Formation and Differentiation of Placental Stem Cells

Jessica Cinkornpumin

Department of Biochemistry
McGill University, Montreal

April 2024

A thesis submitted to McGill University in partial fulfillment of the requirements for the degree of Doctor of Philosophy.

ABSTRACT

The placenta is often an afterthought when the term “pregnancy” is discussed. Yet, one cannot occur without the other. The placenta develops alongside the fetus and is critical for nurturing fetal development to term. This research project focuses on modeling transcriptional mechanisms involved in early placental development to understand how a healthy placenta is established.

The specification of placenta occurs during the early blastocyst stage of the developing embryo, with some of the inner cells specifying the epiblast (later forming the fetus) and the outer cells specifying the trophectoderm (which forms the placenta). Post-implantation, cytotrophoblast cells (CTB) arise from the trophectoderm. These CTB can self-renew and differentiate into syncytiotrophoblasts (STB) and extravillous trophoblasts (EVT), the cells that make up the functional villus structures of the placenta. Villous formation and placental remodeling are complete by the first trimester, and defects in placentation during this stage are believed to cause pregnancy disorders in mid to late gestation. Therefore, this thesis has conducted two interrelated projects to study specification of trophoblast as well as transcriptional regulation of human trophoblast stem cells (hTSCs), EVT, and STB. Since hTSCs derived from CTBs can be cultured in vitro and differentiated to EVT and STB, they are a useful tool to model and study gene regulation as the developing embryo makes early cell-fate decisions.

Conventionally cultured “primed” human embryonic stem cells (hESC) are similar to committed epiblast cells in vivo and are able to differentiate into cells of all three germ layers. However, primed hESCs cannot be converted efficiently to trophoblast. In **Chapter 1**, we reasoned that since specially cultured “naive” hESC transcriptionally and epigenetically resemble preimplantation epiblast, these cells might have improved ability to convert to trophoblast. hESC

reverted to naive state and placed in TSC media (TSCM) transition to cobblestone-like epithelial cells that look similar to hTSC derived from the first-trimester placenta. These cells are termed "transdifferentiated human trophoblast stem cells" (tdhTSC). tdhTSC are transcriptionally similar to hTSC by RNA-seq and have similar methylomes. In addition, they stain positively for pan-placental markers and show capacity for differentiation to other placental lineages. With these cells, we have established a system for studying trophoblast specification, the first specification event in embryonic development.

During early embryonic development, ambient oxygen supply is normally very low (~1-2% O_2). Since oxygen levels often play a key role in controlling self-renewal and cell fate determination in early embryogenesis, in **Chapter 2**, we recapitulate physiological growth conditions in vitro that mimic natural development by culturing 3 hTSC (CT1, CT3, and BT2) cell lines at 2%-5%-20% O_2. hTSC thrive in low oxygen, whereas differentiation of STB and EVT had extreme reduced capacity in hypoxic conditions. Transcriptional comparative analysis revealed a few interesting oxygen sensitive transcription factors, one of them is GCM1 (Glial Cell Missing-1), which has very diminished levels at 2% O_2. GCM1 transcription factor associated with syncytialization of STB in mice but its function in humans was unknown. We determined that GCM1 plays a crucial role in directing both major trophoblast lineages and that knockout of GCM1 in hTSC showed impaired ability to differentiate to STB and EVT. Chromatin immunoprecipitation of GCM1 showed enrichment of GCM1 specific binding near key transcription factors upregulated upon differentiation, including a role in contact inhibition and expression of *CDKN1C*. Inhibition of the PI3K pathway reduces GCM1 expression and prevents spontaneous differentiation in an in vitro model of trophoblast differentiation.

RÉSUMÉ

Le placenta est souvent considéré comme un élément secondaire lorsque l'on parle de grossesse. Pourtant, l'un ne va pas sans l'autre. Le placenta se développe en même temps que le fœtus et joue un rôle essentiel dans le développement de celui-ci jusqu'àterme. Ce projet de recherche se concentre sur la modélisation des mécanismes transcriptionnels impliqués dans le développement précoce du placenta afin de comprendre comment un placenta sain se met en place.

La spécification du placenta débute au stade blastocyste de l'embryon, certaines cellules internes spécifiant l'épiblaste (formera le fœtus) et les cellules externes spécifiant le trophectoderme (formera le placenta). Après l'implantation, les cellules du cytotrophoblaste (CTB) émergent du trophectoderme. Ces CTB peuvent s'auto-renouveler et se différencier en syncytiotrophoblastes (STB) et en trophoblastes extravillositaires (EVT), cellules qui constituent les villosités fonctionnelles du placenta. La formation des villosités et le remodelage placentaire sont terminés au premier trimestre, et les défauts de placentation à ce stade sont souvent la cause des troubles au milieu et à la fin de la grossesse. Les travaux de cette thèse ont mené deux projets pour étudier la spécification du trophoblaste et la régulation transcriptionnelle des cellules souches du trophoblaste humain (hTSC), EVT et STB. Comme les hTSC dérivées des CTB peuvent être cultivées in vitro et différenciées en EVT et STB, elles sont un outil utile pour étudier la régulation des gènes durant la période pendant laquelle l'embryon en développement prend des décisions précoces sur le devenir de ses cellules.

Les cellules souches embryonnaires humaines "amorcées" (CSEh) cultivées de façon conventionnelle sont similaires aux cellules de l'épiblaste in vivo, dont la différentiation est déjà orientée, et sont capables de se différencier en cellules des trois couches germinales. Cependant, les CSEh amorcées ne peuvent pas être converties efficacement en trophoblaste. Dans le chapitre

1, nous avons émis l'hypothèse que puisque les CSEh "naïves" cultivées dans un milieu spécifique ressemblent par les aspects transcriptionnels et épigénétiques à l'épiblaste préimplantatoire, elles pourraient avoir une meilleure capacité à se convertir en trophoblaste. Nos travaux montrent que les CSEh ramenées à l'état naïf et cultivées dans un milieu TSC se transforment en cellules épithéliales de type cobblestone qui ressemblent aux CSEh dérivées du placenta du premier trimestre. Nous avons appelé ces cellules "cellules souches de trophoblaste humain transdifférenciées" (tdhTSC). Par RNA-seq, nous avons constaté que le transcriptome et méthylome des tdhTSC sontsimilaires. Aussi, elles deviennent positives pour les marqueurs pan-placentaires et montrent une capacité de différenciation vers d'autres lignées du placenta. Avec ces cellules, nous avons établi un système pour étudier la spécification du trophoblaste, le premier événement de spécification dans le développement embryonnaire.

Au cours du développement embryonnaire précoce, l'apport en oxygène est très faible (~1-2% O_2). Étant donné que les taux d'oxygène jouent souvent un rôle clé dans l'auto-renouvellement et la détermination du destin cellulaire au cours de l'embryogenèse précoce, nous avons étudié dans le chapitre 2 des conditions de croissance physiologiques in vitro qui imitent le développement naturel. Nous avons utilisé 3 lignées cellulaires de hTSC à 2 %-5 %-20 % d'O_2. hTSC prospèrent dans des conditions de faible oxygène, tandis que la différenciation des STB et EVT a une capacité fort réduite en hypoxie. L'analyse transcriptionnelle comparative a révélé des facteurs de transcription intéressants sensibles à l'oxygène, dont GCM1 (Glial Cell Missing-1), qui est très réduit à 2 % d'O_2. GCM1 est associé à la syncytialisation de la STB chez la souris, mais sa fonction chez l'homme est inconnue. Nous avons donc déterminé que GCM1 joue un rôle crucial dans l'orientation des deux principales lignées trophoblastiques et que le knock-out de GCM1 dans les hTSC mène à une capacité réduite à se différencier en STB et EVT. L'immunoprécipitation de

la chromatine de GCM1 montre un enrichissement de la liaison spécifique de GCM1 à proximité de facteurs de transcription clés régulés lors de la différenciation, et un rôle dans l'inhibition du contact et l'expression de CDKN1C. L'inhibition de la voie PI3K réduit l'expression de GCM1 et empêche la différenciation spontanée dans un modèle in vitro de différenciation du trophoblaste.

ACKNOWLEDGEMENTS

First and foremost, I would like to express my deepest gratitude to my supervisor Dr. William A. Pastor for providing me the opportunity to explore placental research in his laboratory at McGill University. I greatly enjoyed this project and the experience that came with it. I want to personally thank Dr. Pastor for his unwavering commitment to mentorship, continuous support, and encouragement in both my work and life, and patience throughout the past years. I admire the invaluable expertise he has in the field, and I can only aspire to be as academically intellectual and kind.

I am also indebted to my colleagues and peers at this lab, Dr. Yojiro Yamanaka, Dr. Maxime Bouchard, and Dr. Natasha Chang whose given me insightful discussions, constructive feedback, and an enriching workplace to come to. You all have inspired me in many ways academically and personally. I wish you all the best in your future endeavors. I am particularly grateful to Sin Young Kwon, Joy Zhang, Colleen S. Russett, and James Goldberg who were all amazing undergraduates that I had the pleasure to work with. Additionally, it was my greatest pleasure to work with Jacinthe Sirois in which her much-needed support, encouragement, and kindness was instrumental to my accomplishments during my academic journey.

I acknowledge all the contribution from our collaborators listed in the manuscripts and core facilities at McGill who have helped make this research project feasible. I appreciate the financial supports from McGill University Faculty of Medicine, namely the Biochemistry Department (2018), Fonds de recherche Santé Quebec graduate fellowship and studentship (2019-23), and Maysie MacSporran Graduate Studentship (2021).

Finally, to my friends and family, who have always given me solace and motivation throughout my life. I would be remiss to not personally mention my mother, late father, late grandmother, my family across the world, and my new family (Josh Kaiser, our baby Lennon Boone Kaiser, and the extended Kaiser family) their unconditional love, belief in my abilities, and sacrifice and patience are the force behind my success. I am truly fortunate to have you in my life forever and always.

PREFACE

This thesis will be written as manuscript-based format. In Chapter 1, a general literature review will cover the materials discussed in both Chapter 2 and 3. Chapter 2 is a published manuscript with original text and figures. Chapter 3 is in preparation for journal submission. Chapter 4 will be a final discussion encompassing all chapters.

Papers included in this Thesis.

Chapter 2	**Cinkornpumin JK,** Kwon SY, Guo Y, Hossain I, Sirois J, Russett CS, Tseng HW, Okae H, Arima T, Duchaine TF, Liu W, Pastor WA. Naive Human Embryonic Stem Cells Can Give Rise to Cells with a Trophoblast-like Transcriptome and Methylome. *Stem Cell Reports*. 2020 Jul 14;15(1):198-213. doi: 10.1016/j.stemcr.2020.06.003. Epub 2020 Jul 2.
Chapter 3	**Cinkornpumin JK**, Kwon SY, Sirois J, Goldberg J, Zhang J, Renuad SJ, Paul S, and Pastor WA. Reduction of GCM1 Expression by Hypoxia or PI3K Pathway Inhibition Prevents Spontaneous Differentiation of Trophoblast Stem Cells. (Manuscript in preparation, 2024)

CONTRIBUTION OF AUTHORS

All studies for this thesis are performed with the guidance and supervision of Dr. William A. Pastor. The majority of the experiments, data analysis, and figure generation is performed by the candidate of this thesis. Specific contribution of authors for each chapter is described in the AUTHOR CONTRIBUTIONS section. A more detailed description of the other author contributions for each figure is described as follows:

In Chapter 2, the main text writing was primarily written by Dr. William A. Pastor (W.A.P) with edits performed by all-contributing authors. Analysis of published RNAseq and bar graph figure was generated by (W.A.P) (Figure 1A, 1B, 1D, S1A). Ishtiaque Hossian performed the initial ESC naïve conversion (Figure 2A). RNAseq analysis and data illustration was generated by Sin-Young Kwon (S.Y.K) under the guidance of myself and W.A.P (Figure. 3A-D, 6A-C, 7D, S6A, S7A-B). Colleen S. Russet (C.S.R.) assisted in several hCGB assays for Figure 4B. Yixin Gou and Dr. Wanlu Liu performed the methylation analysis and generated the figures (Figure 5A-G, S5A-B) Hsin-Wei Tseng and Dr. Thomas F. Duchaine assisted in the microRNA quantitative RT-PCR (Figure S3A). C.S.R. and Jacinthe Sirois (J.S.) performed the DNA isolation and bisulfite PCR Figure S3B-C.

In Chapter 3, the main text was primarily written by myself with guidance and major edits from W.A.P. S.Y.K performed immunofluorescent staining and western blot for Figure 1C, 1H-I, and S2E. James Goldberg designed the original CRISPR sgRNA guides for GCM1KO1 (Figure 3A). Joy Zhang western blotted for GCM1 in Figure S2F and performed the STB3D hCGB assay in Figure 3F. GCM1 ChIP was shared by Dr. Stephan J. Renaud and ATACseq data was given to us by Dr. Soumen Paul. The analysis of this data was used to generate most of Figure 5. J.S. performed the TSC confluency and CRISPRi experiment for Figure 6A and S2G.

TABLE OF CONTENTS

LIST OF FIGURES

Chapter 2

Chapter 3

LIST OF ABBREVIATIONS

β-catenin	beta-catenin
ΔNp63α	isoform of p63
2D TSC	2-dimensional trophoblast stem cell
3D-TSC	3-dimensional trophoblast stem cell
5iLAF	5 inhibitor LIF Activin A FGF
8CLC	8-cell-like cells
ADAMTS20	ADAM metallopeptidase with thrombospondin type 1 motif 20
AKT	protein kinase B
APAP2	A-kinase anchoring protein 2
Arnt	aryl hydrocarbon receptor nuclear translocator (murine gene)
ASCL2	achaete-scute family bHLH transcription factor 2
ATAC	assay for transposase-accessible chromatin
BCAM	basal cell adhesion molecule
BCL9	B-cell lymphoma 9
BMP	bone morphogenetic protein
BMP4	bone morphogenetic protein 4
BMP7	bone morphogenetic protein 7
BT2	blastocyst-derived cell line 2
C19MC	Chromosome 19 microRNA cluster
cAMP	cyclic adenosine monophosphate
CCR7	c-c motif chemokine receptor 7
CCT	cell column trophoblast
CDH1	cadherin 1
CDK	cyclin dependent kinase
CDKN1C	cyclin dependent kinase inhibitor 1C
CDX2	caudal type homeo box transcription factor 2
CGB	chorionic gonadotropin subunit beta
CGB5	chorionic gonadotropin subunit beta 5
CGB7	chorionic gonadotropin subunit beta 7
ChIP	chromatin immunoprecipitation
COL4A1	collagen type IV alpha 1
CpG	cytosine-phosphate-guanine group
CREB	cAMP response element-binding
CRH	corticotropin-releasing hormone
CRISPR	clustered regularly interspaced short palindromic repeats
CRISPRi	CRISPR interference
CSH1	chorionic somatomammotropin hormone 1
CT1	cytotrophoblast-derive cell line 1
CT3	cytotrophoblast-derive cell line 1
CTB	cytotrophoblast
CTB-CCC	cytotrophoblast-cell column cells
CTB-f	cytotrophoblast -fusing
CTB-p	cytotrophoblast -proliferative
CYP19A1	cytochrome P450 family 19 subfamily A member 1

DAPI	4′,6-diamidino-2-phenylindole
DBD	DNA binding domain
DEG	differentially expressed genes
DKK-1	dickkopf-1
DNA	deoxyribonucleic acid
DPPA5	developmental pluripotency associated 5
DSG3	desmoglein-3
DUSP23	dual specificity phosphatase 23
eEVT	endovascular extravillous trophoblast
EFNB2	ephrin B2
EGF	epidermal growth factor
EGFR	epidermal growth factor receptor
EGFR1	epidermal growth factor receptor 1
ELF5	E74-like factor 5
ELISA	enzyme-linked immunosorbent assay
ENDOU	endonuclease poly(U) specific
Eomes	eomesodermin
EpCAM	epithelial cell adhesion molecule
EPI	epiblast
EPS	extended potential stem cell
ERBB2	Erb-B2 receptor tyrosine kinase 2
ERK	extracellular signal-regulated kinase
ERVFRD-1	endogenous retrovirus group FRD member 1, Syncytin-2
ERVV-1	endogenous retrovirus group V member 1
ERVW-1	endogenous retrovirus group W member 1, Syncytin-1
ESC	embryonic stem cell
Esrrb	estrogen-related receptor b (murine gene)
EVT	extravillous trophoblast
ExM	extraembryonic mesoderm
FACS	fluorescence-activated cell sorting
FGF	fibroblast growth factor
FGF2	fibroblast growth factor 2
FGFR2	fibroblast growth factor receptor 2
FN1	fibronectin 1
FOXH1	forkhead box H1
FPKM	fragments per kilobase of transcript per million mapped
FT190	fallopian tube 190, hTERT
FZD	frizzled
FZD5	frizzled class receptor 5
GAPDH	glyceraldehyde 3-phosphate dehydrogenase
GATA2	GATA-binding factor 2
GATA3	GATA-binding factor 3
GATA4	GATA-binding factor 4
GCM1	Glial Cell Missing-1
GDF3	growth differentiation factor 3
GFP	green fluorescent protein

GGT1	gamma-glutamyltransferase 1
GRM2	glutamate metabotropic receptor 2
GSEA	gene set enrichment analysis
GSK-3β	glycogen synthase kinase 3 beta
H3K27Ac	H3 lysine 27 acetylation
H9	human ESC line, Hut 78
HAND2	hearth and neural crest derivatives-expressed protein 2
HAVCR1	hepatitis A virus cellular receptor 1
hCG	human chorionic gonadotropin
hCGA	human chorionic gonadotropin alpha
hCGB	human chorionic gonadotropin beta
HDAC	histone deacetylase
Hec116	endometrial carcinoma cell line
HEK293T	human embryonic kidney SV40 T antigen
HERV-FRD	human ERV, endogenous retrovirus group V, Syncytin-2
HERV-W	human ERV, endogenous retrovirus group V, Syncytin-1
HERV	human endogenous retrovirus
hESC,	human embryonic stem cell
HIF	hypoxia inducible factor 1
HIF-1α	hypoxia inducible factor 1 subunit alpha
HIF-1β	hypoxia inducible factor 1 subunit beta
HLA-G	human leukocyte class G
HLA-I	human leukocyte class I
HNF1B	hepatocyte nuclear factor-1 beta
hPSC	human pluripotent stem cell
HTR-8	trophoblast cell line infected SVneo
HTRA4	Htr4 serine peptidase
hTSC	human trophoblast stem cell
ICM	inner cell mass
ID1	inhibitor of DNA binding 1
iEVT	interstitial extravillous trophoblast
IGFBP3	insulin like growth factor binding protein 3
ISL1	LIM-homeodomain transcription factor 1
ITGA1	integrin alpha 1 subunit
ITGA2	integrin alpha 2 subunit
ITGA5	integrin alpha 5 subunit
ITGA6	integrin alpha 6 subunit
ITGB6	integrin beta 6 subunit
iTSC	induced trophoblast stem cell
IUGR	intrauterine growth restriction
KCNQ1	potassium voltage-gated channel subfamily Q, KvDMR1
KD	knock-down
KO	knock-out
KRT7	keratin 7
KSR	knockout serum replacement
L1TD1	LINE 1 type transposase domain containing 1

LAMA4	Laminin subunit alpha 4
LGR5	leucine rich repeat containing G protein-coupled receptor
LH/CG-R	luteinizing hormone/choriogonadotropin receptor
LIF	interleukin 6 class cytokine
LMO2	LIM-domain only 2
LncRNA	long non-coding RNA
LPCAT1	lysophosphatidylcholine acyltransferase 1
TPM1	tropomyosin 1
MEF	mouse embryonic fibroblast
mESC	mouse embryonic stem cell
miRNA	micro ribonucleic acid
MMP12	matrix metallopeptidase 12
mRNA	messenger ribonucleic acid
MSX2	Msh homeobox 2
mTSC	mouse trophoblast stem cell
NCAM1	neural cell adhesion molecule 1
NKX-2.5	Nkx homeobox factor 2.5
NODAL	TGF-beta secreted ligand
NOTCH	neurogenic locus notch homolog protein
NOTCH1	neurogenic locus notch homolog protein 1
NOTCH2	neurogenic locus notch homolog protein 2
NOTCH3	neurogenic locus notch homolog protein 3
NOTUM	palmitoleoyl-protein carboxylesterase
NRG1	neuregulin-1
NRP2	neuropilin family receptor protein, SEMA3C
NT	non-targeting
OCT4	POU homeodomain, POU5F1
OVOL1	ovo like transcriptional receptor 1
p21	CDKN1A, cyclin dependent kinase inhibitor 1A
PAGE4	PAGE family member 4
PCA	principal-component analysis
pCCT	proximal cell column trophoblast
PCR	polymerase chain reaction
PDGFRA	platelet-derived growth factor receptor alpha
PE	primitive endoderm
PEG10	paternally expressed gene 10
PEG3	paternally expressed gene 3
PGF	placental growth factor
Phd2	proplyl hydroxylase domain, EGLN1
PI3K	phosphoinositide 3-kinase
PKA	protein kinase A
PLAC8	placental associated 8
PLAU	plasminogen activator, urokinase
PPARγ	proliferator-activated receptor gamma
PPFIA4	PRPRF interacting protein alpha 4
PRDM14	PR/SET Domain 14

PRG2	proteoglycan 2
PROSER2-AS1	proline and serine rich 2-antisense RNA 1
PS	primitive syncytium
PSG	pregnancy-specific glycoprotein
PTO	primary trophoblast organoids
PXGL	PD0325901, XAV939, Gö6983, LIF
qRT-PCR	qualitative real-time PCR
Rho	rhodopsin
RNA	Ribonucleic acid
ROCK	Rho-associated protein kinase
ROS	reactive oxygen species
RPKM	reads per kilobase per million mapped reads
SDC1	stearyl-CoA desaturase
SEMA3C	semaphorin 3C
SEMA3F	semaphorin 3F
SERPINE1	serpine family E member 1
SERPINE2	serpine family E member 2
Seq	sequencing
SOX1	SRY-box transcription factor 1
SOX17	SRY-box transcription factor 17
SOX2	SRY-box transcription factor 2
SOX9	SRY-box transcription factor 9
STAT3	signal transducer and activator of transcription 3
STB	syncytiotrophoblast
SYNCYTIN-1	endogenous retrovirus group W member 1, ERVW-1
SYNCYTIN-2	endogenous retrovirus group FRD member 1, ERVFRD-1
T-cell	T lymphocyte cell
TAP1	transporter 1, ATP binding cassette subfamily
TB-ORG	trophoblast organoid
TCF4	transcription factor 4
TDGF1	Cripto, EGF-CFC family member 1
tdhTSC	transdifferentiated human trophoblast stem cell
TE	trophectoderm
TEAD4	TEA domain transcription factor
TF	transcription factor
TFAP2C	transcription factor AP-2 gamma
TGC	trophoblast giant cell
TGF-β	transforming growth factor-beta
TNIK	TRAF2 and NCK interacting kinase
TP63	tumor protein p63
TPM1	tropomyosin 1
TPM2	tropomyosin 2
TSC-org	trophoblast stem cell organoid
TSCM	trophoblast stem cell media
TSS	transcriptions start site
UCLA1	University of California Los Angeles embryonic stem cell line 1

uNK	uterine natural killer
VCT	villous cytotrophoblast, CTB
VCT-CCC	villous cytotrophoblast-cell column cells
VE-cadherin	cadherin 5
VGLL1	vestigial like family member 1
VHL	Von Hippel-Lindau tumor suppressor
VIM	vimentin
VPA	valproic acid
WIBR3	Whitehead Institute for Biomedical Research line 3
WLS	Wnt ligand secretion mediator
WNT	wingless related integrate site
WNT3A	Wnt family member 3A
WWTR1	WW domain containing transcription regulator 1
XAGE3	X antigen family member 3
YAP1	Yes1 associated transcription regulator
ZFAT	Zinc finger and AT-hook domain containing

CHAPTER 1: INTRODUCTION

1.1 General understanding of the placenta during pregnancy

Throughout the nine months of human pregnancy, the placenta is an essential component of successful fetal development. By dynamically interacting with the maternal decidua under tightly regulated processes, this transient extraembryonic organ enables establishment of pregnancy.(Burton & Fowden, 2015; Maltepe & Fisher, 2015; Turco & Moffett, 2019) In order to perform the functions of future organ systems that are not fully developed or matured in the fetus, the placenta must develop rapidly after conception. Some of the roles that it plays include (1) exchange of nutrients and gas between the mother and fetus; (2) production and secretion of hormones that help maintain a healthy pregnancy; (3) maintaining immunological tolerance of the fetus to the maternal immune system.(Maltepe & Fisher, 2015; Moffett & Loke, 2006) During the 9 months of gestation, the placental component that undergoes the most important dynamic structural and functional changes is the villus. In early pregnancy, the most primitive form of placental villus (mesenchymal villus) become highly vascularized structures that efficiently extract substances from the maternal circulation.(Wang & Zhao, 2010) Once the placenta has developed, placental villus are the primary method of interaction with the maternal system, delivering nutrients and oxygen to the developing fetus and removing fetal waste products. By term, the villi have developed an extensive branching network with an overall epithelial surface of about 12–14 m^2, ensuring a sufficient supply of nutrition for the high growth rates of the fetus.(Burton et al., 2009) Additionally, placental hormones are released into fetal circulation to help control development, growth, and delivery timing. Not only does the placenta aide in developing the fetus, the placenta also greatly affects maternal metabolism by secreting a variety of hormones into the mother's bloodstream. These hormones target most maternal tissues and organs to help maintain

pregnancy, and then mobilize nutrients for birth and lactation.(Napso et al., 2018) In total, these observations reinforce the significance of the placenta in the establishment of the fetal-maternal connection and even beyond the birth of the fetus.

Since the placenta plays so many important roles during fetal development, it should be unsurprising that incomplete formation or improper cellular lineage differentiation can jeopardize correct embryo implantation and fetal development.(Fisher, 2015; Romero et al., 2011) Abnormal placental development in the first-trimester can result in miscarriage or later complications in pregnancy. Some of the frequent causes of maternal and neonatal death during the later stages of pregnancy include preeclampsia, fetal growth restriction, and placenta accreta.(Ananth & Vintzileos, 2006; Maltepe & Fisher, 2015; Romero et al., 2014) One of the confounding factors in better understanding how improper placental development contributes to pregnancy disorders is that the root cause of these disorders occurs during the first trimester of pregnancy. At these early stages, placental tissue availability for *in-vitro* studies is not only more limited due to ethical reasons, but we also cannot accurately predict whether a placenta will eventually develop pathology later in gestation.(Knöfler et al., 2019) Furthermore, detailed molecular investigations are only now becoming more frequent since the cell culture conditions to support self-renewal and long-term propagation of primary trophoblasts was only recently established.(Haider et al., 2018; Okae et al., 2018) From these novel developments in placental studies, my research proposal seeks to identify the origin of placental stem cells and the genes that govern proper formation of the cell lineages found in the villus.

1.2 A briefing on the biological differences between human and mouse model of the placenta

Before the recent progress of *in-vitro* expanded trophoblast stem cell (TSC) lines and self-renewing primary trophoblast organoids (PTOs), our functional knowledge of placental

development was largely based on mouse models.(Latos & Hemberger, 2014; Loregger et al., 2003) Through these studies in mice, specific regulators of major processes in the placenta have been identified, including factors governing placental vascularization, formation of the labyrinth, and function of the junctional zone.(Woods et al., 2018) Additionally, decidualized maternal endometrium (decidua) has also been established as an important regulator of placental development, trophoblast differentiation, and fetal growth.(Khong et al., 1986) However, despite some similarities, there are considerable structural and developmental differences between the murine and human placenta.(Georgiades et al., 2002) As discussed in section 1.8 below, human and mouse placentas show differences in overall morphology, are composed of partially-non overlapping cell types, and have very distinct modes of blastocyst implantation. Trophoblast invasion is more shallow and uterine arterial vessel remodeling is predominantly based on maternal factors in mice.(Carter, 2007) Key molecular regulators of placental development also differ between mice and humans such as FGF signaling, *Eomes* and *Cdx-2* expression patterns. Therefore, my questions about human placental development can only be properly answered by studying human placentas.(Knöfler et al., 2001) In particular, further improvement of current human placenta models is very important to our long-term understanding of pregnancy complications and development of therapeutic treatment options. Many of the critical steps of pathological, or even normal, placentation have not yet been discovered though.(Knöfler et al., 2019) Before discussing how my research has contributed to our understanding of the placenta, the following material will be a review of human placental development and factors that regulate placental cell differentiation.

1.3 The formation of the trophectoderm and early mechanisms in lineage specification

Human development begins with the union of a sperm and ovum, which produces a zygote. The zygote undergoes multiple rounds of rapid mitotic divisions as it journeys to the uterine cavity through the oviduct. When the zygote reaches 12–16 cells (3–4 days postfertilization in humans), it reaches the spherical stage of a morula.(Nikas et al., 1996) Tight cellular adhesion on the outer edges of the morula results in fluid accumulating within the center. After the fluid eventually coalesces to form a blastocoel, the morula has transformed into a blastocyst at around the 32–64 cell stage (approximately 4–5 days postfertilization in humans). At this stage, the first cell specification event has occurred as two distinct populations of cells can be identified: the inner cell mass (ICM) and trophectoderm (TE). The ICM will eventually separate into the pluripotent epiblast (EPI), which gives rise to the embryo proper, and the primitive endoderm (PE), which gives rise to yolk sac endoderm. TE is an extraembryonic segment, which differentiates into the trophoblast lineage components of the placenta.(Alarcon & Marikawa, 2022; Płusa & Piliszek, 2020) As the ICM is still composed of different lineages, TE emergence is the first true lineage commitment event during embryogenesis.

Placenta development continues with the TE then dividing into polar TE (adjacent to the ICM) and mural TE (opposite side of the ICM) based on the embryo's polarity position and differential gene expression.(Petropoulos et al., 2016) The polar TE region next to the ICM is also responsible for the initial interaction between the TE and the uterine epithelium.(Turco & Moffett, 2019) After the developing blastocyst hatches from the zona pellucida, which is a glycoprotein layer initially surrounding the ovum, it attaches to the epithelial surface of the uterine wall and implants into the uterine endometrium (decidua) at around 6–8 days after fertilization.(Baines & Renaud, 2017; Płusa & Piliszek, 2020) After blastocyst implantation into the maternal decidua, TEs differentiate into the first trophoblast lineages at day 8: primitive syncytium (PS) and

mononuclear CTB.(James et al., 2012) The primitive syncytium expands into the maternal endometrium through the epithelium, representing the first invasive placental cell type.(Papuchova & Latos, 2022; Rossant & Tam, 2022) At about day 9, lacunar spaces appear in the PS from the fusion of vacuoles, which is the precursor for uteroplacental circulation when the lacunar spaces eventually reach the maternal capillaries.(Hertig et al., 1956) Under the primary syncytium, a shell of diploid trophoblast cells has formed around the developing embryo.(James et al., 2012) Notably, the formation of the shell coincides with early developing chorionic villi and differentiation into STB, setting the foundation of placentation.(Turco & Moffett, 2019) During this stage, the emergence of the three primary trophoblast subpopulations of the placenta begin to form: cytotrophoblast (CTB), syncytiotrophoblast (STB), and extravillous trophoblast (EVT).(Rossant & Tam, 2022)

1.4 The formation of the cytotrophoblast shell

More specifically, around day 15, the trophoblastic shell forms post-conception from proliferative CTBs that expand laterally at distal sites.(Turco & Moffett, 2019) At these distal sites, where villi make contact with the maternal decidua, STBs are absent. Instead, trophoblast cells from the cell column make contact with the decidua basalis, then spread laterally to form the cytotrophoblastic cell. This outermost site of the placenta encircling the embryo lacks maternal cells, and is thought to be an essential component for anchorage of the placenta to the decidua, as well as protecting the embryo from oxidative stress.(Burton & Jauniaux, 2017) Placental development progresses between the cytotrophoblast shell and proliferating CTB progenitors. CTB differentiation results in the formation of the functional villous placenta containing two types of villi, anchoring villus and floating villus. At the anchoring villus base, CTB form a cell column, while floating villus end in the intervillous space of fetal-maternal interface.(Damsky et al., 1992)

A more detailed review of how these trophoblast subpopulations contribute to the functional villi will be discussed below.

1.5 The function, differentiation, and gene expression of cytotrophoblast

After the epithelial-like TE cells are exposed to the endometrial epithelium upon implantation, they begin to transform into mononuclear CTB, which maintains self-renewal capabilities, acting as the progenitor population for subsequent STB and EVT lineages. These proliferative CTB then form primary villi by breaking through the expanding PS. The PS is also invaded by the extraembryonic mesoderm (ExM) from the other side, which potentially originates from the ICM.(Papuchova & Latos, 2022) As CTB differentiate from the TE, some of the TE markers that are still expressed include GATA2, GATA3, TEAD4, and TFAP2C. Based on analysis of 6-week primary trophoblast and CTB derived from established cell culture conditions, there are now believed to be 3 subpopulations of CTB: CTB, CTB-proliferative (CTB-p), and CTB-fusing (CTB-f). The CTB and CTB-p populations have very similar gene expression profiles and contain the self-renewing stem cell population. Some of the identifying markers include *PAGE4*, *PEG10*, *CDH1*, and *EGFR*.(Haider et al., 2018; Liu et al., 2018; Zhou et al., 2022) Known stem and progenitor cell markers (*LGR5*, *L1TD1* and *TP63*) are also observed to be upregulated, as well as Wingless/Integrated (WNT) signaling molecules (WLS and TNIK), the SEMA3F-NRP2 signaling complex, and the CTB marker BCAM. The CTB-p population often expresses Ki67, which partitions them from CTB in the single-cell analysis by Arutyunyan et al.(Arutyunyan et al., 2023) The additional population of CTB found in the placental villus, labeled CTB-fusing, eventually become STB. As CTB commit to CTB-f, they downregulate WNT (*WLS*, *TNIK* and *LGR5*) and BMP signals (BMP7), while upregulating the BMP antagonist *GREM2* and endogenous retroviral genes (*ERVW-1*, *ERVFRD-1*, *ERVV-1*) known to mediate trophoblast

fusion.(Arutyunyan et al., 2023) Some transcription factors have been identified to regulate CTB self-renewal proliferation, and stemness by inhibiting differentiation, such as *TEAD4* and its cofactor *YAP1* in the HIPPO pathway.(Meinhardt et al., 2020; Saha et al., 2020) Another Hippo signaling cofactor, WWTR1, has also been reported to optimize trophoblast progenitor self-renewal and is believed to be essential for regulating EVT differentiation.(Ray et al., 2022) The mechanistic function of WWTR1 is to directly regulate *TP63* expression, which reinforces self-renewal and restricts premature differentiation. Overall, these interactions drive CTB proliferation and prevent epithelial-to mesenchymal transition and differentiation.(Li et al., 2014)

1.6 The function, differentiation, and gene expression of syncytiotrophoblast

As primary villi surface branches continue to proliferate and differentiate, a villous structure is formed that consists of an ExM-derived core containing fetal capillaries covered by two trophoblast layers: the proliferative villous CTB and one of its potential lineages, the STB. The latter is produced by cell fusion of the developing villous CTB (CTB-f) and forms the syncytium that is the exchange site between the maternal and fetal bloodstreams.(Papuchova & Latos, 2022) As previously mentioned, there are actually two types of human STB: the primitive STB that mediates embryonic implantation, and the definitive STB that lines chorionic villus from the third week onwards. While it is unclear whether definitive STB arise from primitive STB or are a distinct lineage, it is known that definitive villous STB exchanges materials with the maternal blood and ensures optimal pregnancy function. This exchange is supported functionally by an enlarged cell surface that helps the efficient transport of nutrients, gases, and metabolites through microvilli, numerous channels, and transporters.(Jaremek et al., 2021) The other primary function is the synthesis and secretion of a variety of pregnancy hormones, including human chorionic gonadotropin (hCGA and hCGB), placental growth factor (PGF), pregnancy-specific

glycoproteins (PSGs), placental lactogen (CSH1), and corticotropin-releasing hormone (CRH).(Papuchova & Latos, 2022) Lastly, an important characteristic of STB is absence of human leukocyte antigen class I (HLA-I) molecules, which makes it undetectable to potentially reactive maternal T-cells.(Moffett & Loke, 2006)

The tightly controlled process of STB replenishment involves biochemical and morphological changes that are regulated by the coordinated differentiation and fusion of the underlying CTB.(Yang et al., 2003) While the direct signal is unknown, one of the differentiation requirements is exit from the cell cycle, followed by repression of progenitor state-associated genes and activation of STB-associated genes related to nutrient transport, hormone synthesis, and immunomodulation.(Lu et al., 2017; Papuchova & Latos, 2022) This differentiation process is coordinated by a subset of transcription factors (TFs) and signaling inputs, such as the syncytialization-promoting TF hCG.(Yang et al., 2003) At early stages of placenta development, hCG is secreted by CTB and is suggested to induce primitive syncytium formation. During later stages, it is produced by STB and acts as a positive regulator of the syncytialization process. Mechanistically, this positive regulation begins with the binding of hCG to luteinizing hormone/choriogonadotropin receptor (LH/CG-R), which induces high levels of cAMP and activates protein kinase A (PKA). Next, PKA phosphorylates the cAMP response element-binding (CREB) TF, which eventually promotes expression of specific fusogenic genes and *GCM1*, which will be mentioned again later.(Gerbaud & Pidoux, 2015) *GCM1*, glial cells missing transcription factor 1, is a particularly important gene in the syncytialization process as it directly drives expression of the critical fusogenic proteins SYNCYTIN-1 and SYNCYTIN-2. These proteins, encoded by the human endogenous retroviruses (HERV) HERV-W and HERV-FRD, interact with receptors that are localized on the target-cell membrane and induce the critical STB formation

process of cell fusion.(Liang et al., 2010; Yu et al., 2002) To concurrently downregulate CTB genes, *OVOL1* is thought to indirectly promote STB differentiation by suppressing CTB genes, such as *MYC*, *ID1*, *TP63* and *ASCL2*.(Renaud et al., 2015) Together, these mechanisms drive the critical formation and proper functioning of STB for a successful term pregnancy.

1.7 The function, differentiation, and gene expression of extravillous trophoblast

During the early phases of placental development, within the cytotrophoblast shell, the other differentiated trophoblast cell type is produced, the invasive extravillous trophoblasts (EVTs). However, once mature placental villi have formed, EVTs originate from the differentiation of cell column trophoblasts in the tips of anchoring villus that contact the endometrium.(Lv et al., 2019) In these villi, rows of proliferative proximal cell column trophoblasts (pCCTs) develop, representing the progenitor cell pool of differentiated EVTs. EVTs begin their differentiation process in cell columns but invasive EVTs emerge only when the anchoring villus attach to the maternal decidua. These CCTs are proliferative and likely emerge from CTB or CTB-p and eventually differentiate into EVTs. As they commit to the CCT population, they downregulate the WNT pathway (*WLS*, *TNIK* and *LGR5* expression), upregulate *NOTCH1*, shift integrin expression to *ITGB6* and *ITGA2*, and upregulate markers characteristic of epithelial–mesenchymal transition (*LPCAT1*).(Arutyunyan et al., 2023) In this subgroup of cells, characterized by expression of *NOTCH1* and *ITGA2*, the phenotype is an intermediate between CTB and EVT. For example, they express the CTB-related TF *CDH1*, but at the same time express the EVT-associated TFs *TPM1* and *TPM2*. Another marker for these cells during trophoblast development is EpCAM, which is present in CTB and the column base around 6 weeks but is only observed in proximal CCTs after 8 weeks.(Lee et al., 2018)

Column trophoblasts are primarily divided based on whether they are located at sites that are proximal or distal in anchoring columns and can be identified by expression of specific NOTCH and integrin genes.(Haider et al., 2016; Zhou et al., 1997) Proximal CCTs express high levels of *NOTCH1*, *SOX9*, and *ITGA2* and likely represents a progenitor population because they also express the CTB genes *TP63*, *ITGA6*, and *YAP1*.(Lee et al., 2018) Comparatively, distal CCTs express higher levels of *ITGA5*, *NOTCH2* and *HLA-G*, indicating a more mature population of CCTs at the other end of the anchoring column from proliferative CTBs.(Haider et al., 2014) At the distal end of the anchoring villus, there are two types of EVTs, one that is proliferative and the other expressing the metalloprotease gene *ADAMTS20* and *ITGA1*. This second type of non-proliferative EVT was identified as the transition point that split into either endovascular EVTs (eEVTs) or interstitial EVTs (iEVTs). These are both endpoint EVTs, as iEVTs invade through decidual stroma and eEVTs travel to the maternal spiral arteries.(Arutyunyan et al., 2023) Observed in Arutyunyan et al. 2023, they provided evidence that eEVTs (expressing *NCAM1*, *GGT1*, *PPFIA4*, and *MMP12*) emerge from the distal end of the cell column based on their close proximity to the non-proliferative EVTs. Additionally, by single-molecule fluorescent in-situ hybridization, they showed NCAM1-expressing cells close to the cytotrophoblast shell when in proximity to a spiral artery. iEVTs were observed surrounded by decidual stromal and immune cells and upregulate *PLAC828* and plasminogen activator inhibitor genes *SERPINE1* and *SERPINE2*, while downregulating expression of *PLAU*.(Arutyunyan et al., 2023)

The diversity of EVT subtypes have highly specialized properties and are therefore regulated by TFs for their unique function. Depending on the cell type, these TFs promote EVT in 2 directions: maintaining proliferation or EVT cell cycle exit, differentiation, and invasiveness.(Baines & Renaud, 2017) One of the primary pathways that determine the identity of

EVTs is WNT signaling, which is also essential for the reinforcement of the CTB progenitor state.(Haider et al., 2018) In EVT, WNT/TCF4 signaling promotes motility and invasion through WNT3A, while DKK-1 blocks those functions by inhibiting WNT signaling.(Pollheimer et al., 2006) Another set of signaling pathways with a regulatory role in EVT identity is LIF/STAT3 and NOTCH. In a DNA-binding activity experiment in first-trimester trophoblast, STAT3 binding was increased in invasive cells.(Corvinus et al., 2003; Fitzgerald et al., 2005) Manipulation in primary trophoblast models, on the other hand, reveals that NOTCH1 represses CTB markers TEAD4 and TP63 while increasing expression of the EVT progenitor-specific genes *MYC* and *VE-cadherin*.(Haider et al., 2016) In more differentially developed EVT, the upregulation of NOTCH2 and NOTCH3 promotes the migratory and invasive potential of EVTs, while its downregulation has the opposite effect and decreases expression of the arterial marker *EFNB2*.(Hunkapiller et al., 2011; Zhao et al., 2017) Other factors that are associated with regulation of EVT development via the WNT signaling pathway, here mentioned again, is GCM1 and its potential downstream targets. GCM1, which is suggested to be downregulated by hypoxic conditions, is a known master regulator of STB formation but is also believed to play an important role in regulating EVT differentiation.(Chiang et al., 2009; Wang et al., 2022b)

An additional function and role of the invasion of uterine stroma by iEVTs during early pregnancy is to interact with decidual stromal cells, macrophages, and uterine natural killer (uNK) cells to allow immunological acceptance between the placenta and fetus.(Moffett et al., 2017) Besides migration into the spiral arteries, iEVTs also invade decidual lymphatic veins to help drain fluid and exchange hormones with the maternal system prior to the onset of the maternal–placental circulation.(Moffett et al., 2017; Windsperger et al., 2017) iEVTs undergo a final differentiation step into multinucleated trophoblast giant cells when they reach the myometrium, ultimately losing

their ability to invade further.(Knöfler et al., 2019) Migration of EVT into the maternal spiral arteries is another important step in placental development as remodeled vessels are observed as far as the first third of the myometrium in early pregnancy.(Wallace et al., 2012)

Remodeling of the maternal spiral arteries is accomplished by the 2 differentiated EVT subtypes iEVT and eEVT. As iEVTs reach the spiral arteries, they initiate the remodeling process from the outside in the decidua by modifying the smooth muscle layer of spiral arteries. This prepares the vessels for later invasion of the spiral artery endothelial layer by eEVT.(Smith et al., 2009; Whitley & Cartwright, 2010) eEVTs, which have a vascular adhesion phenotype, invade the endothelial layer of the vessel and alter the morphology of the maternal spiral artery endothelial cells. Previously, the maternal cells were thought to be completely replaced by eEVT, but it was later demonstrated that endothelial cells were still present with a modified shape similar to eEVT.(Wei et al., 2022) This process of vessel remodeling results in the transformation of narrow vessels with relatively high resistance to highly dilated, low-resistance conduits.(Smith et al., 2009) By remodeling the maternal vessels, iEVTs and eEVTs ensure that volumetric blood flow is increased later in pregnancy to the uterus, but it is slow enough to prevent damage to the villi.(Hustin et al., 1990; Knöfler et al., 2019) During this process, trophoblast plugs made up of eEVT are produced during the first weeks of pregnancy that block the spiral arteries in the decidua near the implantation site.(Bulmer et al., 2020; Pijnenborg et al., 1980; Roberts et al., 2017; Wallace et al., 2012) These plugs completely restrict blood flow at 6–7 weeks of gestation, keeping the intervillous oxygen tension around 2–3% O_2.(Zhao et al., 2021) Then, at around 12–13 weeks of gestation, the plugs dissolve and oxygenated maternal blood around 8% O_2 begins to flow into the intervillous space.(Burton et al., 2021) This significant increase in flow is also thought to coincide with the completion of trophoblast-independent remodeling of the upstream radial

arteries, which may act as the rate-limiting step for vessels regulating the flow of maternal blood into the intervillous space. The process of plugging spiral arteries is believed to be a key factor in proper development as it allows the placenta and embryo to develop in a low oxygen environment for the majority of the first trimester. There is even supporting evidence that premature oxygen level increase and early blood flow are potentially associated with miscarried pregnancies.(Hustin et al., 1990; James et al., 2018) In total, these observations highlight the essential functions and extensive structural remodeling from EVTs in early placentation that are necessary for a successful pregnancy.

1.8 Mechanistic commonalities and differences between human and mouse placental model

Due to their similarity to human genetics and diversity of molecular tools, studying mouse TSCs (mTSCs) have revealed numerous key regulators, including regulatory mechanisms of TFs and our overall understanding of general trophoblast development. For example, some key factors in placental trophoblast are present in both mice and human, such as the trophoblast self-renewal and differentiation regulator GATA3.(Chiu & Chen, 2016; Home et al., 2017) Mouse and human placentas also have important commonalities, as both of them have a discoid shape and are hemochorial; meaning the placental lineages invade and erode maternal vessels, leading to direct connection to the maternal blood.(Woods et al., 2018) Other critical regulatory genes, however, have different timing and expression patterns in the two species.(Knöfler et al., 2001) Additionally, even though they are functionally similar and share conserved genes, there are also many differences between them, such as size, shape, cellular organization, gestational length, and overall structure.(Carter, 2007) One of the major cell types present in murine placentas but absent in human placentas is the sinusoidal trophoblast giant cell (TGC).(Outhwaite et al., 2015) In mice this cell secretes many hormones and is responsible for the initial contact during invasion of the

uterine wall. In humans, these processes are accomplished by STB and primitive syncytium, respectively. This highlights another difference during early placenta development in that murine placentas lack a primitive syncytium.(Hemberger et al., 2020) Additionally, while murine spongiotrophoblasts and TGCs share similarities to human EVTs, they do not represent a strong counterpart.(Shimizu et al., 2023) Therefore, since human and mouse pregnancy have different physiological features, and recently established human TSCs (hTSCs) show they do not express key mTSC regulators such as *Cdx2*, *Eomes*, *Esrrb*, and *Sox2*, a human model system is necessary to fully understand trophoblast lineage differentiation specific to humans.(Blakeley et al., 2015)

One of the primary areas that human placenta development differs from the mouse is spatiotemporal gene expression, which is the location and timing of when certain genes activate in specific tissues during development. OCT4 expression is restricted to the ICM at about day 4.5 in mice compared to day 6 in human blastocysts. Furthermore, while mouse blastocysts express *Oct4* mutually exclusively in the ICM compared to *Cdx2* in TE, OCT4 is initially co-expressed with CDX2 in the human blastocyst and is only later exclusive to the ICM just before implantation.(Niakan & Eggan, 2013) As previously mentioned, core TE-specific mouse TFs (*Elf5* and *Eomes*) are not present in human TE, even though trophoblast subpopulations express ELF5 in early implanted embryos. Mouse TEs also interact with the maternal endometrium with an opposite polarity, since mice TE attach to the endometrium via the mural subtype and human TE attach via the polar subtype.(Liu et al., 2022) Even conserved expression of *GATA* TFs also differs, as *Gata2* is expressed both in outer morula cells and later TE populations in the mouse, but only in later TE subtypes in humans.(Gerri et al., 2020; Home et al., 2017) Overall, comparison between human and mouse placentas confirmed that their development is comparable only during the first half of gestation.(Soncin et al., 2018)

1.9 Restrictions and recent advances in placental research

Until recently, studying human primary trophoblast development depended on whether placental tissues were available from early stages of pregnancy. Placentas from normal term pregnancies and late-stage pregnancy disorders are the easiest to obtain. When studying placentas from pregnancy disorders, though, there is no way to determine whether the pathology was the cause or a result of the complication. In term placentas, most trophoblast functions are significantly reduced, such as the expansion and invasiveness of EVTs. Among the many different functions of trophoblast lineages, only the in vivo formation of STB can be reliably studied with human term placenta.(Knöfler et al., 2019) When searching for the source of trophoblasts in placentas, CTB isolations were originally thought to be a homogenous stem-cell like population that was bi-potential since they were both fusogenic and undergo EVT formation. While studying early placental stages, however, researchers found that CTBs traditionally isolated contained both CTB and CCT, with EVT and STB seeming to develop from different CTB subpopulations.(Aboagye-Mathiesen et al., 1996) Additionally, STBs differentiate from CTBs that are positioned in a monolayer around villus. The possibility of a non-homogenous bi-potential population of CTBs was first suggested by observations that sequential trypsinization isolated trophoblasts with different properties. For example, Haider et al. observed in 2016 that digestion of first trimester placenta could isolate CCT and another CTB subtype that only differentiated into EVT and STB, respectively.(Haider et al., 2016; Haider et al., 2018) This was later supported when multilayered cell clusters from the tips of first trimester villous explants were limited to EVT outgrowth without STB regenerative capabilities.(Aboagye-Mathiesen et al., 1996; James et al., 2005) The isolated EVT progenitor population was unlike normal CTB preparations because it had a slow proliferation rate, with almost 20% of cells transforming into HLA-G positive EVTs and lacking

STB differentiation.(James et al., 2007) Development of new methods to isolate pure populations of CCTs has improved EVT differentiation rates to >90% and has led to a better understanding of the different signaling pathways that generate EVT and STB progenitor populations. Later findings suggested that traditionally isolated CTBs were not a stem cell population, but that a definitive trophoblast stem cell (TSC) population was still present within placental villus.(Haider et al., 2016; Okae et al., 2018)

The recent establishment of a human TSC model by Okae et al. 2018 isolated this TSC population, allowing researchers to finally study the different components of trophoblast lineage differentiation in humans. This first population of human TSC was isolated by enzymatically digesting first trimester placental villi, purifying ITGA6-positive CTBs, and then culturing them in a novel medium formulation that was able to maintain cell-cultured CTB far longer than any previous attempts. After several passages, the proliferative TSC subset took over the culture, establishing TSC lines that remained in an undifferentiated state for up to 5 months. One of the first surprising characteristics of human TSCs came from the initial transcriptomic analysis, which revealed that critical markers of trophoblast identity were *cytokeratin 7*, *GATA3*, *TEAD4*, and *TP63*, while multiple murine markers were absent or weakly expressed.(Okae et al., 2018) While self-renewing placental organ cultures were also later derived from first trimester placenta (Haider et al., 2018), the nature of cultured TSCs still has a number of questions to be answered. Certain aspects have been confirmed, such as hTSCs being definitively placental, having a very long or indefinite replicative life, and possessing the capabilities to differentiate into EVTs and STBs. hTSCs are also epithelial cells that share key surface markers with primary villus CTBs. However, it still remains unclear whether current hTSCs are CTBs that happened to adapt to in vitro culture or if they represent an unspecified CTB subpopulation or precursor.(Cinkornpumin et al., 2020)

1.10 Transcriptional regulators of early development

While multiple organoid and TSC models have been developed, an important part of improving these models is standardizing a set of genes and TFs that regulate differentiation of CTBs into STBs and EVTs. This begins with an understanding of genes responsible for the separation of the three blastocyst lineages: the epiblast, primitive endoderm, and trophectoderm. In a paper by Petropoulos et al. 2016, the transcriptome of blastocysts from day 3 to day 7 of human embryogenesis were studied. The second strongest segregating factor emerged early day 5, which marked the formation of the blastocyst and emergence of each lineage. The first was TE and ICM segregation, shown by well-known TE linage markers (*GATA2* and *GATA3*) and known ICM markers (*SOX2* and *PDGFRA*). Surprisingly, ICM cells during late day 5 were observed to separate with respect to EPI and PE lineage-specificity. Among the genes with known EPI markers were pluripotency-related genes (*SOX2*, *TDGF1*, *DPPA5*, *GDF3*, and *PRDM14*), while genes implicated in primitive endoderm specification (*PDGFRA*, *FGFR2*, *LAMA4*, and *HNF1B*) were observed in a different population. The EPI lineage was completely separated from PE at day 6, but at day 5 EPI genes were still partially expressed in PE cells. By day 6, EPI-specific genes that were believed to be important in embryonic preimplantation development for both mice and human were present, such as *PRDM14*, *GDF3*, *TDGF1*, *NODAL*, *SOX2*, and *NANOG*. Genes reported in day 6 PE populations included known PE-specific factors such as *COL4A1*, *HNF1B*, *PDG*FRA, *GATA4* and *FN1*, marking the full separation of EPI and PE progenitors(Petropoulos et al., 2016).

As for TE, it is further divided into polar TE (near the ICM) and mural TE (far from the ICM) based on the polarity position of the embryo and certain gene expression differences. Some genes that are associated with trophoblast differentiation, such as *CCR7* and *CYP19A1*, are upregulated in human polar TE, suggesting that they have a distinct role in determining trophoblast

lineages.(Petropoulos et al., 2016) Many of the TFs expressed in TE continue to be present in CTB, including *GATA2/3*, *TEAD4*, and *TFAP2C*. For example, previous studies in both mice and humans have shown that TEAD4 promotes TSC self-renewal and stemness by promoting cell cycle gene expression, while also silencing STB and invasive EVT differentiation associated genes.(Saha et al., 2020) Similarly, repression of the TEAD4 cofactor YAP1 revealed that it promotes self-renewal, proliferation, and stemness by regulating cell cycle- and STB-related genes.(Meinhardt et al., 2020) CDX2 is a critical TF in murine TE and is also present in human TE. However, unlike the mouse, CDX2 expression in human placental development diminishes post-implantation, and is absent in TSCs and week 6 CTBs. This raises a few questions as to whether CDX2 is actually a human trophoblast marker, if another progenitor subpopulation exists during the first trimester, or if the current hTSC media lacks the necessary components to maintain CDX2 expression.(Liu et al., 2021; Okae et al., 2018) ELF5, on the other hand, is present in both mTSCs and hTSCs, but downregulated during differentiation. Epigenetic regulation is also conserved, as the *Elf5/ELF5* promoter undergoes DNA methylation in both species.(Hemberger et al., 2010; Ng et al., 2008) In humans, MSX2 is reported to play a pivotal role in deciding placental cell fates because it was established as an important component of STB lineage repression.(Hornbachner et al., 2021) TP63 is another gene believed to be specific to the human trophoblast, with high expression observed in CTB and hTSCs. Functionally, it is considered a master regulator of trophoblasts, as it promotes self-renewal, restricts epithelial-to-mesenchymal transition, and blocks premature differentiation.(Li et al., 2014)

1.11 Embryonic stem cells and their capacity for trophoblast differentiation

There has long been interest in deriving TSC from embryonic stem cells (ESC). ESCs are derived from the pre-implantation epiblast, the pluripotent stem cells that give rise to the embryo. Upon implantation, the epiblast undergoes dramatic changes including epithelialization, increased DNA methylation, and embryonic potency gene expression profile, that prime the epiblast to rapidly respond to external differentiation cues during gastrulation to form the embryo proper. Once this occurs, the epiblast is said to transition from the ‘‘naive’’ pluripotent state to the ‘‘primed’’ pluripotent state. This is followed by gastrulation, where the epiblast differentiates, and pluripotency is lost. Unfortunately, isolation of ESCs and TSCs to study early developmental stages have proven to be very different in mice and humans. In mice, ESCs that were cultured from the blastocyst inner cell mass exhibit naive pluripotency and can differentiate into every embryonic lineage.(Nichols & Smith, 2009) Similarly, murine trophoblast stem cells (mTSCs) can be isolated from blastocysts or early post implantation embryos and can differentiate into all placental lineages.(Tanaka et al., 1998) Interestingly, mESCs are a brief developmental window artificially perpetuated in vitro, but mTSCs are actually a cell population in mouse embryos. They are found in a niche called the extra-embryonic ectoderm, which forms shortly after implantation and does not have a human counterpart.(Maltepe & Fisher, 2015; Tanaka et al., 1998; Uy et al., 2002) Reflecting their cells of origin, mESCs and mTSCs are fixed in their differentiation potential, as they only contribute to embryonic and placental lineages, respectively. Furthermore, mESCs can only be transformed to mTSCs in vitro by genetic manipulation; but the resulting cells are still not properly reprogrammed.(Cambuli et al., 2014; Niwa et al., 2005)

Since these mESCs and mTSCs do not have equivalent behaviors or even locations in human stem cells, finding human counterparts has been complicated. Using murine TSC culture

conditions to obtain hTSCs from blastocysts has been unsuccessful, with hTSC derivation only occurring in 2018 with a largely unrelated growth media.(Kunath et al., 2014; Okae et al., 2018) In contrast to the more naïve mESCs, hESCs cultured in conventional medium (with serum and fibroblast growth factor 2 [FGF2]), have an epithelial morphology, high levels of DNA methylation than naïve ESC, and a transcriptome that is closer to primed post-implantation epiblast.(Nakamura et al., 2016; Nichols & Smith, 2009) To counteract this, several formulations for culturing naive hESCs have been developed. Two of the most promising formulations, 5iLAF and t2iL + Go¨, have low DNA methylation and robust reactivation of pre-implantation genes (Takashima et al., 2014; Theunissen et al., 2014), compared to other formulations that are closer to intermediate positions on the naive-primed spectrum.(Pastor et al., 2016)

Similarly, murine and human ESCs lineage restriction that appeared to preclude conversion to trophoblast. Primed hESCs treated with BMP4 and inhibitors of Activin and FGF signaling can upregulate placental genes, but the resulting cells quickly stop dividing and differentiate. Furthermore, multiple groups have questioned whether they are fully placental, with evidence suggesting incomplete reprogramming to a placenta-like state with partial mesoderm expression patterns.(Amita et al., 2013; Lee et al., 2016; Roberts et al., 2014) Intriguingly though, naive hESCs may reflect an earlier or less fixed developmental state than mESCs. Their gene and transposon expression pattern are especially primitive, corresponding to early epiblast or even late morula.(Theunissen et al., 2016) Naive hESCs also have features typically associated with placental cells, including high TFAP2C levels and nuclear localization of YAP protein.(Pastor et al., 2018; Qin et al., 2016) In a recent paper, a subpopulation of cells in t2iL + Go¨ naive culture had a unique expression pattern compared to both naive and primed hESCs. The cell identity was not examined, but the placental markers *VGLL1*, *GATA2*, *GATA3*, and *XAGE*3 were upregulated,

while the pluripotency markers *OCT4* and *NANOG* were negative.(Messmer et al., 2019) This provided the basis for further study of hESCs cultured in naive medium to determine whether they can spontaneously differentiate to the placental lineage, described in Chapter 2 of this thesis.(Cinkornpumin et al., 2020)

1.12 Molecules and signaling pathways important for in vitro culture of placental cells

Today, a number of different conditions have been developed for 2D TSCs and 3D organoids.(Okae et al., 2018; Turco et al., 2018). Unexpectedly, each of them lack certain mouse TSC stem-cell maintenance signals, such as FGF4 and transforming growth factor-beta (TGF-b) signaling.(Tanaka et al., 1998) Instead, the first trophoblast model that established continued proliferation of human TSCs treated with epidermal growth factor (EGF), and inhibition of histone deacetylase (valproic acid), Rho associated protein kinase (Y27632), TGF-β signaling (A83-01) and glycogen synthase kinase-3 (CHIR99021).(Okae et al., 2018) The other group, Haider et al., used EGF, the TGF-β signaling inhibitor A83-01, the BMP signal inhibitor Noggin, and the activators of WNT signaling, R-spondin, CHIR99021 and prostaglandin E2, which previously established epithelial organoids from other human tissues. Both studies suggest that WNT and EGF signaling activation, as well as inhibition of the TGF-β pathway, may be sufficient for long-term expansion of human TSC cultures and placental organoids.(Haider et al., 2018)

In their work, Okae et al. 2018 isolated CTB, EVT, and STB cells from first-trimester placentas. RNA sequencing (RNA-seq) confirmed genes that were expressed in the CTB (*ITGA6* and *TP63*), EVT (HLA-G), and STB (CGB and CSH1) populations. Functional gene annotation showed CTB population possessing an overrepresentation of WNT and EGF signal transduction pathways (‘‘regulation of FZD by ubiquitination’’ and ‘‘EGFR1’’). This was significant because WNT and EGF signaling are required for proliferation of various epithelial stem cells, including

skin stem cells and intestinal stem cells.(Leng et al., 2020; Sato et al., 2009; Zhao et al., 2020) That implied that the conditions to maintain other epithelial stem cells may be the same for CTB/TSC cells. Some of the other factors that were eventually included in the culture conditions were Y27632 and CHIR99021. Y27632 is a Rho-associated protein kinase (ROCK) inhibitor that was added to all experiments because it was considered essential for cell attachment, while absence of CHIR99021led to differentiation of TSCs into HLA-G+ EVT-like cells. Enhanced proliferation of TSCs in long-term culture was also supported by the TGF-b inhibitors A83-01 and SB431542, as well as the histone deacetylase (HDAC) inhibitor valproic acid (VPA). For the EVT media, TGF-ß inhibitors promoted differentiation of TSC into EVT-like cells, with A83-01 more potent than SB431542. NRG1 and Matrigel were also included to promote epithelial-to-mesenchymal transition and produce EVT-like cells that strongly expressed HLA-G. To form STB, TSC were treated with forskolin, a cAMP agonist that generated aggregates that fused to form large syncytia. In this syncytia, STB markers CGB and *SDC1* were highly expressed, while *ITGA6*, *CDH1*, *HLA-G*, and *VIM* were minimally expressed. These cultured TSCs matched traditional criteria suggested by Lee et al. 2016 which proposed robust criteria for human trophoblast cells that included: expression of *GATA3*, *KRT7*, and *TFAP2C*, lack of HLA class I profile, hypomethylation of the ELF5 promoter, and expression of the miRNA C19MC.(Lee et al., 2016) TFAPC2 immunostaining was not performed, but TSC cells meet all other criteria, with high expression of TFAPC2 in RNA-seq for CTB cells. Upon additional analysis, it can be noted that the EVT-like cells derived from TSC likely correspond to the distal cell column for a few reasons. First, the transcriptome profiles for EVT-like cells and primary EVT isolations were very similar. Since EVT cells were primarily isolated from villous tissues, most were cell column derived. Second, the EVT-like cells that differentiated gradually lost their capacity to proliferate. Unlike the

proliferative proximal cell column, both in vivo EVT cells and early EVT cells residing in distal cell columns are non-proliferative.(Okae et al., 2018) While 2D culture of TSC has proven to recapture some aspect of in vivo placentation, others have tried to generate 3D organoids to further uncover alternative mechanisms of expansion and differentiation.

In the first of two trophoblast organoid papers in 2018, Turco et al. produced organoids based on media containing EGF, FGF2, CHIR99021 (a WNT activator), A83-01 (a TGFβ and SMAD inhibitor) and R-spondin 1. They were isolated similarly to Okae et al. 2018 by enzymatically digesting first trimester placentas and enriching for a proliferative trophoblast marker; in this case EPCAM was used. Their identity as trophoblasts was also confirmed using the Lee et al. 2016 criteria, with the trophoblast organoids self-organizing into matching components of placental villus (although inverted, with STB found on the inside of organoids), staining for EPCAM and CDH1, and expressing Ki67 and TP63 similar to villus in vivo. Structurally, the basement membrane was in contact with Matrigel on the outside of the organoid, so the syncytia lined the central cavity. In EVT differentiation media, HLA-G+ cells migrated from the organoid, formed tracks in the digested Matrigel, and eventually adhered to the plastic of the culture tray.(Turco et al., 2018) Haider et al. 2018 utilized a similar CTB/TSC media condition to Okae et al. 2018 and Turco et al. 2018 to generate human trophoblast organoids. In their paper, WNT signaling was confirmed to maintain stemness and proliferation of trophoblast organoid culture systems. In their WNT negative condition, they saw decreased expression of the WNT stem cell receptor *LGR5* and the CTB self-renewal markers *ELF5*, *TEAD4*, *CDX2*, and *TP63*. In contrast, the EVT markers *HLA-G*, *NOTCH2*, *PRG2*, and *ERBB2* were activated without WNT activators. The STB markers *ENDOU* and *CGB* were also decreased during the differentiation of the EVT linage. Notably, the critical EVT progenitor regulator of formation and survival, NOTCH1, was

observed in the cell column.(Haider et al., 2016) Of all these novel culture conditions, the expression patterns of trophoblast subtypes was similar in 2D and both trophoblast organoids to its in vivo culture equivalent.(Haider et al., 2018)

1.13 Oxygen conditions and regulation during placentation processes

In placental development, many factors can govern trophoblast cell differentiation. One of the factors that control this process is hypoxia, a condition of severe low O_2 levels, which promotes CTB proliferation and TP63 expression via HIF-1α and HIF-1β in a similar fashion to the low oxygen of the fallopian tube and uterine cavity during placentation.(Jiang et al., 2000; Wang et al., 2022b) Since the placenta grows significantly during a period of relative hypoxia, this is an essential component of understanding placental development. As was previously mentioned, an important event during early gestation is the exposure of the blastocyst to severe hypoxia (as low as 2–3% O_2 and PO_2 of 15-20 mm Hg) in the uterus.(Ottosen et al., 2006) After implantation, the trophoblast population expands and EVTs begin to invade the wall of uterine spiral arteries. These vessels become plugged by EVT subtypes, which prevents maternal blood from entering the intervillous space. This results in the maintenance of a severe hypoxic microenvironment that can persist up to week 12 of pregnancy.(Burton et al., 2021) Hypoxic conditions are not necessarily harmful to certain cell types, though, and sometimes can even be beneficial or protective. Several mouse studies suggest that embryonic cells only require low levels of O_2, often referred to as "quiet metabolism." This limits potentially harmful reactive oxygen species (ROS) production and protects the embryo from teratogenesis mediated by free radicals.(Jauniaux et al., 2003) The rise in O_2 levels within the placenta and embryonic compartments to "normal" physiologic levels of 8–10%, when the plugs dissolve at the end of the first trimester (Rodesch et al., 1992) importantly overlaps with the end of organogenesis. At this stage of fetal development, oxygen levels are no

longer low and the risk of teratogenesis therefore decreases since the development of major organs is complete.(Zhao et al., 2021)

While maintaining the CTB stem-cell state under hypoxic conditions is well established, early EVT differentiation is also reliant on low O_2 levels. Early in the first trimester, when local O_2 levels are 2–3%, invasive EVTs begin to differentiate from CTBs in the cytotrophoblast shell. During this transition from an epithelial to a mesenchymal phenotype, EVTs lose CTB cell surface marker expression of TP63 and EGFR while gaining HLA-G.(Li et al., 2014) The production of EVTs when culturing first trimester human villous explants was surprisingly found to be triggered only after exposure to 2–3% O_2, but not at 20% O_2. As they migrate to the decidua, where the O_2 levels are higher, their phenotype begins to change as they mature. This suggests that EVT differentiation begins under low O_2 levels, then matures under relatively higher O_2 conditions.(Treissman et al., 2020) This was confirmed in primary culture, as first trimester explants cultured in low oxygen (<3% O_2) develop 'outgrowths' that are positive for HLA-G and ITGA5 (markers of early distal CCTs).(Chang et al., 2018) Comparatively, differentiation of multinucleated STBs from mononuclear CTBs occurs in a relatively high O_2 microenvironment. In this study, O_2 levels of 19% in trophoblasts cultured in vivo promoted spontaneous CTB cell fusion into STBs, while O_2 levels around 9% resulted in reduced cell fusion and decreased secretion of STB hormones.(Alsat et al., 1996) Notably, the hypoxic conditions responsible for inhibition of STB differentiation in the first trimester is partially reliant on a functional HIF complex.(Wakeland et al., 2017) These finding show O_2 condition during development has an overwhelming effect on the function and formation of the placenta.

1.14 Transcriptional regulation of trophoblast stem cell and downstream lineages

There are also many TFs considered to be essential for the regulation of trophoblast development, which in turn would indicate their potential as markers to predict gestational disease such as PE and IUGR. To find these genes, scientists attempt to look for master regulators of the EVT and STB lineages and then determine what happens when they are dysregulated. One of the genes, mentioned previously, that is considered a potential regulator of both lineages is GCM1.(Wang et al., 2022b) In a 2009 study, experiments in first trimester floating villous explants showed that increasing or decreasing GCM1 expression changed CTB number and proliferation, formation of STB, and the differentiation from CTB to EVT. Ry reducing GCM1 expression, proliferating CTBs accumulated, while overlying STB degenerated due to absence of syncytial fusion. Comparatively, addition of forskolin had the opposite effect when GCM1 expression increased. Similarly, the downregulation of GCM1 inhibits CTB to EVT differentiation. Therefore, this suggests that GCM1 expression is critical for maintaining a balance between CTB proliferation and differentiation of the EVT and STB lineages in the first trimester.(Baczyk et al., 2009)

Since hypoxia and GCM1 regulation are believed to be linked to different aspects of trophoblast maintenance and differentiation, a variety of molecular mechanisms associated with hypoxia have been studied for their connection to GCM1 regulation. One of the first aspects studied was the effect of HIF on GCM1 gene expression, but no direct effect of HIF1 on GCM1 gene expression was detected.(Chiang et al., 2009) Hypoxia does, however, suppress GCM1 activity at both transcriptional and post-translational levels by increasing degradation of GCM1. Although the hypoxic mechanism responsible for controlling activation and inhibition of the pathways is unknown, there are some pathways that have been found to play a role in regulating the increase and decrease of GCM1 activity in the placenta. In primary trophoblasts and placental cell lines, for example, hypoxia inhibits the PI3K-Akt signaling pathway, which is an important

pathway for regulating trophoblast proliferation, differentiation, migration, and invasion.(Chen et al., 2019) One of the observed effects of PI3K-Akt inhibition by hypoxia is the increase in activated GSK-3β. This is one of the regulatory mechanisms of GCM1 because activated GSK-3β phosphorylates the residue Ser^{322} in GCM1, which is a known mechanism that promotes GCM1 degradation.(Chiang et al., 2009) To balance GCM1 expression in the placenta, a counteracting factor is the activation of cAMP-PKA signaling. This will eventually lead to recruitment of DUSP23, which dephosphorylates the Ser^{322} residue and increases GCM1 expression.(Lin et al., 2011) In addition to TFs that regulate GCM1, there are multiple genes that have been observed to interact with GCM1 to control the differentiation of CTBs in both EVTs and STBs.

GCM1 expression has been observed across the surface of primary villi in differentiated EVT and STB, but not in CTB and at the base of columns. GCM1 mRNA expression was observed in proximal cell columns as well (Baczyk et al., 2004), with a gradient-like expression pattern of GCM1 across differentiating cells. One mechanism controlling levels of CTB differentiation is opposing roles between an isoform of TP63, ΔNp63α, and GCM1 regulated CTBs, in which ΔNp63α maintained stemness while GCM1 promoted differentiation. Staining showed that cell column trophoblasts co-express ΔNp63α and GCM1 in first trimester placenta or in the STB layer of term placenta. These double positive cells were believed to be cells transitioning from CTB ΔNp63α+ cells to differentiated GCM1+ EVTs or STBs. By indirectly decreasing GCM1 activity through GATA3, which was previously shown to interact with and inhibit GCM1 (Chiu & Chen, 2016), ΔNp63α suppresses trophoblast differentiation promoted by GCM1. The roles are then reversed upon cAMP activation of GCM1, which induces hCGβ, HTRA4, and SYN1 gene expression for STB differentiation, as well as inhibiting *ΔNp63α* expression and CTB-associated genes *ELF5*, *TEAD4*, and *EpCAM*.(Wang et al., 2022b)

While GCM1 is known to target and regulate fusion genes, there are also many other upstream and maintenance pathways that it is associated with. For example, cell cycle exit and trophoblast fusion are dependent on the interaction of p21 and GCM1 with the Syncytin-2 gene promoter binding site.(Lu et al., 2017) Upstream of GCM1 is the conserved TF peroxisome proliferator-activated receptor gamma (PPARγ), which is implicated in STB syncytialization by promoting transcription of the STB-related genes *GCM1* and *SYNCYTIN-1*.(Armistead et al., 2021; Ruebner et al., 2012) Another signaling pathway that potentially regulates GCM1 is the classic Wnt/B-catenin pathway. Specifically, one study reports that β-catenin/BCL9-Like (BCL9L)/T-cell factor 4 (TCF4) directly targets GCM1 and synctin.(Matsuura et al., 2011) In another study, GCM1 was found to activate FZD5 expression, which helped maintain GCM1 expression during trophoblast differentiation into syncytiotrophoblasts in combination with ß-catenin signaling.(Lu et al., 2013)

As indicated before, GCM1 is a known master regulator of STB formation, but it is also believed to be involved in EVT cell fate regulation.(Wang et al., 2022b) One of the early mechanisms believed to promote EVT invasion was GCM1 stimulation of HTRA4, which is a serine protease involved in fibronectin cleavage.(Wang et al., 2012) Results from Manilla et al. 2021, however, contradict the HTRA4 findings by demonstrating that HTRA4 likely promotes syncytialization instead of suppressing cell fusion, as was suggested by Wang et al. 2012. They believe a strong reason for this discrepancy is due to the difference of cell model and experimental approach used. Wang et al. 2012 studied the effect of HTRA4 on cell fusion using HEK293T cells, which is a human embryonic kidney derived cell line. This is important because HEK293T cells do not represent trophoblasts, do not naturally undergo syncytialization, nor do they express any established syncytialization markers or even naturally express HTRA4. All of this calls into

question whether the interaction between GCM1 and HTRA4 is involved in regulation of EVT lineage differentiation.(Mansilla et al., 2021) In another study, *ASCL2* was observed to be strongly downregulated in EVTs with GCM1 knocked down. This is important because some studies have shown that ASCL2 is present in some CTB populations and proliferative CCT, but its absence was reported to impair the differentiation from TSC to EVT.(Varberg et al., 2021) Using a chromatin immunoprecipitation (ChIP) and quantitative PCR, GCM1 was shown to bind to the *ASCL2* promoter. That suggested that GCM1 binds upstream of *ASCL2* and drives *ASCL2* expression during EVT differentiation. Since WNT signaling was also identified as a highly upregulated term in GCM1 KD EVTs, GCM1 potentially promoted EVT formation by inhibiting WNT signaling. This inhibition of WNT was accomplished, at least in part, by stimulating NOTUM expression to repress WNT/β-catenin signaling.(Jeyarajah et al., 2022) Overall, while these observations suggest a multifaceted for GCM1 in STB and EVT formation function, there is still much to be discovered.

1.15 Rationale and objectives of research proposal

Since CTB can be cultured in vitro as hTSC and directly differentiated to EVT and STB, these cells can be used to model and study gene regulation as the developing embryo makes early cell-fate decisions. For this thesis, we conducted two interrelated projects to study specification of trophoblast as well as transcriptional regulation of hTSC, EVT, and STB.

Conventionally cultured "primed" hESC are similar to committed epiblast cells in vivo and are able to differentiate into cells of all three germ layers. However, primed hESC cannot be converted efficiently to trophoblast. In **Chapter 1**, we reasoned that since specially cultured "naive" hESCs transcriptionally and epigenetically resemble preimplantation epiblast, these cells might have improved ability to convert to trophoblast. This would establish a system for studying trophoblast specification, the first specification event in embryonic development.

In **Chapter 2**, ambient oxygen supply dynamically changes from ~2-3% O_2 during the 1st trimester to ~8-10% O_2 upon migration trophoblast cells and remodeling of the decidua in the 2nd trimester of placentation. Since these changes coincide with major developmental changes, potential regulators of trophoblast lineage specification might be altered by oxygen tension that we seek to uncover.

CHAPTER 2: Naive Human Embryonic Stem Cells Can Give Rise to Cells with a Trophoblast-like Transcriptome and Methylome

(Stem Cell Reports, https://doi.org/10.1016/j.stemcr.2020.06.003)

Jessica K. Cinkornpumin[1], Sin Young Kwon[1], Yixin Guo[4], Ishtiaque Hossain[1], Jacinthe Sirois[1,2], Colleen S. Russett[1], Hsin-Wei Tseng[1], Hiroaki Okae[5], Takahiro Arima[5], Thomas F. Duchaine[1,2], Wanlu Liu[3,4], and William A. Pastor[1,2] *

[1]Department of Biochemistry, McGill University, Montreal, QC H3G 1Y6, Canada. [2]The Rosalind & Morris Goodman Cancer Research Centre, McGill University, Montreal, QC H3A 1A3, Canada. [3]Department of Orthopedic of the Second Affiliated Hospital of Zhejiang University School of Medicine, Zhejiang University, Hangzhou 310029, China. [4]Zhejiang University-University of Edinburgh Institute (ZJU-UoE Institute), Zhejiang University School of Medicine, International Campus, Zhejiang University, 718 East Haizhou Road, Haining 314400, China. [5]Department of Informative Genetics, Environment and Genome Research Centre, Tohoku University Graduate School of Medicine, Sendai 980-8575, Japan
*Correspondence: william.pastor@mcgill.ca

2.1 Abstract

Human embryonic stem cells (hESCs) readily differentiate to somatic or germ lineages but have impaired ability to form extra-embryonic lineages such as placenta or yolk sac. Here, we demonstrate that naive hESCs can be converted into cells that exhibit the cellular and molecular phenotypes of human trophoblast stem cells (hTSCs) derived from human placenta or blastocyst. The resulting ‘‘transdifferentiated’’ hTSCs show reactivation of core placental genes, acquisition of a placenta-like methylome, and the ability to differentiate to extravillous trophoblasts and syncytiotrophoblasts. Modest differences are observed between transdifferentiated and placental hTSCs, most notably in the expression of certain imprinted loci. These results suggest that naive hESCs can differentiate to extra-embryonic lineage and demonstrate a new way of modeling human trophoblast specification and placental methylome establishment.

Keywords: *DNA methylation; amnion; development; differentiation; embryonic stem cells; epigenetics; placenta; pluripotency; trophoblast.*

2.2 Introduction

In most mammals, the first cellular specification event is believed to be acquisition of placental or non-placental identity.(Pfeffer, 2018) Distinct polarized outer and apolar inner cell populations form during the morula phase of development. In the subsequent blastocyst stage, the outer cells give rise to the trophoblast lineage and later form most cells in the placenta. The inner cells give rise to the inner cell mass, which specifies both the hypoblast and pluripotent epiblast. The epiblast generates all embryonic tissues (ectoderm, mesoderm, and endoderm) of the organism. The observations above have been demonstrated by lineage tracing, blastomere transplantation, and chimera experiments in mice.(Chazaud & Yamanaka, 2016) On the basis of observation, immunofluorescent staining, and RNA sequencing (RNA-seq), it is likely that human development follows a similar pattern.(Niakan & Eggan, 2013; Stirparo et al., 2018)

After implantation of the blastocyst into the uterine wall, the trophoblast lineage develops rapidly. Structures called villus sprout and expand. Cytotrophoblasts (CTBs), a population of epithelial cells within the villus, fuse to form syncytiotrophoblasts (STBs), large multinucleated cells that line the surface of the villus, secrete pregnancy hormones, and mediate gas and nutrient exchange with maternal blood. At the tips of villus that contact maternal tissue, CTBs undergo epithelial to mesenchymal transition and differentiate into extravillous trophoblasts (EVTs). EVTs invade maternal tissue, expand and anchor the villus, and remodel maternal arterioles.(Maltepe & Fisher, 2015)

Meanwhile, the epiblast undergoes a series of changes, including epithelialization, increased DNA methylation, and expression of a new set of genes and cell surface receptors. These changes prime the epiblast to differentiate rapidly in response to external cues during subsequent gastrulation. As such, the epiblast is said to transition from the ‘‘naive’’ pluripotent state to the

‘‘primed’’ pluripotent state.(Nichols & Smith, 2009) Upon gastrulation, the epiblast differentiates, and pluripotency is lost.

Stem cells have been used to study these developmental stages in mice and humans. In mice, embryonic stem cells (ESCs) can be cultured from the blastocyst inner cell mass, exhibit naive pluripotency, and can be differentiated into all embryonic lineages.(Nichols & Smith, 2009) Likewise, murine trophoblast stem cells (mTSCs) can be isolated from blastocysts or early post-implantation embryos and can form all placental lineages.(Tanaka et al., 1998) Unlike ESCs, which reflect a brief developmental window artificially perpetuated in vitro, mTSCs are actually present in mouse embryos. Their niche is a structure called the extra-embryonic ectoderm, which forms shortly after implantation and lacks a human counterpart.(Maltepe & Fisher, 2015; Tanaka et al., 1998; Uy et al., 2002) Reflecting their cells of origin, mESCs and mTSCs are fixed in their specifications. In chimera assays, mESCs and mTSCs contribute only to embryonic and placental lineage, respectively. mESCs cannot be converted to mTSCs in vitro except by genetic manipulation (Niwa et al., 2005), and even then the resulting cells are incompletely reprogrammed.(Cambuli et al., 2014)

Finding human counterparts for these stem cells has proven to be more complicated, and their behavior has not always matched that of the murine counterpart. As with mice, human ESCs (hESCs) can be isolated from preimplantation blastocysts.(Thomson et al., 1998) However, in conventional medium (with serum and fibroblast growth factor 2 [FGF2]), hESCs have an epithelial morphology, high levels of DNA methylation, and a transcriptome resembling primed post-implantation epiblast.(Nakamura et al., 2016; Nichols & Smith, 2009) Several formulations for culturing naive hESCs have been developed. Two formulations, 5iLAF (Theunissen et al., 2014) and t2iL + Go¨ (Takashima et al., 2014), show low DNA methylation and strong reactivation

of pre-implantation genes, while other formulations show intermediate positions on the naive-primed spectrum.(Pastor et al., 2016)

Efforts to obtain human trophoblast stem cells (hTSCs) from blastocysts using culture conditions analogous to murine TSCs have not been successful.(Kunath et al., 2014) Primed hESCs treated with BMP4 and inhibitors of Activin and FGF signaling upregulate placental genes.(Amita et al., 2013) However, the resulting cells differentiate and quickly stop dividing. Furthermore, there is argument as to whether they more closely resemble placenta or mesoderm (Roberts et al., 2014), with some evidence suggesting partial but incomplete reprogramming to a placenta-like state.(Lee et al., 2016) Recently, hTSCs were successfully derived from first-trimester placental villi and pre-implantation blastocysts.(Okae et al., 2018) Self-renewing placental organ cultures have also been derived from first trimester placenta.(Haider et al., 2018; Okae et al., 2018) hTSCs are clearly placental, have a very long or indefinite replicative life, and can differentiate to EVTs and STBs. hTSCs are epithelial cells and share key surface markers with villous CTBs. It remains unclear whether hTSCs are simply CTBs successfully adapted to in vitro culture or if they represent a CTB subpopulation or precursor.

Intriguingly, naive hESCs may reflect an earlier or less fixed developmental state than mESCs. Their pattern of gene and transposon expression is especially primitive, corresponding to early epiblast or even late morula(Theunissen et al., 2016). Naive hESCs show some features typically associated with placental cells, including high TFAP2C levels (Pastor et al., 2018) and nuclear localization of YAP protein.(Qin et al., 2016) A recent paper reported the existence of a subpopulation of cells in t2iL + Go¨ naive culture that had an expression pattern dissimilar from both naive and primed hESCs.(Messmer et al., 2019) The identity of these cells was not determined, but they show upregulated expression of placental markers, such as VGLL1, GATA2,

GATA3, and XAGE3, and are negative for the pluripotency markers OCT4 and NANOG. Thus, even hESCs cultured in naive medium may undergo spontaneous differentiation to placental lineage.

We sought to determine whether naive hESCs can differentiate to the trophoblast lineage and form hTSCs. In addition to helping us understand the nature of naive human pluripotency, such a capability would allow generation of hTSC lines from existing hESC lines and could potentially be used to model human placental specification.

2.3 Results

2.3.1 Similarity of hTSCs to Stem Cells in First-Trimester Placenta

To compare hTSCs and cells differentiated in vitro with primary placental cells, we conducted principal-component analysis (PCA) of published RNA-seq data from hTSCs and primary placental cell types.(Okae et al., 2018) hTSCs clustered closer to CTBs than to differentiated EVTs and STBs, with in-vitro-differentiated cells positioned relatively close to their isolated in vivo counterparts (Figure S1A). Yet, there was still considerable distance between hTSCs and CTBs. While this may partially reflect adaptation to in vitro culture, we considered that hTSCs may represent a distinct subpopulation of CTBs.

A recent report described a subpopulation of proliferative cells at the base of the CTB cell column in first-trimester placental villi.(Lee et al., 2018) These cells appear to give rise to EVTs and STBs and may be the core stem cell population in first-trimester placenta. These cells upregulate a number of genes relative to both CTBs and EVTs, and are distinguished by the surface markers ITGA2 and EpCAM.(Lee et al., 2018) Interestingly, hTSCs express far higher levels of ITGA2 and EPCAM than bulk CTBs (Figure 1A). Furthermore, genes identified as upregulated in

these primary ITGA2+ EpCAM+ cells are expressed at globally higher levels in hTSCs than CTBs or differentiated placental cells (Figure 1B). We confirmed by flow cytometry that hTSCs are strongly positive for ITGA2 and EpCAM and downregulate expression of these genes upon differentiation (Figures 1C, 1D, and S1B). Together, these data suggest that hTSCs may correspond to a real reported stem cell population in placenta and may explain some of the modest divergence observed between CTBs and hTSCs. Also, although neither marker is specific to placenta, ITGA2 and EpCAM may be used to sort hTSCs from heterogeneous populations.

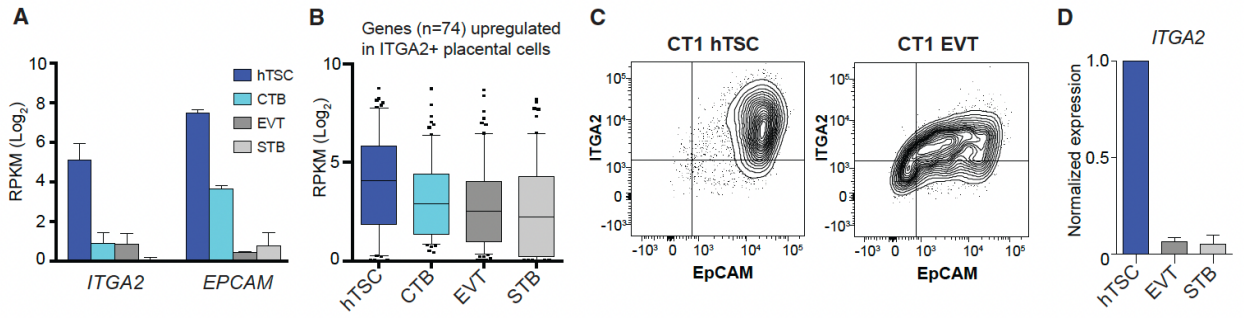

Figure 1. Similarity of hTSCs to reported ITGA2+ EpCAM+ Progenitor Population. (A) Expression of ITGA2 and EPCAM in hTSCs and primary placenta cells. Data are taken from Okae et al. (2018), with n = 3–4 independent experiments per cell type. (B) Seventy-four genes were identified as upregulated in ITGA2+ cells by Lee et al. (2018) and also present in Okae et al.'s RNA-seq dataset. The expression of these genes is plotted using RNA-seq data from Okae et al., with each gene represented as a single point in the boxplot. **(**C) Flow cytometry plot of ITGA2 and EpCAM in CT1 hTSCs and EVT. Representative of n = 5 independent experiments. (D) Downregulation of ITGA2 upon directed differentiation of CT1 (qRT-PCR, mean + SE of n= 2 independent experiments).

2.3.2 Transdifferentiation of Naive hESCs to Putative hTSCs

To determine whether naive hESCs could be converted to placental lineage, we used an established reporter line (WIBR3 OCT4-ΔPE-GFP) that expresses GFP only upon acquisition of naive pluripotency.(Theunissen et al., 2014) We treated the cells with a rapid naive induction

protocol that entails culture with PXGL media (Guo et al., 2017), an improved version of the well-established t2iL + Gö naive media.(Takashima et al., 2014) We observed GFP^{+} colonies with dome-shaped naive morphology (Figures 2A and 2B) and strong upregulation of naive markers (Figure S2A). Ten days after the start of reversion, we plated the hESCs directly into hTSC medium. Although a mixed population of cells formed, within 4 days of transition we observed colonies of epithelial cells that resembled hTSCs (Figure 2C) and stained strongly positive for the pan-placental markers KRT7 and TFAP2C and the CTB marker TEAD4 (Figure 2D). After 11 days of culture in hTSC medium, we sorted a pure population of putative hTSCs using the surface marker profile $ITGA2^{hi}$ $EpCAM^{hi}$ $ITGA1^{lo}$ (Figure 2E). ITGA2 and EpCAM were chosen on the basis of the observations above, and ITGA1 was selected against because it is expressed on differentiated placental cells (Nagamatsu et al., 2004) but is low in hTSCs (Figures 2E and S2B). We also stained for HLA-G to gate against differentiated $HLA\text{-}G^{hi}$ cells, although we eventually ceased use of this marker because it was less sensitive than ITGA1. The resulting transdifferentiated hTSC (tdhTSC) line (termed WIBR3-tdhTSC line 1) was morphologically indistinguishable from hTSCs of placental origin (Figure 2F) and had similar surface marker expression (Figure S2C). To rule out the possibility of contamination with placental hTSCs, we conducted short tandem repeat (STR) analysis and confirmed that WIBR3-tdhTSC L1 has the same genetic markers as the starting WIBR3 hESCs (Table S1). A list of all transdifferentiations conducted and cell lines generated in this paper are included in Table S2.

As discussed in the introduction, there is evidence that a very small proportion of cells in t2iL + Gö steady-state culture may already express placental markers, and it is possible that some cells in naive culture conditions have not fully attained naive state. To establish that genuine naive hESCs, rather than a side population, are what give rise to tdhTSCs, we sorted GFP^{hi} and

GFP^{lo} WIBR3 OCT4-ΔPE-GFP naive-cultured cells into hTSC medium (Figure 2G). The GFP^{hi} hESCs (true naive) gave rise to ITGA2^{+} EpCAM^{+} cells with far higher efficiency, as demonstrated by fluorescence-activated cell sorting (FACS) 16 days later (Figure 2H). ITGA2^{hi} EpCAM^{hi} ITGA1^{lo} cells were sorted to give rise to an additional line, WIBR3 tdhTSC line 2 (Figures 2H and S2D). The GFP^{lo} hESCs by contrast gave rise to very few ITGA2^{+} EpCAM^{+} cells (Figure 2H).

We also reverted and transdifferentiated a second embryonic stem cell line, UCLA1 (Diaz Perez et al., 2012), via the same strategy (Figures S2E and S2F). All lines generated showed uniform staining for KRT7, TFAP2C, and TEAD4 (Figure 2I).

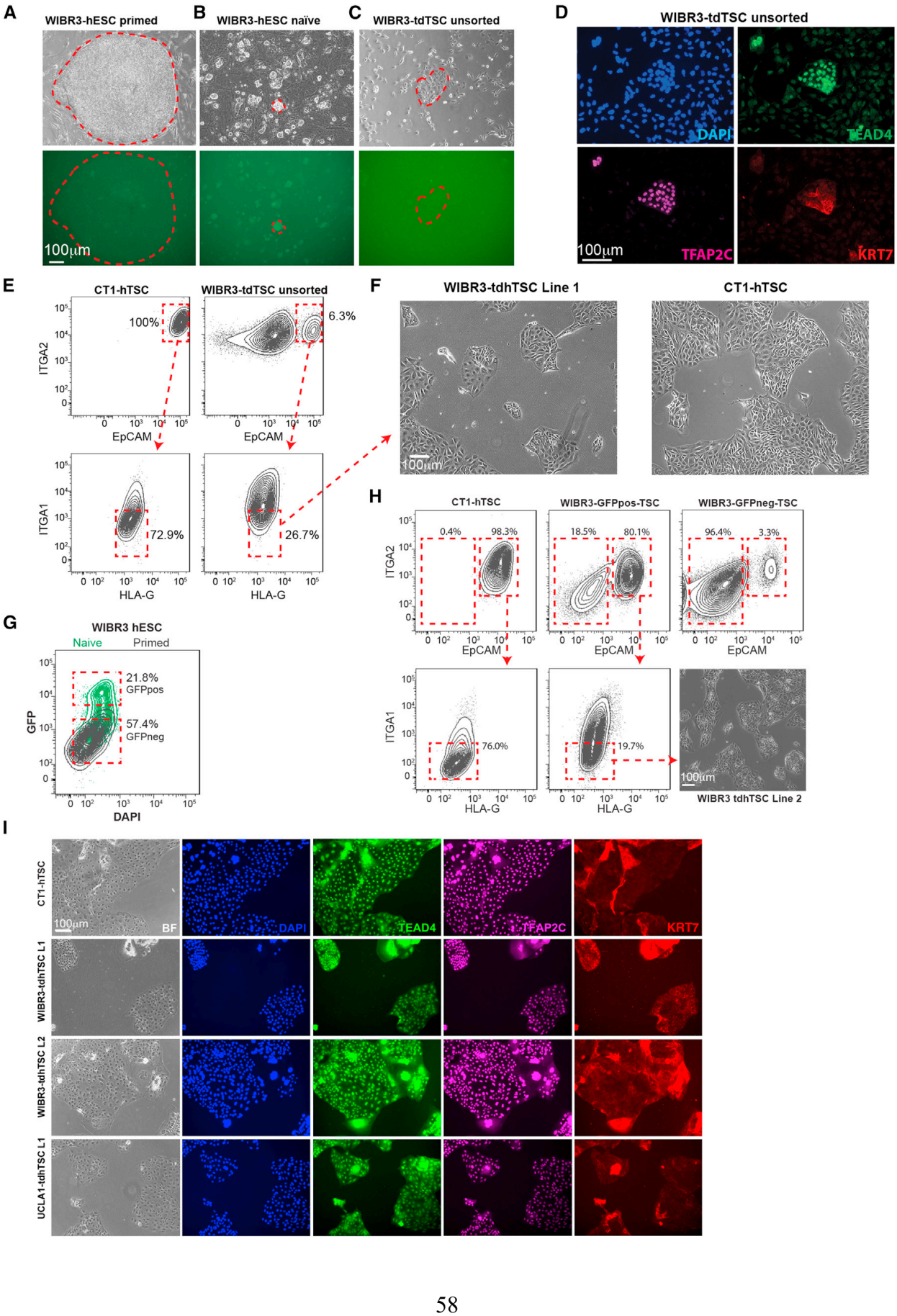
A
WIBR3-hESC primed
B
WIBR3-hESC naïve
C
WIBR3-tdTSC unsorted
100μm
D
WIBR3-tdTSC unsorted
DAPI
TEAD4
TFAP2C
KRT7
100μm
E
CT1-hTSC
WIBR3-tdTSC unsorted
100%
6.3%
ITGA2
EpCAM
ITGA1
72.9%
26.7%
HLA-G
F
WIBR3-tdhTSC Line 1
CT1-hTSC
100μm
G
WIBR3 hESC
Naive
Primed
21.8%
GFPpos
57.4%
GFPneg
GFP
DAPI
H
CT1-hTSC
WIBR3-GFPpos-TSC
WIBR3-GFPneg-TSC
0.4%
98.3%
18.5%
80.1%
96.4%
3.3%
ITGA2
EpCAM
ITGA1
76.0%
19.7%
HLA-G
100μm
WIBR3 tdhTSC Line 2
I
CT1-hTSC
WIBR3-tdhTSC L1
WIBR3-tdhTSC L2
UCLA1-tdhTSC L1
100μm
BF
DAPI
TEAD4
TFAP2C
KRT7

Figure 2. Transdifferentiation of hESCs to Putative hTSCs and Purification via FACS Sorting. (A) Upper panel: light microscopy image of a colony of primed WIBR3 OCT4-DPE-GFP hESCs, with the colony circled with a dashed line. Lower panel: lack of GFP signal. (B) Light and fluorescent image of WIBR3 OCT4-DPE-GFP hESCs after 10 days of naive reversion. Many GFP+ colonies are present, with one representative colony circled. (C) Naive hESCs after 4 days of culture in hTSC medium. Note the presence of a colony of epithelial cells and the loss of GFP signal. (D) Immunofluorescent image of WIBR hESCs after 10 days in hTSC medium. Note a distinct population of TFAP2C+ TEAD4+ KRT7+ cells. (E) FACS of WIBR3 hESCs grown in hTSC medium for 11 days and comparison CT1 hTSCs. Note distinct population of $ITGA2^{hi}$ $EpCAM^{hi}$ cells which was sorted to produce WIBR3 tdhTSC line 1. (F) Light microscopy of CT1 and WIBR3 tdhTSC line 1. (G) Flow cytometry of WIBR3 OCT4-DPE-GFP hESCs in naive (green) and primed (black) conditions are overlaid. GFPhi and GFPlo cells from naive culture, populations indicated with boxes, were sorted into hTSC medium. (H) Flow cytometry of GFP^{hi} and GFP^{lo} cells after 16 days in hTSC medium. Note much higher $EpCAM^{hi}$ $ITGA2^{hi}$ population in the GFP^{hi} population. (I) Immunofluorescent staining for hTSC/CTB (TEAD4) and pan-placental (TFAP2C, KRT7) markers in lines indicated. Representative of n = 2 independent experiments.

2.3.3 Validation of Putative Transdifferentiated hTSCs

To confirm placenta-like identity of the putative tdhTSCs, we conducted RNA-seq of the starting hESC lines, tdhTSCs, and control placental (CT1, CT3) and blastocyst-derived (BT2) hTSCs. As a further comparison, we sequenced RNA from two epithelial cell lines: FT190-transformed fallopian tube epithelium and Hec116 endometrial carcinoma. A full list of samples and mapping statistics is in Table S3, with gene expression levels in Table S4.

Appropriately, tdhTSCs show dramatically reduced expression of core pluripotency transcription factors and gain of established placental markers and CTB/hTSC genes (Figures 3A and 3B). Minimal expression of amnion or somatic differentiation markers was observed. PCA of gene expression data showed three clear clusters: hESCs, hTSCs, and tdhTSCs, and non-placental epithelial lines (Figure 3C), with tdhTSCs intermingled with genuine hTSCs.

Classifying cells as placental on the basis of expression of a small number of markers is controversial.(Roberts et al., 2014) Classic pan-placental markers, such as TFAP2C, GATA3, and KRT7 are expressed in many non-placental tissues, as are the hTSC/CTB genes ELF5, TP63, and TEAD4.(Uhlén et al., 2015) Even the pregnancy hormone hCG is produced in pituitary cells.(Chen et al., 1976) Therefore, we used a non-biased approach to identify genes expected to show increased expression in placenta. We analyzed gene expression data from early primate embryogenesis (Nakamura et al., 2016) and identified 107 genes specific to trophoblast as compared with epiblast, hypoblast, and gastrulating cells, 89 of which were expressed (reads per kilobase of transcript per million mapped reads [RPKM] > 1) in at least one of our RNA-seq samples (Table S5). As predicted, hTSCs show dramatically higher expression of these trophoblast-specific genes than do pluripotent or epithelial cells (Figure 3D). Crucially, tdhTSC lines express trophoblast genes at levels similar to hTSCs of placental origin.

Moreover, the tdhTSCs show other classic hallmarks of placental identity.(Lee et al., 2016) They exhibit high expression of microRNAs generated from the Chromosome 19 microRNA cluster (C19MC) (Figure S3A), demethylation of the *ELF5* promoter (Figure S3B), and reduced staining with pan-HLA antibody relative to non-placental epithelial cell lines (Figure S3C). They were also capable of directed differentiation to STB lineage, upregulating STB markers and secreting large quantities of hCG (Figures 4A, 4B, S4A, and S4C). Differentiation of WIBR3 tdhTSCs to EVT lineage resulted in spindle-shaped morphology, gain of the EVT markers ITGA1 and HLA-G, and upregulation of EVT genes (Figures 4A, 4C, S4B, and S4C). UCLA1 tdhTSC L1 show impaired differentiation to mature EVTs (Figure 4A and data not shown), although so do some blastocyst-derived hTSC lines.(Okae et al., 2018)

Combined, these results demonstrate similarity of tdhTSCs to genuine hTSCs.

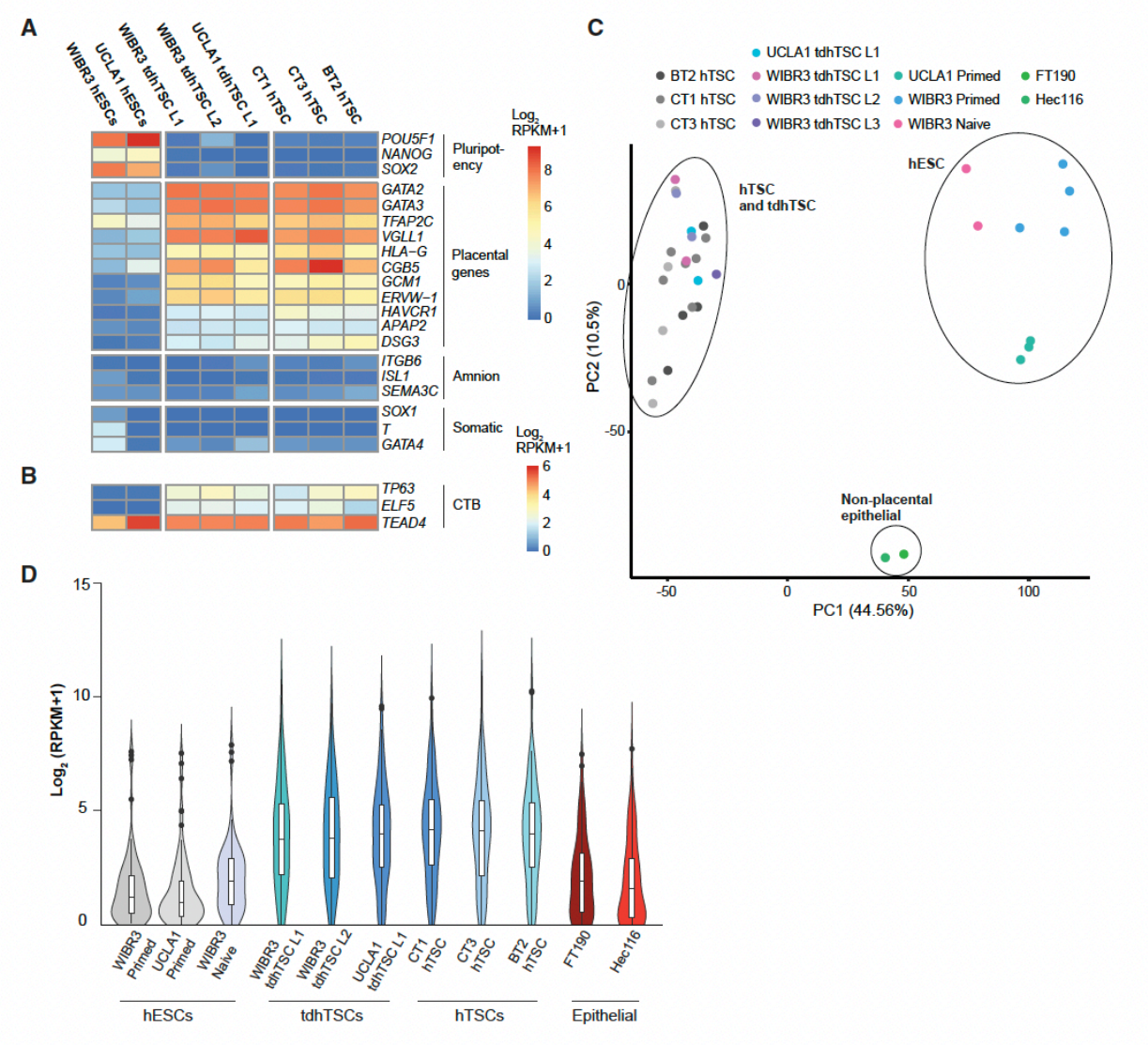

Figure 3. Validation that Transdifferentiated hTSCs Express Placental Genes. (A) Gene expression of indicated markers in each sample type are indicated by coloration. Expression from replicates of each sample type are averaged. n = 2 (all tdhTSC lines), n = 3 (UCLA1 hESC), n = 4 (WIBR3 hESCs, CT3, BT2), n = 7 (CT1) biological replicates. (B) Same as (A) except with a different color scale. (C) Principal-component analysis for gene expression of the lines indicated. Each dot is one biological replicate. (D) Expression of 89 trophoblast-specific genes, as identified by analysis of pre-implantation primate embryos (Nakamura et al., 2016), is indicated for each cell type. Expression of each gene, using an average of all replicates for a given cell type, is indicated as a single point on the violin plot. Box indicates 25th, 50th, and 75th percentiles. n = 1 (epithelial cell), n = 2 (all tdhTSC lines, naive hESCs), n = 3 (UCLA1 hESCs), n = 4 (WIBR3 hESCs, CT3, BT2), n = 7 (CT1) biological replicates.

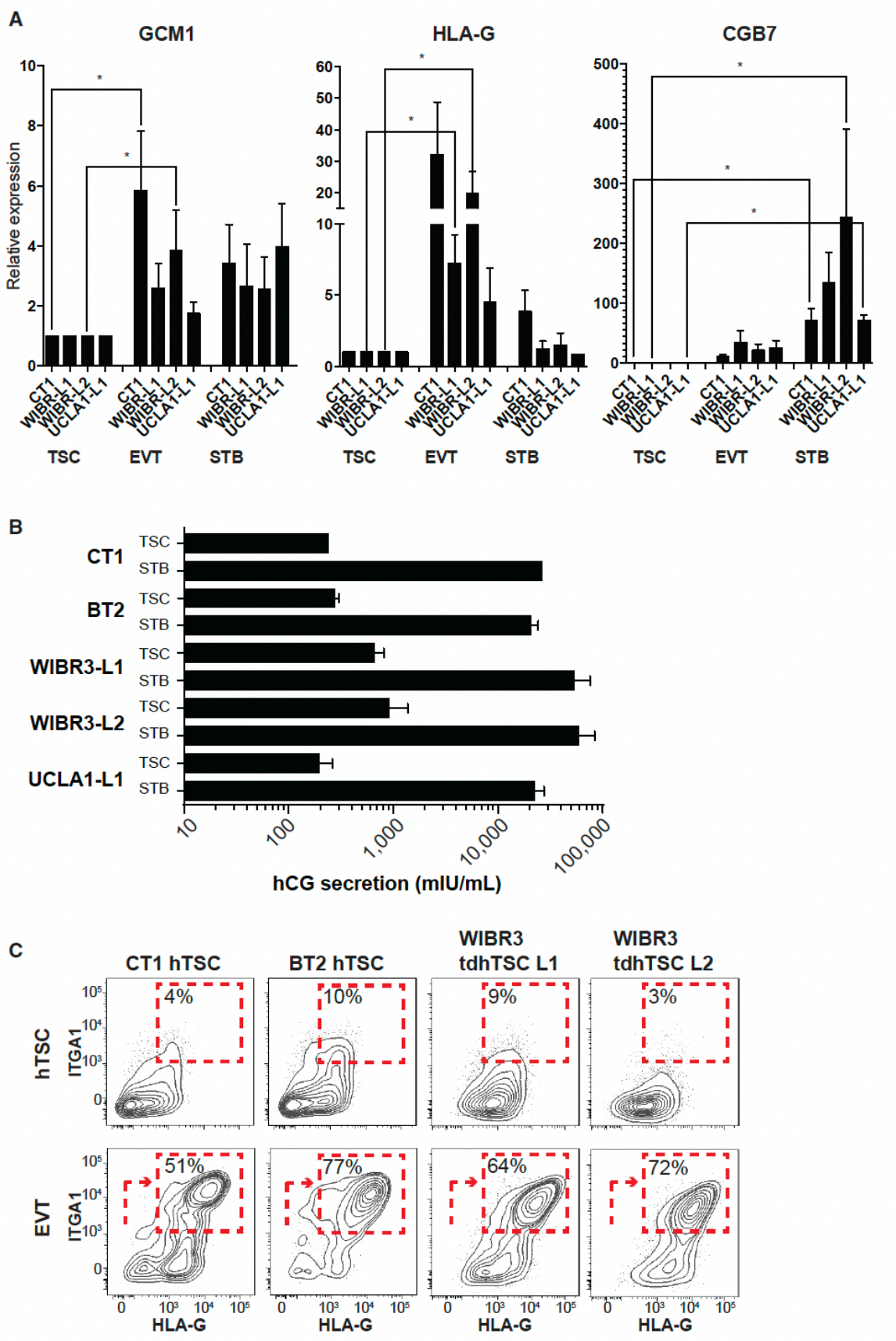
A
GCM1
HLA-G
CGB7
Relative expression
CT1
WIBR-L1
WIBR-L2
UCLA1-L1
TSC
EVT
STB
B
CT1
BT2
WIBR3-L1
WIBR3-L2
UCLA1-L1
TSC
STB
10
100
1,000
10,000
100,000
hCG secretion (mIU/mL)
C
CT1 hTSC
BT2 hTSC
WIBR3 tdhTSC L1
WIBR3 tdhTSC L2
hTSC
EVT
ITGA1
HLA-G
4%
10%
9%
3%
51%
77%
64%
72%

Figure 4. Differentiation Capacity of tdhTSCs. (A) qRT-PCR for markers of EVT (GCM1, HLA-G), and STB (GCM1, CGB7) differentiation of lines indicated, normalized to GAPDH. Error bars indicate mean + SE for n = 3–5 independent experiments. *$p < 0.05$ in one-tailed t test. (B) ELISA assay for hCG secretion after directed differentiation to STB. Error bars indicate mean + SE for n = 2 biological replicates, except CT1 for which there is one replicate. (C) Flow cytometry of hTSCs and EVT, for the EVT markers HLA-G and ITGA1, for the lines indicated. Representative of n = 5 independent experiments.

2.3.4 Gain of Placenta-like DNA Methylation Pattern in tdhTSCs

The placenta has a highly distinctive DNA methylation profile compared with hESCs or somatic cells. Global methylation levels are much lower in placenta and especially low in hTSCs.(Okae et al., 2018) Despite this reduced overall DNA methylation level, some CpG islands have increased DNA methylation in placenta and hTSCs, a pattern that is often recapitulated in the CpG island methylator phenotype, which occurs in many somatic cancers.(Smith et al., 2017) We sought to determine whether tdhTSCs acquired this distinctive placenta-like methylome. Also, because DNA methylation is a highly heritable mark, we reasoned that even if tdhTSCs have acquired an overall hTSC-like phenotype, they might still bear traces of their cell of origin or their period as naive hESCs.

We performed whole-genome bisulfite sequencing of CT1, CT3, WIBR3 primed hESCs, and WIBR3 tdhTSC line 1 and line 2 (Table S3). Methylation levels and patterns observed for CT1 and WIBR3 hESCs are similar to published data (Figures 5A and S5A). The global CpG DNA methylation level of the tdhTSCs is similar to that of placental hTSCs and far lower than that of hESCs (Figure 5A). The methylation level of individual CpG islands and gene promoters in tdhTSCs is far better correlated with that of placental hTSCs than with hESCs (Figures 5B, 5C, and S5B). On a global level, tdhTSCs appear to acquire a placenta-like methylome.

We then focused on the phenomenon of placenta-specific CpG island methylation. We used published data to identify 788 CpG islands with substantially higher methylation in CT1

hTSCs compared with WIBR3 hESCs (see Experimental Procedures and Table S6). Interestingly, these CpG islands include the promoters of genes critical for neural lineage (*SOX1*, *PAX6*), cardiac development (*HAND2*, *NKX-2.5*), and transforming growth factor β family signaling (*NODAL*, *FOXH1*), suggesting that DNA methylation may be a mechanism for shutting off these lineages in placenta. The WIBR3 tdhTSCs show a strong increase in DNA methylation at these 788 CpG islands relative to primed cells (Figures 5D and 5E), demonstrating that tdhTSCs have gained placenta-specific methylation.

We next considered the phenomenon of "gatekeeper" genes: key placental genes whose promoters are methylated in hESCs, thus precluding conversion to placental fate. Analogous methylation is a critical obstacle to complete conversion of murine ESCs to mTSCs.(Cambuli et al., 2014) To address this question, we identified 2,107 promoters methylated in WIBR3 hESCs that show dramatically lower DNA methylation in CT1 hTSCs (see Experimental Procedures and Table S6). These regions show dramatic loss of methylation in WIBR3 tdhTSCs (Figure 5F). Of these genes, 172 are upregulated in hTSCs relative to primed hESCs and have an average RPKM > 1 in hTSCs, possible gatekeepers (Table S6). This set includes key placental factors, including *ELF5* and a number of hCG and STB fusion genes. Globally, these genes show increased expression in tdhTSC lines, comparable with placental hTSCs (Figure 5G). There is thus no general inability to reactivate placental gene expression in tdhTSCs, even at genes whose promoters are heavily methylated in starting hESCs.

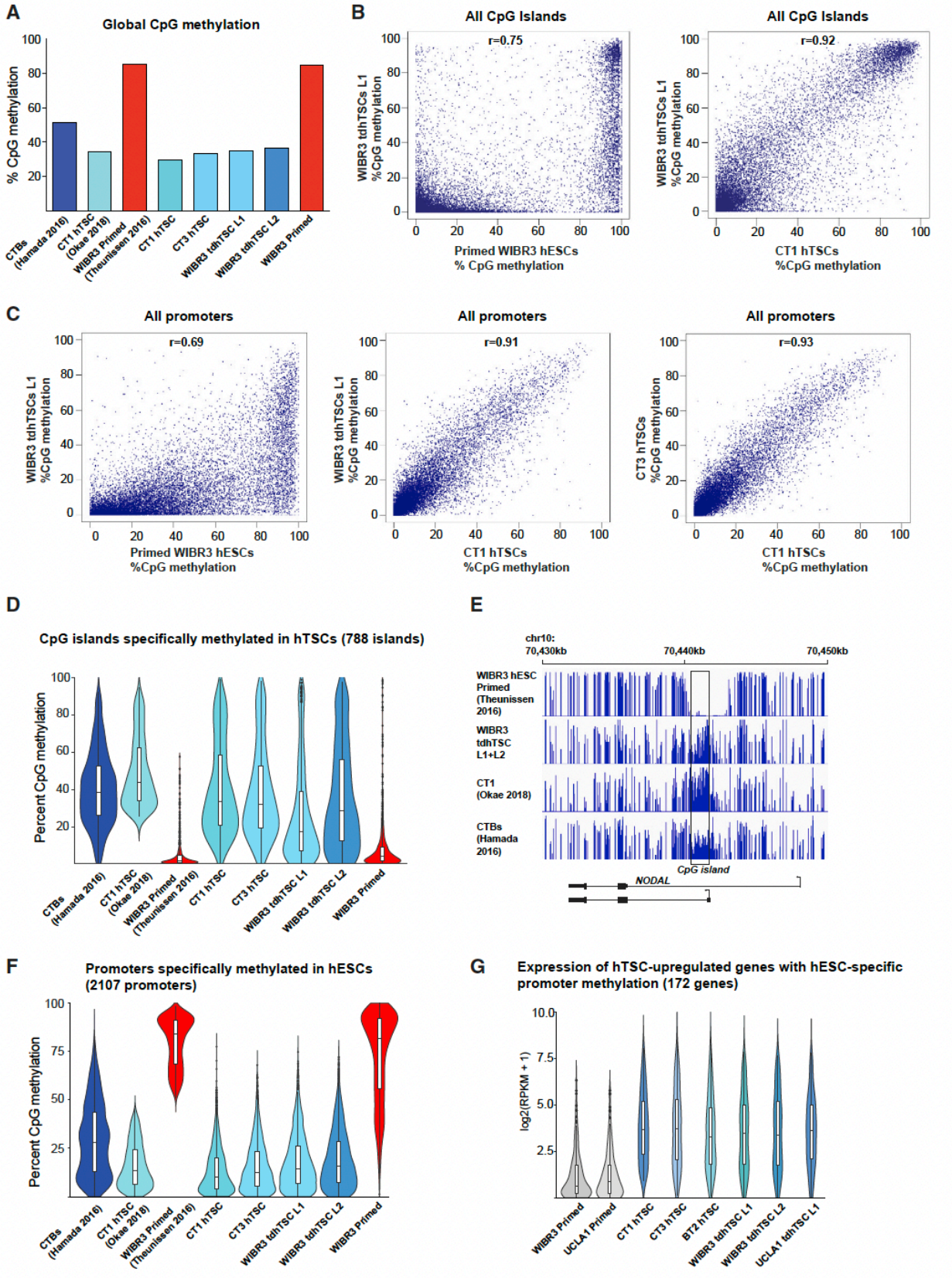
A
Global CpG methylation
% CpG methylation
CTBs (Hamada 2016)
CT1 hTSC (Okae 2018)
WIBR3 Primed (Theunissen 2016)
CT1 hTSC
CT3 hTSC
WIBR3 tdhTSC L1
WIBR3 tdhTSC L2
WIBR3 Primed
B
All CpG Islands
r=0.75
WIBR3 tdhTSCs L1 %CpG methylation
Primed WIBR3 hESCs % CpG methylation
All CpG Islands
r=0.92
WIBR3 tdhTSCs L1 %CpG methylation
CT1 hTSCs %CpG methylation
C
All promoters
r=0.69
WIBR3 tdhTSCs L1 %CpG methylation
Primed WIBR3 hESCs %CpG methylation
All promoters
r=0.91
WIBR3 tdhTSCs L1 %CpG methylation
CT1 hTSCs %CpG methylation
All promoters
r=0.93
CT3 hTSCs %CpG methylation
CT1 hTSCs %CpG methylation
D
CpG islands specifically methylated in hTSCs (788 islands)
Percent CpG methylation
CTBs (Hamada 2016)
CT1 hTSC (Okae 2018)
WIBR3 Primed (Theunissen 2016)
CT1 hTSC
CT3 hTSC
WIBR3 tdhTSC L1
WIBR3 tdhTSC L2
WIBR3 Primed
E
chr10:
70,430kb
70,440kb
70,450kb
WIBR3 hESC Primed (Theunissen 2016)
WIBR3 tdhTSC L1+L2
CT1 (Okae 2018)
CTBs (Hamada 2016)
CpG island
NODAL
F
Promoters specifically methylated in hESCs (2107 promoters)
Percent CpG methylation
CTBs (Hamada 2016)
CT1 hTSC (Okae 2018)
WIBR3 Primed (Theunissen 2016)
CT1 hTSC
CT3 hTSC
WIBR3 tdhTSC L1
WIBR3 tdhTSC L2
WIBR3 Primed
G
Expression of hTSC-upregulated genes with hESC-specific promoter methylation (172 genes)
log2(RPKM + 1)
WIBR3 Primed
UCLA1 Primed
CT1 hTSC
CT3 hTSC
BT2 hTSC
WIBR3 tdhTSC L1
WIBR3 tdhTSC L2
UCLA1 tdhTSC L1

Figure 5. Global Methylation Patterns of tdhTSC. For all data, data in parentheses indicate data mined from published sources, data without parentheses indicate original data. (A) Global CpG methylation level in samples indicated. (B) Correlation of CpG island methylation in each of the two samples is indicated. Each CpG island represents as a single point, all CpG islands with adequate coverage are plotted. (C) Correlation of promoter methylation between two samples is indicated. All autosomal promoters with adequate coverage are plotted. (D) Violin plot indicating degree of CpG island methylation in samples indicated among 788 CpG islands that show higher DNA methylation in CT1 hTSCs relative to primed hESCs. (E) DNA methylation of a region of genome that includes the CpG island promoter of *NODAL*. Height of bars corresponds to percentage CpG methylation, from 0% to 100%. Data from WIBR3 tdhTSC L1 and L2 are merged to allow sufficient sequencing depth for visualization. (F) Violin plot showing methylation level of 2,107 promoters that show higher DNA methylation in primed hESCs relative to CT1 hTSCs. (G) Expression of 172 possible "gatekeeper" genes, genes that have upregulated expression in hTSCs and higher promoter methylation in hESCs. Expression of each gene, using an average of all replicates for a given cell type, is indicated as a single point on the violin plot. Box indicates 25th, 50th, and 75th percentiles. n = 2 (all tdhTSC lines), n = 3 (UCLA1 hESCs), n = 4 (WIBR3 hESCs, CT3, BT2), n = 7 (CT1) biological replicates.

2.3.5 Dysregulation of Select Imprinted Genes in tdhTSCs

Nonetheless, we detected examples of aberrant methylation in tdhTSCs in which their past as naive or primed hESCs was apparent. As expected, many imprinted regions showed aberrant hypomethylation in hTSCs (Figure 6A), a predictable consequence of having once been naive hESCs.(Pastor et al., 2016) More surprisingly, three imprints showed selective hypermethylation in tdhTSC: *PEG3*, *ZFAT*, and *PROSER2-AS1*. *PEG3* is low expressed in primed hESCs and is prone to hypermethylation in culture, while *ZFAT* and *PROSER2-AS1* are placental imprints that converge toward methylation in pluripotent and somatic cells.(Barbaux et al., 2012; Hamada et al., 2016) Apparently, they resisted demethylation in both the naive and trophoblastic states.

We calculated differentially expressed genes, comparing hTSCs with both primed hESCs and tdhTSCs (Figures 6B and 6C; Table S7). Very few genes show substantial dysregulation in tdhTSCs relative to hTSCs, but they include *PEG3*, *ZFAT*, and *PROSER2-AS1*, all of which show

striking downregulation consistent with their hypermethylation (Figures 6C and S6). In summary, while tdhTSCs have a broadly hTSC-like methylome, they do carry vestiges of their past that have some impact on their transcriptional program.

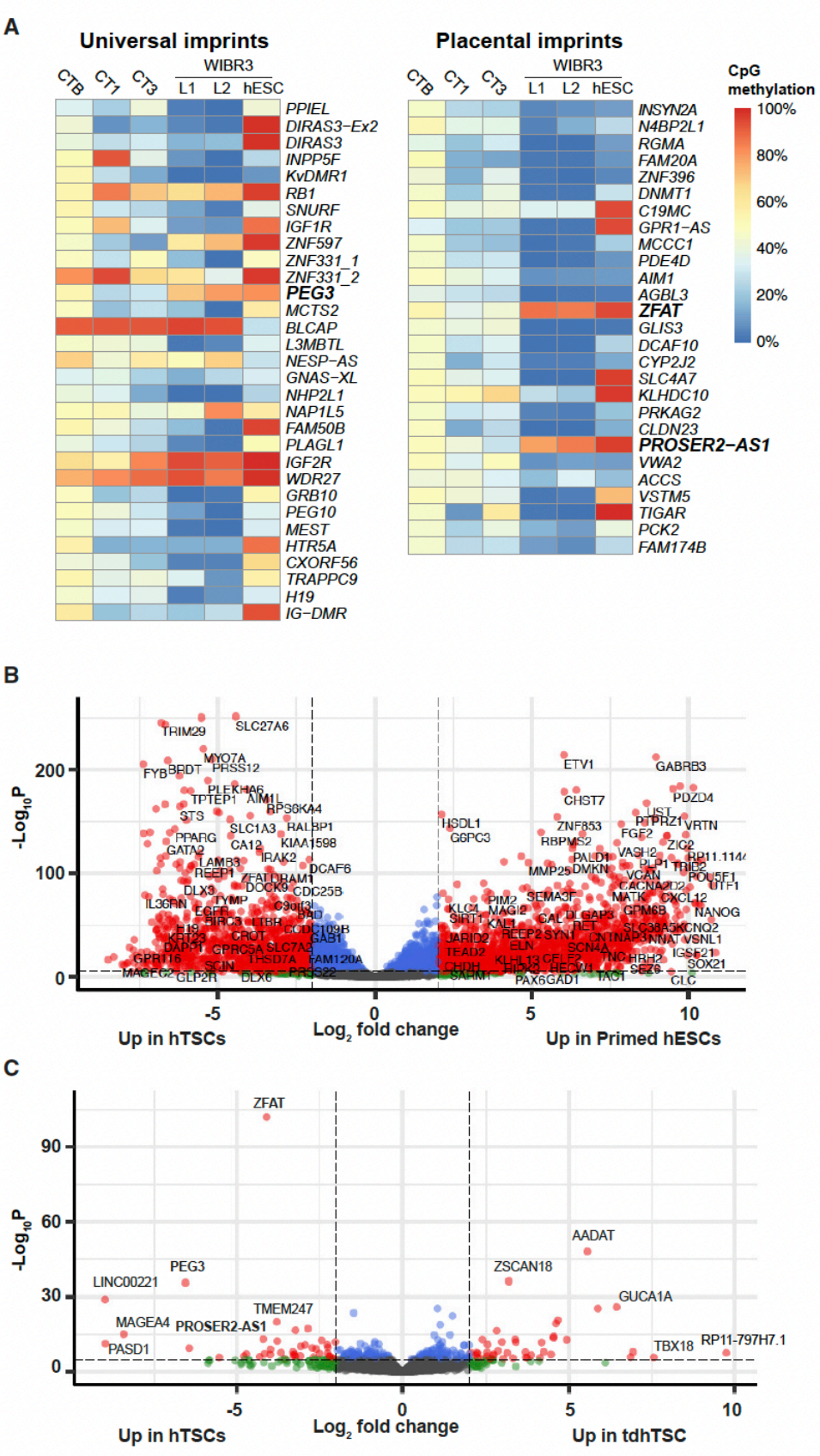
A
Universal imprints
Placental imprints
CTB
CT1
CT3
WIBR3
L1
L2
hESC
CpG methylation
100%
80%
60%
40%
20%
0%
PPIEL
DIRAS3−Ex2
DIRAS3
INPP5F
KvDMR1
RB1
SNURF
IGF1R
ZNF597
ZNF331_1
ZNF331_2
PEG3
MCTS2
BLCAP
L3MBTL
NESP−AS
GNAS−XL
NHP2L1
NAP1L5
FAM50B
PLAGL1
IGF2R
WDR27
GRB10
PEG10
MEST
HTR5A
CXORF56
TRAPPC9
H19
IG−DMR
INSYN2A
N4BP2L1
RGMA
FAM20A
ZNF396
DNMT1
C19MC
GPR1−AS
MCCC1
PDE4D
AIM1
AGBL3
ZFAT
GLIS3
DCAF10
CYP2J2
SLC4A7
KLHDC10
PRKAG2
CLDN23
PROSER2−AS1
VWA2
ACCS
VSTM5
TIGAR
PCK2
FAM174B
B
-Log10P
Log2 fold change
Up in hTSCs
Up in Primed hESCs
C
-Log10P
Log2 fold change
Up in hTSCs
Up in tdhTSC
ZFAT
PEG3
LINC00221
MAGEA4
PROSER2-AS1
PASD1
TMEM247
AADAT
ZSCAN18
GUCA1A
TBX18
RP11-797H7.1

Figure 6. Imprinting Abnormalities in tdhTSC. (A) CpG methylation level of all universal (organism-wide) and placental imprints in cell types indicated. CTB, primary cytotrophoblasts; L1, WIBR3 tdhTSC L1; L2, WIBR3 tdhTSC L2. CTB data from Hamada et al. (2016), original data shown for all other samples. (B) Volcano plot of genes differentially expressed in hTSCs (CT1, CT3, and BT2) versus primed (WIBR3 and UCLA1 hESCs). Red dots correspond to differentially expressed genes ($p_{adj} < 0.05$, fold-change > 4). (C) Volcano plot of genes differentially expressed in hTSCs (CT1, CT3, and BT2) versus tdhTSCs (WIBR3 tdhTSC lines 1, 2, and 3, and UCLA1 line 1). Red dots correspond to differentially expressed genes ($p_{adj} < 0.05$, fold-change > 4).

2.3.6 Conversion of Non-naïve Cells to hTSC-like Cells

A recent report details the generation of "expanded potential stem cells" (EPS cells). EPS cells have a transcriptional program and level of DNA methylation similar to primed hESCs but can reportedly be differentiated into trophoblast by treatment with BMP4. When cultured in hTSC medium, trophoblast-like colonies can be identified, picked, and propagated.(Gao et al., 2019) A second report countered the first claim, showing that EPS cells treated with BMP4 formed cells with amnion-like, rather than trophoblast-like, properties.(Ge Guo et al., 2021) However, it remained unclear whether tdhTSCs could be derived from EPS hESCs, so we analyzed RNA-seq data from the EPS-derived tdhTSCs. Although they were not sequenced in parallel with placental hTSCs, making direct comparison difficult, they express trophoblast genes at levels similar to placental hTSCs (Figure S7A) and do not express amnion-specific genes at high levels (Figure S7B). Interestingly, two of the three tdhTSC lines made from EPS cells showed low *PEG3* expression, and all showed low *ZFAT* and *PROSER2-AS1* expression (Figure S6).

To perform a direct comparison, we grew three hESC lines (WIBR3, UCLA1, and H9) in naive medias (5iLAF, PXGL), in medias that produce cells with a mixture of naive and primed properties (EPS, RSet), and in primed medium, and subsequently transferred them to hTSC medium for 15 days. Surprisingly, all conditions were able to produce at least some population of

ITGA2^{hi} EpCAM^{hi} ITGA1^{lo} cells (Figures 7A and S7C; Table S2). However, naive conditions generally produced more efficient transdifferentiation as measured by production of ITGA2^{hi} EpCAM^{hi} ITGA1^{lo} cells (Figure S7C). WIBR3 cells had markedly inefficient transdifferentiation from EPS medium (Figure S7C), to the extent that we were not able to isolate a pure line. Furthermore, while tdhTSC lines isolated from naive cells showed uniformly low staining for the amnion marker ITGB6 (Ge Guo et al., 2021), lines generated from EPS, RSet, or primed UCLA1 or H9 cells showed heterogeneous staining for this mark and higher expression as measured by RT-PCR (Figures 7B–7D). Expression of the gene *HAVCR1*, specific to trophoblast over amnion (Ge Guo et al., 2021), was uniformly higher in tdhTSCs generated from naive cells (Figure 7D). Finally, while naive hESCs gave rise to uniformly TEAD4^{+} TFAP2C^{+} KRT7^{+} tdhTSC colonies after sorting, EPS, RSeT, and primed-derived tdhTSCs contained a second population of cells with markedly lower TEAD4 staining (Figure S7D). It remains unclear whether EPS, RSet, and primed cells gave rise to a mixture of hTSCs and amnion-like cells, or cells with properties of both, but naive cells are clearly optimal for generation of hTSCs.

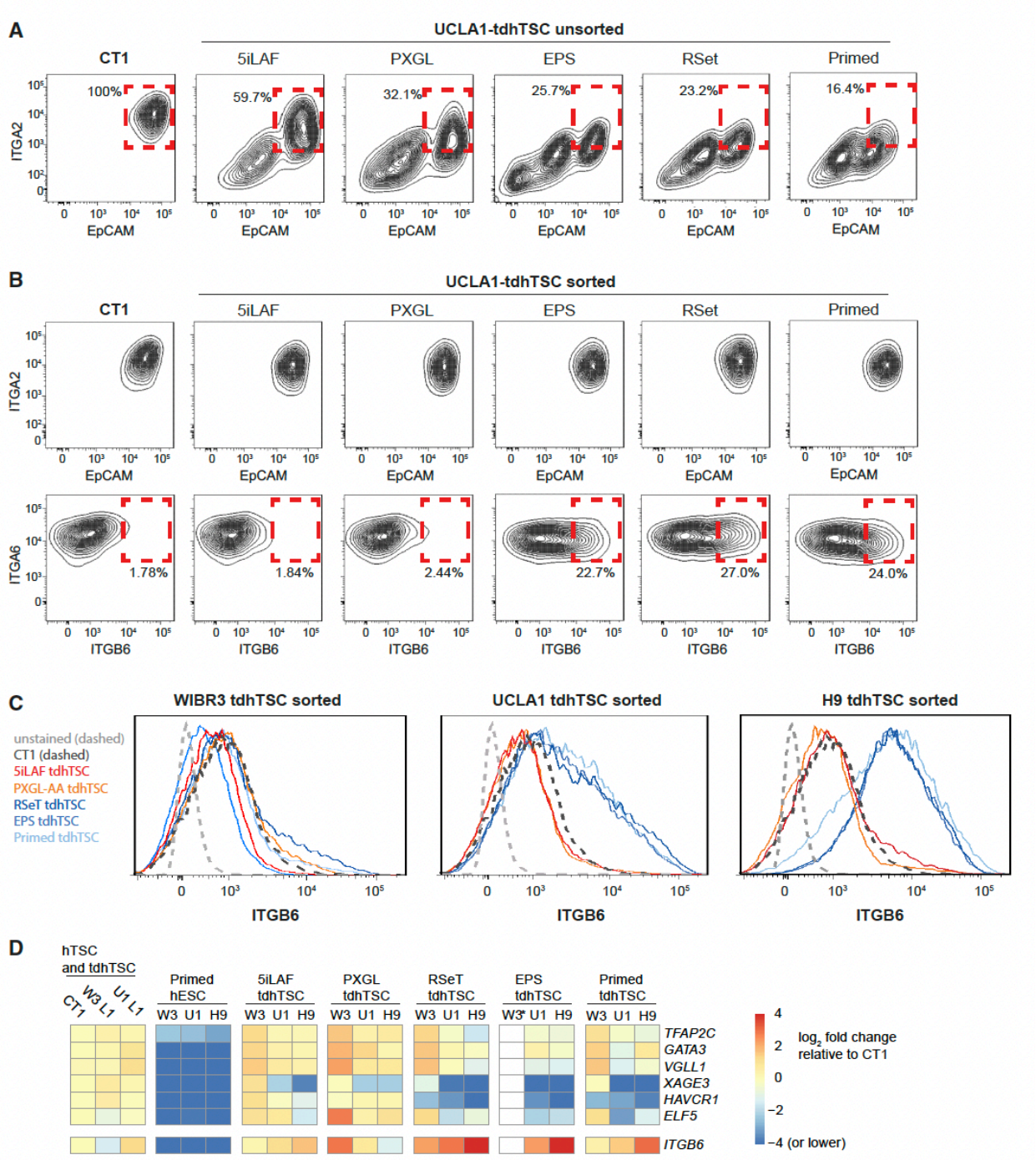

Figure 7. Comparative Transdifferentiation Capacity from Different Media Conditions. (A) Flow cytometry of UCLA1 hESCs cultured in various conditions and then grown in hTSC medium for 15 days. Percentage of ITGA2^{hi} EpCAM^{hi} cells is indicated. (B) Flow cytometry 20 days after sorting. Note higher ITGB6 signal in putative tdhTSCs derived from hESCs in non-naive conditions. (C) Flow cytometry histogram of ITGB6 signal for putative tdhTSCs derived from hESC lines, and growth condition indicated.

(D) qRT-PCR quantification of placental markers and *ITGB6* in indicated cell lines normalized to *GAPDH*. W3, WIBR3; U1, UCLA1. *WIBR3 EPS-derived tdhTSCs could not be studied because conversion efficiency was too low to produce a pure ITGA2^{hi} EpCAM^{hi} line. n = 1 biological replicate.

2.4 Discussion

We find that naive hESCs can be converted into hTSC-like cells. Very recently, another report also demonstrated production of hTSC-like cells from naive hESCs.(Dong et al., 2020) Whereas we cultured naive cells in hTSC medium for 10–22 days and purified tdhTSCs using surface markers, Dong and colleagues cultured naive cells in hTSC medium for 5–10 passages and report pure tdhTSC lines. There is an unproven but plausible reconciliation of these findings: successfully transdifferentiated tdhTSCs may grow faster than other cell types in mixed transdifferentiations, and may dislodge other cells as tdhTSC colonies expand, resulting in their taking over mixed cultures even without sorting.

2.4.1 Imprinting in tdhTSCs

It is probably impossible to generate perfectly placenta-like tdhTSCs from hESCs by any current method. Certain parental imprints are retained only in placenta and accordingly these regions show biallelic hyper- or hypomethylation in hESCs.(Okae et al., 2014) hESC lines frequently show aberrations even in non-placental imprints (Rugg-Gunn et al., 2007), and culture in naive conditions results in widespread imprint erasure.(Pastor et al., 2016; Theunissen et al., 2016) Considering the importance of imprinting in placental development, it is somewhat remarkable that tdhTSCs are as similar to hTSCs as they are. Human conceptuses that lack maternal imprinting give rise to hydatidiform moles, aberrant placentas with little or no embryonic tissue.(Nguyen & Slim, 2014) Nonetheless, only three imprinted genes failed to activate upon transdifferentiation. The failure to reactivate *PEG3* is somewhat surprising, because this imprint

is demethylated and chromatin-opened in naive hESCs.(Pastor et al., 2016) This may be a consequence of the relatively brief period in which the hESCs used in this study were cultured in naive medium. *ZFAT* and *PROSER2-AS1* by contrast do not show open chromatin in naive hESCs (Pastor et al., 2016), are not reactivated in tdhTSCs derived from EPS cells, and may be the most refractory to activation in tdhTSCs.

More surprising is two imprints which were not differentially expressed: *IGF2* and *CDKN1C*. Demethylation of the H19 and KvDMR1 loci, respectively, should be expected to abrogate long-range promoter-enhancer interactions necessary for the expression of these two genes.(Soejima & Higashimoto, 2013) *CDKN1C* is of particular note because it is strongly implicated in molar pathology, and its loss eliminates contact inhibition in hTSCs.(Takahashi et al., 2019) However, expression of these genes was highly variable across both hTSC and tdhTSC replicates and trended lower in tdhTSCs (Table S3).

2.4.2 Transdifferentiation Capacity of Human Pluripotent Cells

While we show that naive hESCs are more efficient in transdifferentiating to tdhTSCs, it remains unclear whether hTSC-like cells can be generated from non-naive cells or how such cells might be different or impaired. There are now reports of generation of trophoblast-like cells from EPS cells (Gao et al., 2019), primed hESCs treated with BMP4 and an S1P3 agonist (Mischler et al., 2021), and primed hESCs cultured in micromesh.(Li et al., 2019) Our results certainly do not rule out this possibility. However, distinguishing tdhTSCs from contaminating, possibly amnion-like cells, is not a trivial endeavor: the contaminating cells share surface markers (ITGA2, ITGA6, and EpCAM) and show only subtle morphological differences from hTSCs. Amnion expresses many of the same core transcription factors as placenta.(Ge Guo et al., 2021) Amnion identity must be firmly ruled out, preferably by direct comparison with placental hTSCs.

While hESCs can convert to tdhTSCs, naive murine ESCs require genetic manipulation to make such a transition and even then do so incompletely.(Cambuli et al., 2014) There are at least two possible explanations, which are not mutually exclusive: human naive pluripotent cells may reflect an earlier developmental state than murine naive cells or human pluripotent cells may retain greater plasticity than previously appreciated. The latter phenomenon deserves serious consideration. Remarkably, cells from day 5 human blastocysts (stage BL3), if harvested and reaggregated into an empty zona pellucida, will compact and cavitate, forming blastocysts of normal appearance with a $NANOG^+$ ICM.(De Paepe et al., 2013) Similar results are obtained if only outer (trophectoderm) or inner (ICM) cells are added to an empty zona pellucida, implying that lineage is not restricted until well after blastocyst formation. Furthermore, the barrier to placental transdifferentiation is sometimes crossed in the context of malignancy: early germ cells, which reactivate much of the transcriptional program of the pluripotent epiblast, can give rise to choriocarcinomas (trophoblast-like tumors) in both mice and humans.(Alison et al., 1987; Rijlaarsdam et al., 2015) Future studies may also indicate when and how in human development a firm barrier to placental differentiation is established.

2.5 Experimental Procedures

Naïve Reversion: Primed hESCs were routinely passaged in TeSR-E8 media (Stemcell Technologies). In the first na.ve reversion we conducted (which led to the generation of WIBR3 tdhTSC L1 and L2), primed hESCs were cultured in special primed media (DMEM-F12 supplemented with 15% FBS, 5% KSR, 1X Glutamax, 1X non-essential amino acids, 0.1mM β-mercaptoethanol and 8 ng/ml FGF) on mitomycin C inactivated mouse embryonic fibroblast (MEF) feeder layers for one passage prior na.ve reversion. In subsequent reversions, cells were cultured in TeSR-E8 until na.ve induction.

In accordance with published protocol (Guo et al., 2017) 200,000 primed hESCs were dissociated into single cells using 30% TrypLE Express and plated onto a MEF feeder layer in special primed media (in the first reversion) or TeSR E8 (in subsequent reversions) supplemented with 10 μM ROCKi at 5% O2. After 24h, primed hESCs were cultured for 3 days in na.ve induction medium (24.5 ml DMEM F-12, 24.5 ml Neurobasal media, 0.25 ml N2, 0.5 ml B27, 1x Glutamax, 150 μM L-ascorbic acid, 0.1mM β-mercaptoethanol, 1μM PD0325901, 10μM ROCKi, 0.75mM vaporic acid and 10ng/ml recombinant hLIF). Following induction, reverting na.ve hESCs were cultured in PXGL maintenance medium (24.5 ml DMEM F-12, 24.5 ml Neurobasal media, 0.25 ml N2, 0.5 ml B27, 1xGlutamax, 150 μM L-ascorbic acid, 0.1mM β-mercaptoethanol, 1μM PD0325901, 2μM G.6983, 10μM ROCKi, 2μM XAV939 and 10ng/ml recombinant hLIF) indefinitely. Reverting na.ve cells started showing dome-like morphology with refractive edges 7 days post-induction. We observed that culture with ascorbate (described as optional in previous protocols) enhanced subsequent transdifferentiation (data not shown). Culture of RSet cells was conducted with a commercially available reagent (Stemcell Technologies 05975) and

manufacturer protocol. EPS cells were generated and cultured by published protocol.(Gao et al., 2019) Cells were cultured in RSeT or EPS media for 11 days before culture in hTSC media.

Embryonic Stem Cell Culture: Primed hESCs were routinely cultured with TeSR-E8 (StemCell Technologies) on hESC Qualified Matrigel (Corning). hESCs were reverted to naive state using a one-step induction adapted from published protocols (Guo et al., 2017) Further details are provided in Supplemental Experimental Procedures.

TSC Culture and Differentiation: hTSCs were cultured according to published protocol (Okae et al., 2018) with the following alterations. 0.5–1 × 10^5 cells were plated on each well of a 6-well plate, and cells were passaged every 5–7 days. We observed that reduced oxygen levels promote hTSC self-renewal but inhibit directed differentiation, so we cultured hTSCs in 5% O_2 5% CO_2 but performed differentiation to EVT or STB at 20% O_2 5% CO_2.

EVT and STB differentiation were performed according to published protocol, with the following alterations. For STB differentiation the density of the cells when plated was doubled to 150,000 per 6-well plate well and cells were cultured for 3 days in STB (2D) medium before collection and assessment. For EVT, 150,000 cells were plated initially, but procedures for differentiation remained unchanged.

The three lines described in this paper as CT1, CT3, and BT2 correspond to the published lines TS^{CT1}, TS^{CT3}, and TS^{BLAST2}, respectively.(Okae et al., 2018)

For consistency, all stem cells used in RNA-seq were cultured in 5% O_2.

Transdifferentiation of Naive hESCs to hTSC Culture: Naive hESCs were passaged to Matrigel (Corning)-coated plates at 20%–30% confluency into TSC culture medium. Cells were grown on collagen-coated plates in subsequent passages, akin to control hTSCs. Cells were grown to confluency before fluorescent cell sorting, which is described further in Supplemental Experimental Procedures.

STR Analysis: STR analysis was performed at the SickKids Center for Applied Genomics Facility using GenePrint10 (Promega).

Flow cytometry: Cells were dissociated with TrypLE Express (Gibco 12604) and quenched with Soybean trypsin inhibitor (Gibco 17075), then passed over a 70µm filter to remove aggregates. Cells were then centrifuged 3 minutes at 200xg and resuspended in 1ml FACS buffer (1xPBS, 1%BSA) and counted.

Cells were stained with appropriate fluorescent antibodies at a concentration of 1µg antibody per one million cells in a volume of 1ml. When fewer cells were used, antibody and volume were scaled down accordingly. Cells were incubated with antibody for 20 minutes in the dark at 4ÅãC, then centrifuged, washed with 1ml of FACS buffer, resuspended in 300µl FACS buffer and analyzed. DAPI was included immediately before flow to distinguish dead cells. Flow cytometry was performed using a BD FACSAria Fusion instrument, FACS with a BD LSRFortessa instrument, and analysis was performed using FlowJo v10.

A table indicating which antibodies were used and in which figures is shown below:

hCG ELISA: hCG secretion was measured using an hCG AccuBind ELISA (Monobind) according to manufacturer instructions.

Generation of RNA-Seq Libraries: RNA extraction was performed using QIAGEN RNeasy Micro Kit, except for two samples (WIBR3 primed replicate 1, WIBR3 naive day 10) that were extracted using RNAzol RT (Sigma). RNA quality was confirmed using Bioanalyzer. mRNA was enriched from 500 ng total RNA using NEBNext Poly(A) mRNA Magnetic Isolation Module Kit and libraries were generated using Swift RNA Library Kit.

Samples were run on an Illumina NovaSeq instrument at the La Jolla Institute for Allergy and Immunology Sequencing Core, or on a HiSeq 4000 at Michael Smith Genome Sciences Center. Three samples were sequenced at both locations to confirm similarity of results.

RNA-Seq Analysis

Mapping and RPKM Calculation: FASTQ files were mapped to hg19 using the STAR aligner (v2.5.3a) with default parameters. Bam files were analyzed by RNA-SeQC to confirm library quality. Read counts were calculated with htseq-count and RPKM was calculated using cufflinks (v2.2.1) with default settings.

PCA: PCA was performed using prcomp function in R and plotted with the ggfortify package. Genes with RPKM < 2 in all samples were excluded from analysis.

Identification of Trophoblast-Specific Genes: Cynomolgus monkey single-cell RNA-seq data normalized using the RPM method were obtained from Nakamura et al.(Nakamura et al., 2016)

Trophoblast-specific genes were identified by calculating differentially expressed genes between trophoblast cells (11 cells each in the categories “Pre-implantation Early trophoblast,” “Pre-implantation late trophoblast,” and “Post-implantation parietal trophoblast”) and all other cells. Differentially expressed genes were identified as false discovery rate (FDR) < 0.05 using the kruskal.test function and p.adjust function in R. As a further filter, trophoblast-specific genes were required to show at least 4-fold higher expression in placental cells over all non-placental cell types and to have an average RPM > 7 in placental cells.

Differential Gene Expression Calling and Volcano Plot: Read counts obtained from htseq-count were used for differential gene expression with DESeq2. Genes with raw read count >100 were plotted using EnhancedVolcano package in R.

Generation of Whole-Genome Bisulfite Sequencing Libraries: Genomic DNA was collected using a QIAGEN Blood and Tissue Kit, including RNase A treatment. DNA concentration was measured using Nanodrop. DNA (500 ng) was fragmented using a Covaris M220 instrument and 250 ng was processed with a Zymogen bisulfite conversion kit. The equivalent of 50–100 ng of DNA was used to generate the sequencing library with the Accel-NGS Methyl-Seq DNA Library Kit (Swift Biosciences).

Libraries were sequenced as 150-bp paired-end reads at the Michael Smith Genome Sciences Center on a HiSeq 4000 instrument.

Bisulfite Sequencing Analysis: The adaptor sequences of paired-end 150 bp WGBS raw reads were first trimmed based on the FastQC (v.0.11.8) report using Cutadapt (v.1.9.1).(Martin, 2011)

Then the last 15 bp of read1 and first 15 bp of read2 were cut according to Swift kits manual using Cutadapt (v.1.9.1).(Martin, 2011) Trimmed paired-end reads were then aligned to human reference genome (GRCh38) using BSMAP (v.2.7.4) (Xi & Li, 2009) allowing two mismatches. Methylation levels over each cytosine were then calculated using BSMAP (v.2.7.4) methratio.py scripts. Potential unconverted reads were removed with a customized function incorporated in the methratio.py script.(Cokus et al., 2008) Methylation levels over different genomic regions were extracted using a customized Python script. Differentially methylated regions (DMRs) were defined using CT1 (Okae et al., 2018) and WIBR3 (Theunissen et al., 2016) with customized R script over promoters and CpG islands regions. Promoters were defined as upstream 1 kb and downstream 200 bp of transcription start site. Chromosome Y was excluded from the DMR analysis. Regions with coverage (C + T count) greater than 50 in both samples were kept. p values were calculated with Fisher's exact test and then adjusted with the Benjamini-Hochberg procedure (FDR).

Additional thresholds were then applied. To identify regions with CT1-specific CpG island methylation, we required (1) FDR < 0.05, (2) a ≥25% absolute difference in CpG methylation level between CT1 hTSCs and WIBR3 hESCs, and (3) ≥50 CTs mapped over the region in all eight bisulfite sequencing samples. To identify regions with hESC-specific promoter methylation, we required (1) FDR < 0.05, (2) a ≥50% absolute difference in CpG methylation level between CT1 hTSCs and WIBR3 hESCs, and (3) ≥50 CTs mapped over the region in all 8 samples.

ELF5 Methylation Analysis: The ELF5 promoter was amplified using primers described previously (Lee et al., 2016). Further details are contained in the Supplemental Experimental Procedures.

Alterations to Images: Brightness and contrast of light microscopy images was uniformly altered in some figures to enhance clarity.

Ethical Permissions: All experiments were approved by the McGill University Faculty of Medicine institutional review board and the CIHR Stem Cell Oversight Committee.

Data and Code Availability: RNA-seq and bisulfite sequencing data have been deposited to the Gene Expression Omnibus database under the accession number GSE152104.

2.6 Author Contributions

J.K.C., S.Y.K., I.H., J.S., C.S.R., and H.-W.T. conducted the experiments. S.Y.K. and Y.G. conducted the bioinformatic analysis. H.O. and T.A. provided hTSC lines and technical advice. T.F.D., W.L., and W.A.P. supervised the experiments and analysis.

2.7 Acknowledgments

We thank the Goodman Cancer Research Center Flow Cytometry core, the SickKids Center for Applied Genomics Facility, the La Jolla Institute for Allergy and Immunology Sequencing Core, and the Canada Michael Smith Genome Sciences Center at BC Cancer for their dedicated service. We thank the Rudolph Jaenisch (MIT) and Thorold Theunissen (Washington University) labs for providing WIBR3 OCT4-ΔPE-GFP hESCs, and the Amander Clark lab (UCLA) for providing UCLA1 hESCs. This work was funded by the New Frontiers in Research Fund (NFRF) grant NFRFE-2018-00883 and the Canadian Institutes of Health Research (CIHR)

project grant PJT-166169 to W.A.P., the Zhejiang Provincial Natural Science Foundation of China, LQ20C060004 to W.L., and PJT-165996 to T.F.D. J.K.C. was supported by a Fonds de recherche Santé Québec graduate fellowship. J.K.C. and I.H. were supported by studentships from the McGill University Faculty of Medicine.

2.8 Supplementary Information

Naive Human Embryonic Stem Cells Can Give Rise to Cells with a Trophoblast-like Transcriptome and Methylome

Jessica K. Cinkornpumin et al.

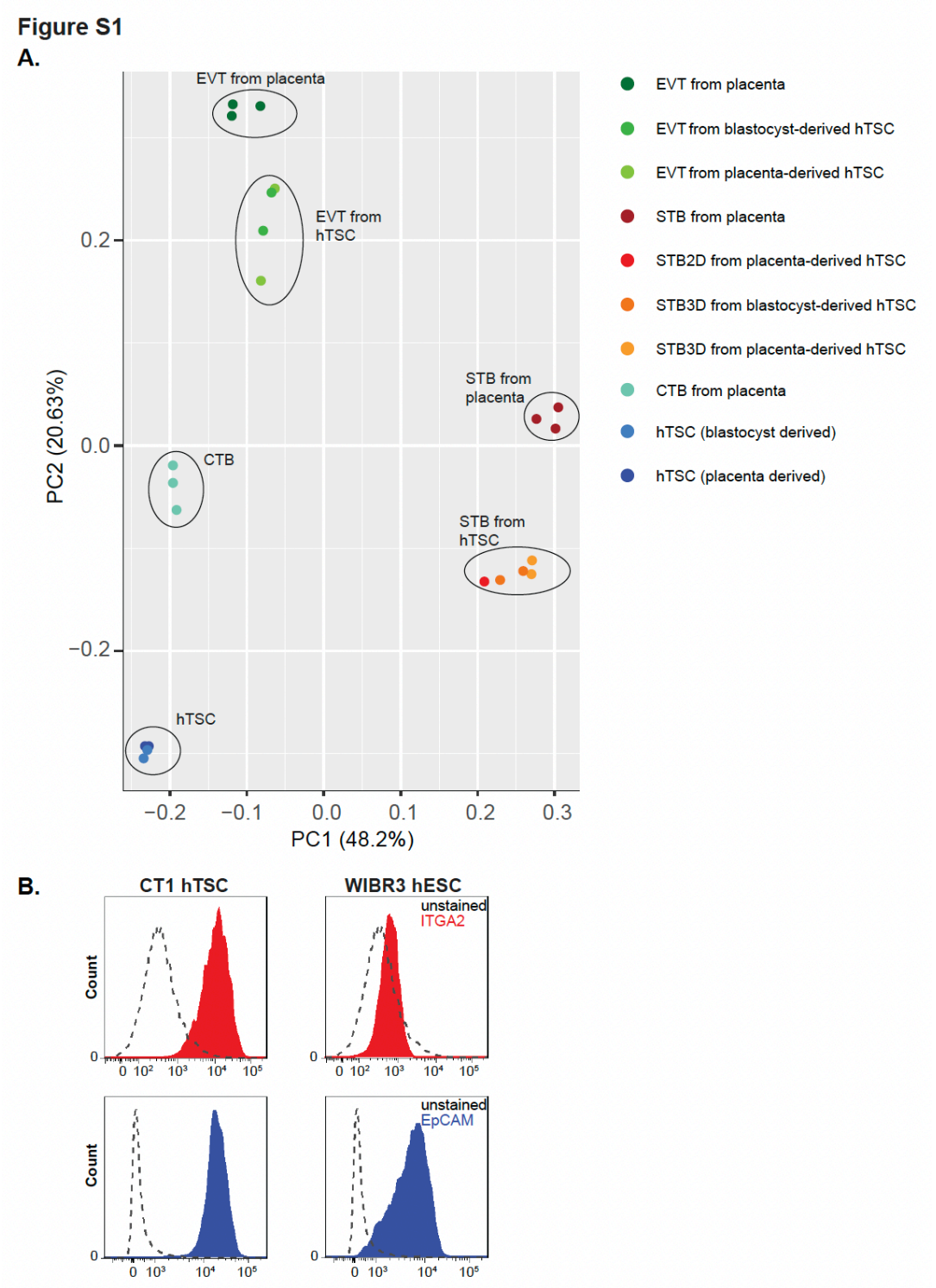

Figure S1. Principle component analysis of gene expression of different placental cell types. Related to Figure 1. A. Principle component analysis was performed using RNA-seq data from Okae et al.(Okae et al., 2018) Cells analyzed include cell types isolated directly from placenta (CTB= cytotrophoblast, STB= syncytiotrophoblast, EVT=extravillous trophoblast) and lines cultured and differentiated in vitro. These

include blastocyst-derived hTSC lines (BT1 and BT2), placental-derived hTSC lines (CT1 and CT2), as well as EVT and STB derived from these lines. “2D” and “3D” STB refer to two differentiation protocols. B. Flow cytometry for ITGA2 and EpCAM in hTSCs and hESCs. Staining profile is indicated relative to unstained control.

Figure S2

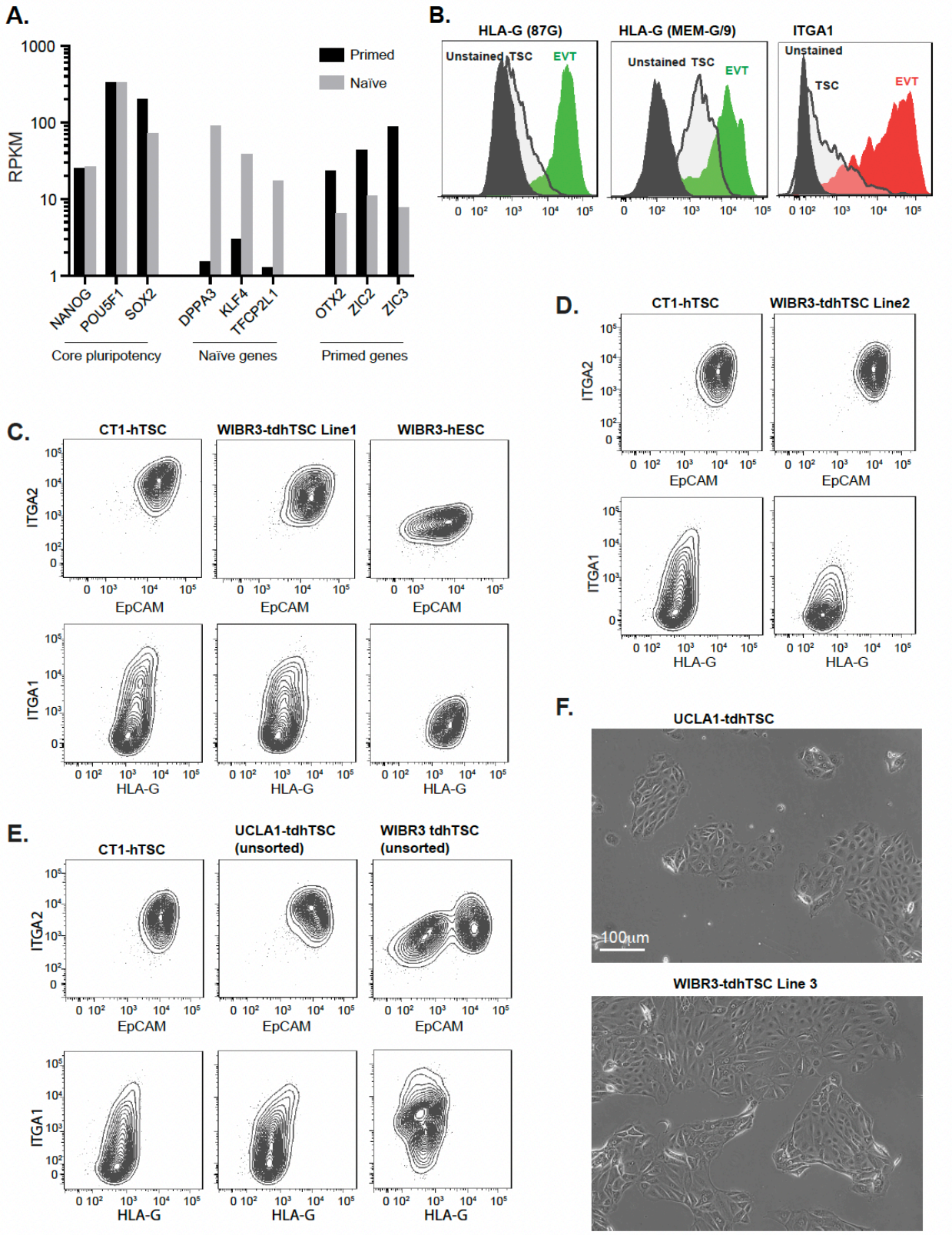
A.
Primed
Naïve
RPKM
1000
100
10
1
NANOG
POU5F1
SOX2
DPPA3
KLF4
TFCP2L1
OTX2
ZIC2
ZIC3
Core pluripotency
Naïve genes
Primed genes
B.
HLA-G (87G)
HLA-G (MEM-G/9)
ITGA1
Unstained TSC
EVT
Unstained
TSC
C.
CT1-hTSC
WIBR3-tdhTSC Line1
WIBR3-hESC
ITGA2
ITGA1
EpCAM
HLA-G
D.
CT1-hTSC
WIBR3-tdhTSC Line2
E.
CT1-hTSC
UCLA1-tdhTSC (unsorted)
WIBR3 tdhTSC (unsorted)
F.
UCLA1-tdhTSC
100μm
WIBR3-tdhTSC Line 3

Figure S2. Transdifferentiation of hESCs to putative hTSCs and purification via FACS sorting. Related to Figure 2. A. Expression of primed and naïve hESC markers in primed and Day 10 naïve cells (which were used as the starting point for generation of WIBR3 tdhTSC Line 1) as measured by RNA-sequencing of one replicate. B. Flow cytometry validation of HLA-G and ITGA1 antibodies used in other figures. Note elevated HLA-G and ITGA1 signal in EVT. Representative of n= 5 – 15 independent experiments per antibody C. Flow cytometry of WIBR3 tdhTSC Line 1, 16 days after sorting, with CT1 and WIBR3 hESCs as comparisons. Representative of n= 2 (hESCs), and n=3 (WIBR3 tdhTSC L1) independent flow cytometry experiments conducted with these lines. D. Flow cytometry profile of WIBR3 tdhTSC Line 2. Representative of n= 3 independent experiments. E. UCLA1 and WIBR3 hESCs were reverted and transferred to hTSC media, with flow cytometry conducted 7 days later. Note formation of ITGA2^{hi} EpCAM^{hi} ITGA1^{lo} cells in both lines. Same CT1 control was used in D. and E. F. Photographs of sorted ITGA2^{hi} EpCAM^{hi} ITGA1^{lo} UCLA1 tdhTSC Line 1 and WIBR3 tdhTSC Line 3.

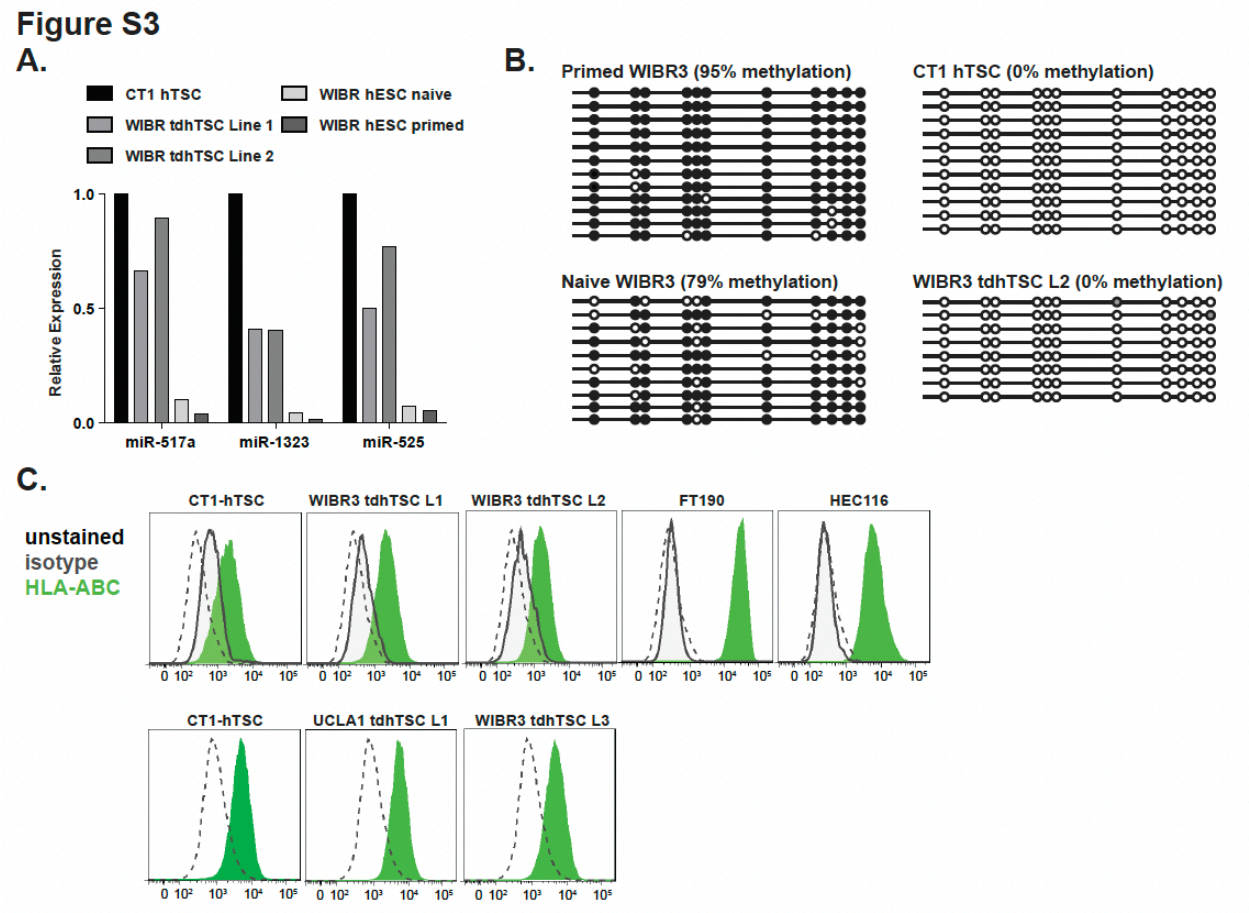

Figure S3. Transdifferentiated hTSCs show hallmarks of placental identity. Related to Figure 3. A. RT-PCR of three miRNA that are generated from the placental C19MC transcript. n=1 biological replicate. B. Bisulfite PCR of the ELF5 locus for the Primed, Naïve and WIBR3 tdhTSC L2, as well as control CT1 line. Each CG site is indicated with a circle, with an empty circle indicating an unmethylated CG, a black circle indicating methylation, and a gray circle indicating non-informative sequencing. Note modest demethylation in naïve culture and dramatic demethylation upon transdifferentiation. C. Flow cytometry for a pan-HLA antibody in CT1, WIBR3 tdhTSC Lines 1 and 2, FT190 and Hec116. Unstained, isotype control, and pan-HLA staining profiles are indicated. Representative of n=2 independent experiments.

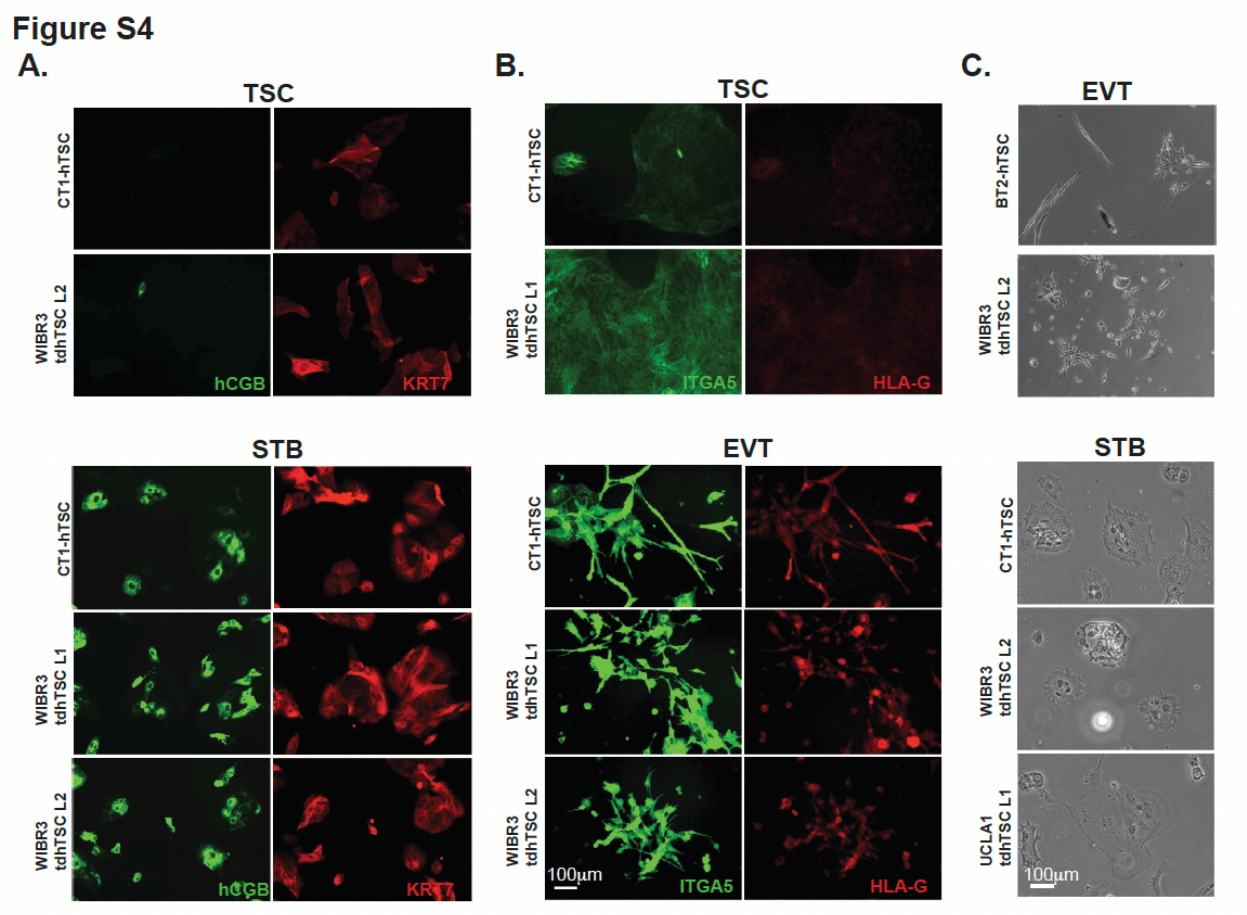

Figure S4. Differentiation capacity of tdhTSCs. Related to Figure 4. A, B. Immunofluorescent staining of cells indicated with STB marker (hCGB), EVT markers (ITGA5, HLA-G) or a pan-placental marker (KRT7). Note gain of hCGB upon STB differentiation (A) and gain of spindly mesenchymal morphology and increased staining for ITGA5 and HLA-G upon EVT differentiation (B). C. Light microscopy photos of EVTs and STBs indicated.

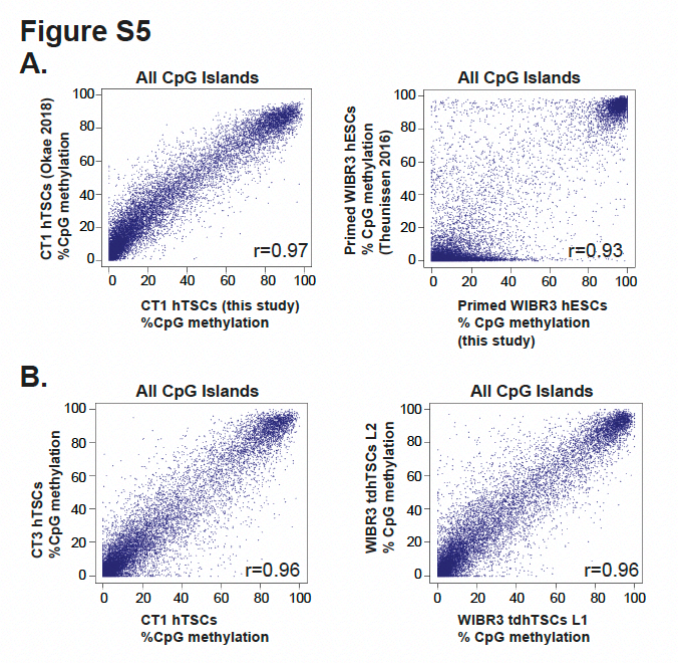

Figure S5. Global methylation patterns of tdhTSC. Related to Figure 5. A. Scatterplot showing CpG island methylation for each CpG island in our sample (X-axis) and published data (Y-axis). Note high correlation between new and published data. B. Scatterplot showing CpG island methylation for similar samples (CT1 vs. CT3, WIBR3 tdhTSC L1 vs. L2).

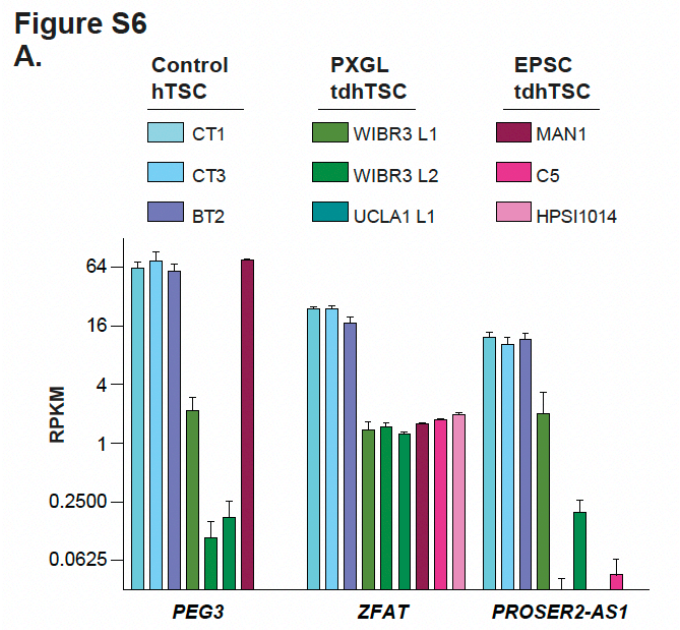

Figure S6. Imprinting abnormalities in tdhTSC. Related to Figure 6. A. Expression of the three imprinted genes indicated in control and tdhTSCs. Data for EPS tdhTSCs are from published sources.(Gao et al., 2019) n=2 (all tdhTSC lines), n=4 (CT3, BT2) or n=7 (CT1) biological replicates.

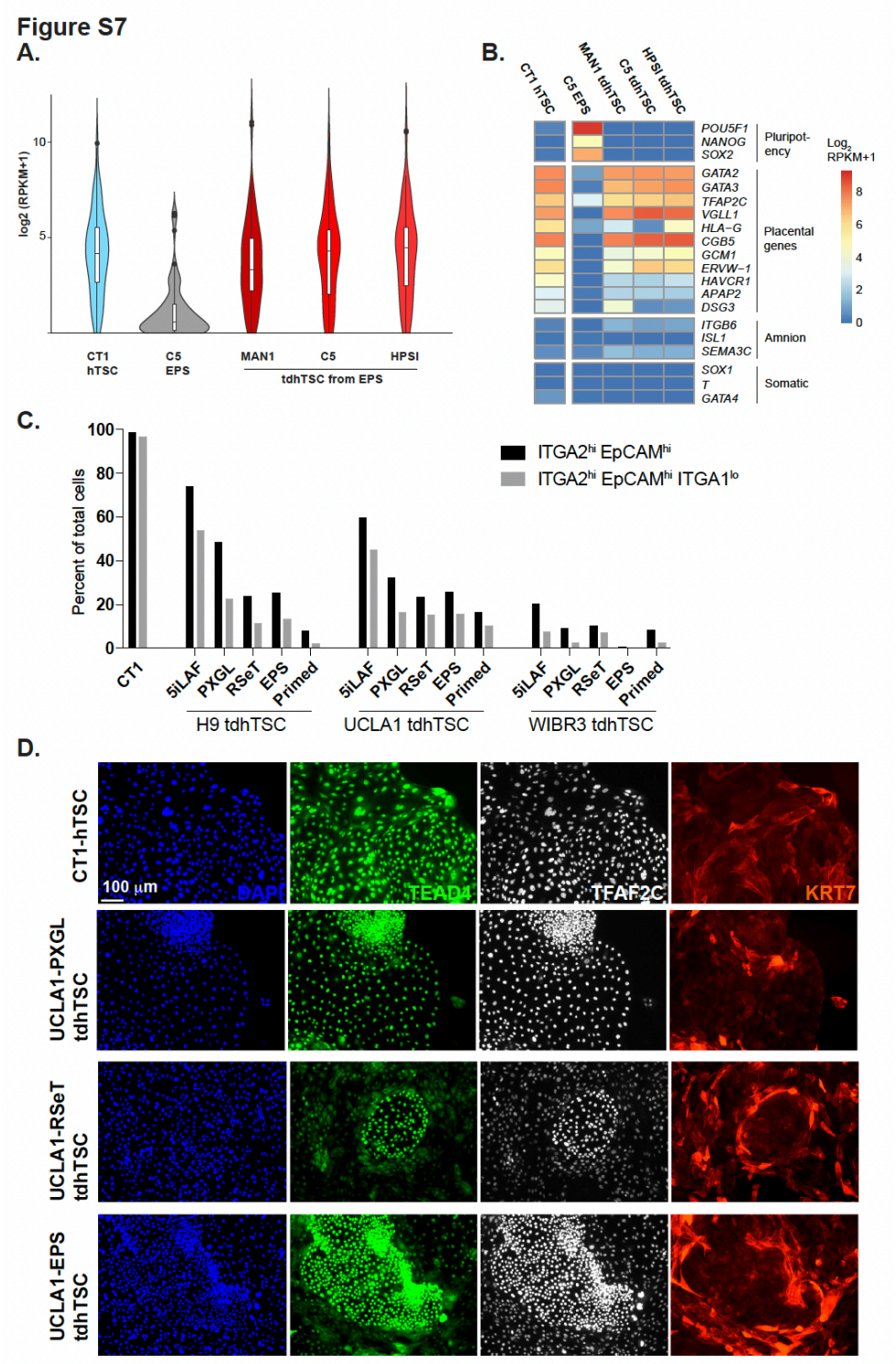

Figure S7. Comparative transdifferentiation capacity from different media conditions. Related to Figure 7. A. Expression of 89 placental genes (same as in Figure 3D) in tdhTSCs derived from EPS cells. Expression of each gene, using an average of all replicates for a given cell type, is indicated as a single point on the violin plot. n=2 (EPS and tdhTSC) or n=7 (CT1) biological replicates. Data for EPS cells and

EPS tdhTSCs are from published sources.(Gao et al., 2019) B. Expression of markers indicated from RNA-seq data. Data for EPS cells and EPS tdhTSCs are from published sources.(Gao et al., 2019) Data from n=2 (EPS and tdhTSC) or n=7 (CT1) biological replicates are averaged. C. Percentage of $ITGA2^{hi}$ $EpCAM^{hi}$ and $ITGA2^{hi}$ $EpCAM^{hi}$ $ITGA1^{lo}$ cells after hESCs of the line and starting conditions indicated are cultured in hTSC media for 15 days. n=1 experiment. D. Immunofluorescent images of control CT1 hTSCs and tdhTSCs derived from hESCs cultured in naïve (PXGL) and primed-like (EPS, RSeT) conditions. Note uniform staining for the three indicated markers in CT1 and PXGL-derived hTSCs, but a mixture of $TEAD4^{hi}$ and $TEAD4^{lo}$ cells in EPS or RSeT derived tdhTSCs. n=1 experiment.

2.9 Supplemental Table Captions

(Stem Cell Reports, https://doi.org/10.1016/j.stemcr.2020.06.003)

Table S1. STR analysis of WIBR3 hESCs and TSC. Related to Figure 2.

Table S2. Descriptions of transdifferentiations. Related to Figures 2 and 7. Description of circumstances of generation of each cell line, efficiency of production of ITGA2hi EpCAMhi and ITGA2hi EpCAMhi ITGA1lo cells, and figures in which each cell line was used.

Table S3. Sample description and mapping statistics. Related to Figures 3, 5, 6.

Table S4. RPKM of all samples. Related to Figures 3, 5, 6.

Table S5. Expression of trophoblast-specific genes in RNA-seq samples. Related to Figure 3. Expression data used to generate Figure 3D.

Table S6. Methylation data. Related to Figures 5,6. CpG islands with CT1-hTSC-specific methylation, promoters with hESC-specific methylation, and putative gatekeeper genes and their expression levels in different samples are all shown.

Table S7. Genes differentially expressed between control hTSC and tdhTSC. Related to Figure 6. First two panels: Genes that show differential expression between hTSCs (CT1, CT3, BT2) and primed hESCs (WIBR3, UCLA1) are listed, along with fold-change and log2 read count per million. Positive fold-change value indicates higher expression in hESCs. Third and fourth panels: Genes that show differential expression between control hTSCs (CT1, CT3, BT2) and tdhTSCs (WIBR-tdhTSC Line 1, WIBR3-tdhTSC Line 2, UCLA1 tdhTSC) are listed. Positive fold-change value indicates higher expression in tdhTSCs.

CHAPTER 3: Reduction of GCM1 Expression by Hypoxia or PI3K Pathway Inhibition Prevents Spontaneous Differentiation of Trophoblast Stem Cells

Jessica Cinkornpumin[1], Sin-Young Kwon[1], Jacinthe Sirois[1,2], James Goldberg[1], Joy Zhang[1], Stephen J. Renaud[3], Soumen Paul[4,5,6], and William A. Pastor[1,2]

[1]Department of Biochemistry, McGill University, Montreal, Quebec, Canada [2]The Rosalind & Morris Goodman Cancer Institute, McGill University, Montreal, Quebec, Canada [3]Schulich School of Medicine and Dentistry, University of Western Ontario, London, Ontario [4]Department of Pathology and Laboratory Medicine, University of Kansas, Kansas City, United States [5]Institute of Reproduction and Perinatal Research, University of Kansas, Kansas City, United States [6]Department of Obstetrics and Gynecology, University of Kansas, Kansas City, United States

Keywords: Placenta, cytotrophoblast, Trophoblast stem cell, extravillous trophoblast, syncytiotrophoblast, GCM1, CDKN1C, differentiation, placental villi, cell column, hypoxia

3.1 Abstract

The placenta develops alongside the embryo and nurtures fetal development to term. During the first stages of embryonic development, due to low blood circulation, the blood and ambient oxygen supply is normally very low (~1-2% O2) and gradually increases upon placental invasion. While a hypoxic environment is associated with stem cell self-renewal and proliferation, persistent hypoxia may have severe effects on differentiating cells and could be the underlying cause of placental disorders. We find that human trophoblast stem cells (TSC) thrive in low oxygen, whereas differentiation of syncytiotrophoblast (STB) and extravillous trophoblast (EVT) is critically affected by hypoxic conditions. We find that the pro-differentiation factor GCM1 (human Glial Cell Missing-1) is downregulated in low oxygen. Knock-out of GCM1 in TSC caused impaired EVT and STB formation and function, reduced expression of genes that respond to differentiation, and maintenance of self-renewal genes. Chromatin immunoprecipitation of GCM1 showed enrichment of GCM1 specific binding near key transcription factors upregulated upon differentiation, including a role in contact inhibition and expression of *CDKN1C*. Finally, we find that reduction of GCM1 expression by inhibition of the PI3K pathway prevents spontaneous differentiation in an in vitro model of trophoblast differentiation.

3.2 Introduction

Placentation establishes the maternal-fetal interface that further ensures the successful progression of the pregnancy.(Huppertz, 2007) During the first major specification event at the early blastocyst stage, the embryo undergoes a series of divisions and cell migrations This forms the outer cell mass, termed the trophectoderm (TE) and inside, the inner cell mass, which contains the epiblast that gives rise to the embryo proper. Cells from the TE, upon implantation, quickly differentiate into cytotrophoblast (CTB) that can give rise to the 2 major placental lineages: the extravillous trophoblast (EVT) and syncytiotrophoblast (STB). The early implantation embryo is comprised of many villi made up of CTBs that quickly divide and differentiate into STB that create a space, the cytotrophoblast shell, for the emerging villus structures. CTBs line the inside of the villus and STBs line the outside of the villus and mediate nutrient, oxygen (O_2), and waste exchange. At the tips of this villus, the CTBs then differentiate into EVTs through the cell column. As these EVTs mature, subtypes of EVTs act to remodel the maternal decidua to anchor the placenta and spiral arteries to allow for proper blood flow to the placenta. Establishing this network of organized cell types and tissue structures is essential to fetal health and development as it is essential to maintain the connection between the mother and the fetus.(Baines & Renaud, 2017; Hamilton & Boyd, 1960; Hemberger et al., 2020; Knöfler et al., 2019; Lyall et al., 1999; Turco & Moffett, 2019)

During the first trimester of human pregnancy, some EVTs establish plugs blocking the uterine spiral arteries. For the initial stages of the first trimester, the conceptus develops in a relatively low oxygen environment (~2.5% O_2, Hypoxia).(Jauniaux et al., 2001; Rodesch et al., 1992) After approximately eight weeks, the trophoblast plugs disintegrate and endovascular extravillous cytotrophoblasts (eEVT) invade the uterine spiral arteries where they degrade resident

smooth muscle and endothelial cells (ECs) and replace them with a trophoblast cells.(Sato, 2020) This expands the arterial, provides blood to the placenta, and raises oxygen tension (~8.6% O_2).(Chang et al., 2018; Genbacev et al., 1997; Rodesch et al., 1992) The hypoxic niche supports embryonic organogenesis and placental angiogenesis, promotes cytotrophoblast proliferation, and suppresses trophoblast differentiation, largely due to the activity of oxygen-regulated transcription factors (TFs) that mediate physiological adaptation to changes in oxygen tension.(Genbacev et al., 1997; Simon & Keith, 2008; Tuuli et al., 2011) In previous observations, mice carrying deletions of *Hif1α/Hif2α* or binding patterner, *Arnt,* both led to midgestational embryonic lethality possibly due to reduce proliferation of junctional zone progenitor cells and decrease in labyrinth vascularization. Inactivation of *Hif1* antagonist *Phd2*, *Vhl*, and Pparg, while also embryonic lethal, saw expansion of the junctional zone at the cost of reduce labyrinth volume.(Barak et al., 1999; Cowden Dahl et al., 2005; Gnarra et al., 1997; Kozak et al., 1997; Maltepe et al., 1997; Takeda et al., 2006) When explants of human placental villi are cultured in high oxygen, ITGA1 expression is gained at the edges of the explant where villous tips are found, marking mature EVTs. In low oxygen, instead of ITGA1 expression at these same villous tips, proliferation of KRT7 marked cells (a pan-trophoblast marker) and increased expression of HLA-G cells are found.(Genbacev et al., 1997) In this approach, oxygen tension is seen to play an essential role in defining human trophoblast stem cells and differential placental states. This suggests that oxygen levels might have an active role in regulating differentiation during placenta formation.

Several mechanisms play important roles in TE specification, such as HIPPO signaling that relies on its co-activator, Yes-associated protein (YAP) to interact with TEA domain 4 (TEAD4) causing it to nuclear-localize and turn on essential TE establishing gene, CDX2, in pre-implantation mouse and human embryos and maintaining stemness in murine TSCs.(Home et al.,

2012; Meinhardt et al., 2020; Saha et al., 2020) WNT-NOTCH signaling is more crucial post-implantation and therefore important for differentiation of the trophoblast sub-lineages. WNT-NOTCH signaling factors denote several roles in the formation of the villus and the cell column.(Dietrich et al., 2022; Haider et al., 2016; Knofler & Pollheimer, 2013; Sonderegger et al., 2010; Zhao et al., 2017) Another such TF, Glial cells missing 1 (*GCM1*), is expressed in all sub-lineages of the trophoblast, yet its role is still not well defined. Single cell analysis of pre-gastrulation embryo and first trimester placenta, show *GCM1* expression in CKT7 positive cell lineages as early as CTBs and its further induction in differentiated subtypes of STBs and invasive EVTs.(Arutyunyan et al., 2023; Liu et al., 2018; Petropoulos et al., 2016; Xiang et al., 2020) GCM1 is important for the induction of EVT associated genes, ASCL2 and the WNT antagonist, NOTUM, and knockdown of GCM1 prevents downstream differentiation into either STBs or EVTs.(Jeyarajah et al., 2022) Since GCM1 induction coincides with the branch point of differentiation and increase in oxygen levels, it suggests that GCM1 and oxygen could have a more dynamic function in placental formation that warrants further investigation.

3.3 Results

3.3.1 Hypoxia Maintains Trophoblast Stemness and Increases Cell Proliferation

To determine the effect of hypoxia on hTSC growth, we took hTSCs commonly maintained in 20% O_2 and cultured them in 20%, 5% and 2% O_2. After the first 72hrs of culture we performed flow cytometry for the hTSC cell surface markers ITGA6 and EpCAM, and the EVT markers ITGA1 and HLA-G (Fig. 1A). We observed noticeable depletion of ITGA1 and slightly increased HLA-G expression in lower oxygen in several hTSC lines (Fig. 1A, 1B), similar to what was observed in explants by Genbacev and colleagues. Continued culture of these cells in their

respective oxygen conditions resulted in near complete loss of ITGA1^{hi} expression cells in both 5% and 2% O_2 (Fig. S1A). Similarly, hTSCs cultured in 20% O_2 showed some spontaneous expression of the STB marker hCGB, which was reduced in low oxygen (Fig. 1C, 1D). Regions of dense cell-to-cell contact showed expression of the differentiation marker NOTCH1 in hTSCs at 20% O_2, but not in lower oxygen (S1B). In addition to lower expression of differentiation markers, we observed higher cell density in lower oxygen culture conditions (Fig. 1C, 1E). Collectively, these results indicated that low oxygen aids in stemness and proliferation, while high oxygen promotes spontaneous differentiation.

Based on the above findings, we took TSC from the varying oxygen levels described above to observe differentiation potential in these diverse oxygen conditions. TSC cultured in any of the varying oxygen levels successfully differentiated to EVT or STB if differentiation was undertaken at 20% O_2 (Fig. 1F, 1H, 1J). However, when we perform the same differentiation in the low oxygen levels, we observed dramatic impairment of differentiation (Fig. 1G, 1I). EVT differentiated in low oxygen failed to downregulate EpCAM or upregulate ITGA1 and HLA-G (Fig. 1F, 1G), while STBs 2% O_2 showed a higher percentage of cells retaining TEAD4 and a lower percentage expressing hCGB (Fig. 1I, 1J). Thus, oxygen promotes both spontaneous and directed differentiation of hTSCs.

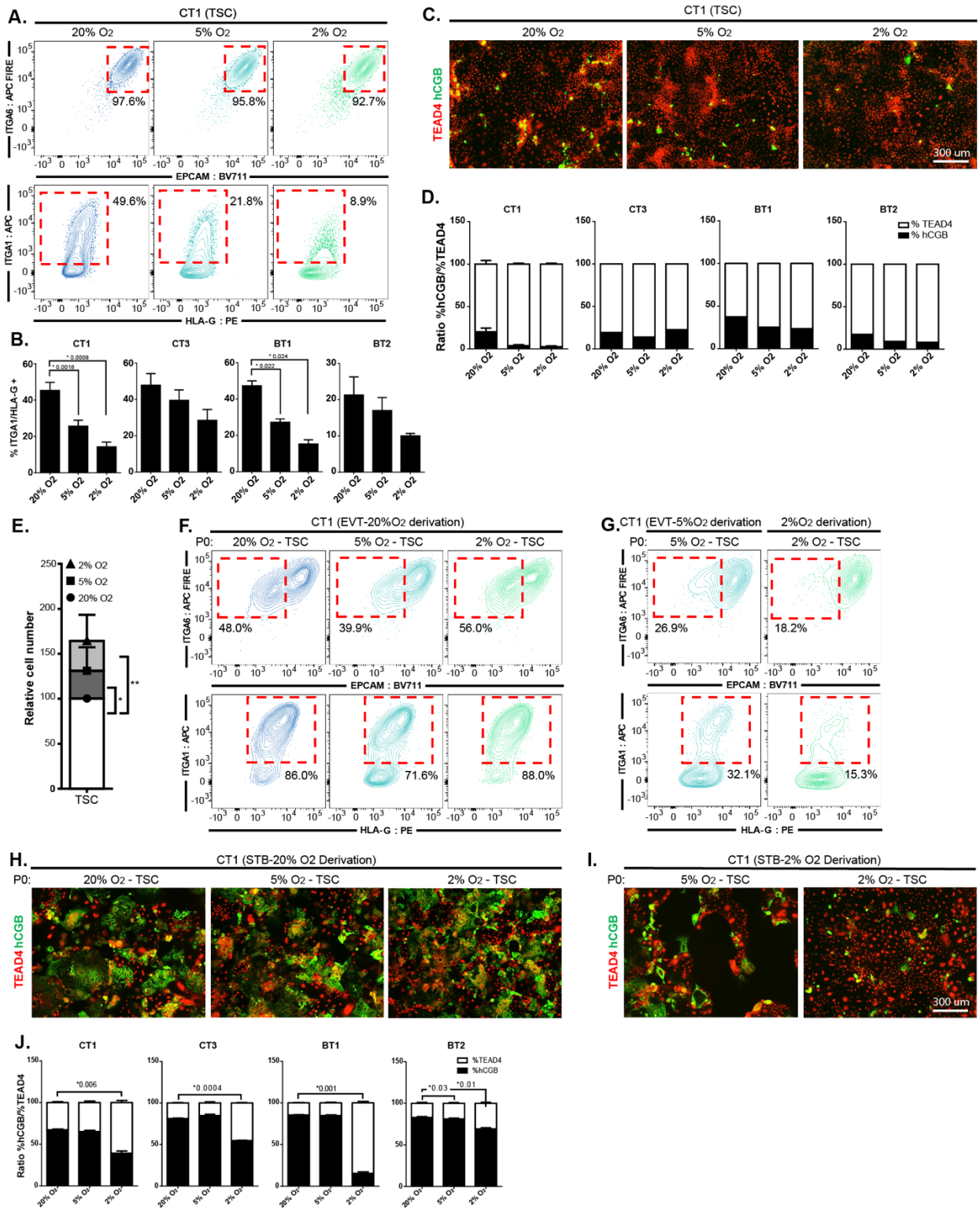

Figure 1. TSC culture in varying oxygen conditions reveal reduction of differentiation capacity. A. Trophoblast stem cells were cultured for 72hrs in varying levels of oxygen (20%, 5%, 2% O_2). Flow cytometry was used to assess the effects of culture in varying oxygen tensions. ITGA6 and EpCAM being

markers for TSCs, and ITGA1 and HLA-G being a marker to EVT differentiation. **B.** We compared the measurement of ITGA1+/HLA-G+ across multiple cell lines and observed similar phenotypes (4 cell lines, n=3 for each cell line). **C., D.** Spontaneous differentiation of hTSC to STB is indicated by loss of TEAD4 and increase in hCGB staining in a cell. **C.** Shows representative images of cells, with lower STB formation in low O_2. **D.** Quantification of spontaneous hCGB expression across multiple cell lines (4 cell lines, n=4 for each cell line). **E.** Relative numbers of TEAD4+ cells per unit area (4 cell lines, n=4 for each cell line). **F.** EVT differentiation in 20% O_2 starting with hTSC in oxygen concentration indicated. Successful differentiation is marked by the upregulation of surface markers ITGA1 and HLA-G and downregulation of EPCAM. **G.** EVT differentiation undertaken at oxygen level indicated. **H., I., J.** Successful STB differentiation is shown by the fusion of syncytium of multiple cells (**H.**, **I.**), the loss of TEAD4 expression (**H.**, **I.**), and expression of hCGB (**H., I., J.**). As with EVT, TSC cultured in any oxygen level can differentiate properly to STB, but in the presence of reduced oxygen levels they have an inability to make STB. * p <0.05; unpaired t test comparing each sample to the controls. mean ± SEM

3.3.2 Trophoblast Differentiation Transcription Factor, GCM1, is Oxygen Sensitive

We performed RNA-sequencing (RNAseq) on 3 TSC lines (CT1, CT3, BT2; female) cultured in the 3 oxygen conditions (20%, 5%, 2% O_2). Principle component analysis (PCA) shows a strong dependence of gene expression on oxygen conditions (Fig. 2A, S2A). Gene cluster and enrichment analysis indicate that the genes in Cluster 1 (gene up regulated in 2% O_2) correspond to hypoxia response and WNT activation, while both Cluster 1 and Cluster 2 (upregulated in 20% O_2) showed enrichment for various placental terms (Fig. 2B, 2C).

Genes associated with EVT and STBs expression such as *ITGA1*, *OVOL1* and various chorionic gonadotropin genes were among the genes downregulated in the 2% O_2 condition (Fig. 2D, 2E, Table S1, S2B). Using published gene expression data, we identified 100 genes specific to EVT and STB differentiation and 100 genes specific to TSC relative to these cell types. hTSC genes were higher in 2% O_2, while EVT and STB genes were lower, further indicating that hypoxia broadly suppresses differentiation gene expression (Figure 2F, Table S2). Interestingly, consistent with flow cytometry data (Figure 1A) and observations in explant, HLA-G was positively

regulated by hypoxia (Figure 2E), indicating that hypoxia promotes expression of this marker even as it suppresses the overall EVT differentiation program.

Analysis of known TF targets appropriately indicated that HIF1A was the most enriched TF associated with Cluster 1 (hypoxia) expression, while *GCM1* was associated with high oxygen (Figure S2C, S2D). *GCM1* (Glial cells missing 1), which is expressed in hTSCs, but upregulated upon differentiation (Figure S2E), was itself strongly downregulated in low oxygen conditions at the RNA and protein level (Fig. 2D, 2E, S2F, Table S1). GATA3, which is reported to repress GCM1 by an indirect mechanism (Wang et al., 2022a), was upregulated in 2% O_2, but only slightly, suggesting another mechanism at work. We then used CRISPR interference (CRIPSRi) to repress *VHL*, the prolyl hydroxylase which oxidizes HIF1α in high ambient oxygen and targets it for destruction. Repression of *VHL* in 20% O_2 led to dramatic upregulation of *IGFBP3*, the most hypoxia responsive gene in hTSC and a known HIF1α target.(Natsuizaka et al., 2012) Hypoxia induces *IGFBP3* in esophageal squamous cancer cells through HIF-1α-mediated mRNA transcription and continuous protein synthesis.(Natsuizaka et al., 2012) We also observed downregulation of *GCM1* expression, indicating that *GCM1* is negatively regulated by the canonical HIF1α pathway (Figure S2G).

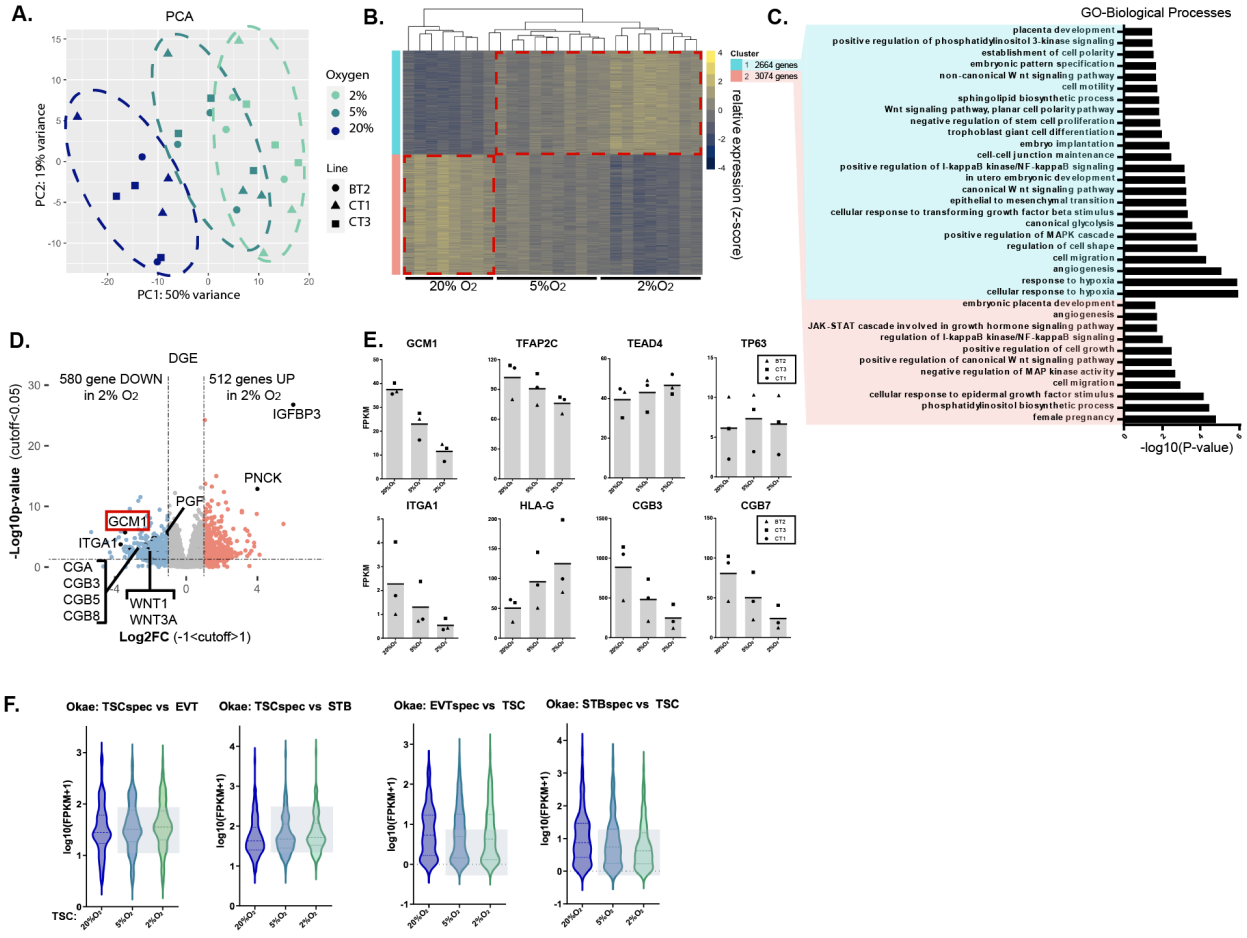

Figure 2. RNAseq of TSC in ambient oxygen versus hypoxia reveals many downregulated differentiation genes. A. Principle component analysis (PCA) showing gene expression difference when TSC are cultured in varying oxygen conditions. (3 cell lines; BT2, CT1, CT3; n=3 for each line in each condition) **B.** Hierarchical Gene Clustering indicate the 5% O_2 and 2% O_2 cluster more closely together than to 20%O_2 TSC. 5% O_2 seem to have an ambiguous repression expression profile between the two spectrums. Red dotted lines indication the shift in gene expression from 20% O_2 and 2% O_2 labeled as Cluster 1 and Cluster 2 **C.** GSEA analysis of Cluster 1 and Cluster 2 using DAVID (https://david.ncifcrf.gov/tools.jsp/). **D.** Volcano plot comparing the gene expression differences between TSCs cultured in 20% O_2 to TSCs cultured in 2% O_2. **E.** Bar graph of specific genes of interest using averaged FPKM of each cell type from the 3 replicates. **F.** Violin plots of overall FPKM of specific genes sets plotted for each TSC oxygen culture conditions (Gene set derived from Okae et al. 2018, Download .xlsx (7.63 MB)).

3.3.3 GCM1 is Essential for the Differentiation into Trophoblast Lineages

Since GCM1 is highly sensitive to oxygen levels and implicated in hTSC differentiation (Wang et al., 2022a), we generated GCM1-knockout (GCM1KO) by deleting a small genomic region in exon 2 just after the ATG-start site to disrupt the translation of the DBD (DNA binding domain) (Chiu & Chen, 2016) and subsequent functional protein regions in TSC (Fig. 3A). This is labeled as GCM1KO1. Unexpectedly, this deletion made a less preferrable alternative slice site available, which spliced in before exon 3 (Fig. S3A). While this deletion still had the desired frameshift, we generated an addition line deleting the entirety of exon 3 (Fig. 3A, S3A). This is labeled GCM1KO2. TSCs targeted with a non-targeting (NT) sgRNA showed ubiquitous nuclear expression of GCM1, with TEAD4 loss in the highest GCM1 expressors (Fig. 3B), while both GCM1 KO lines showed loss of specific GCM1 signal (Fig. 3B). To functionally study GCM1 ability to drive differentiation, we performed differentiation into EVTs and STBs. In both cases, GCM1KO TSC failed to exit stemness and differentiate; reminiscent of the results seen when cultured in low oxygen (Fig. 3C-3G). GCM1KO-EVTs failed to turn on ITGA1^{hi}/HLA-G^{hi} (Fig. 3C, 3D). Likewise, both GCM1KO cell lines failed to form STB (using STB3D method described in Okae et al. 2018). Instead of differentiating into STB3D, expressing SDC1 and secreting abundant hCGB; they continued active proliferation and formed large clusters that lacked expression of these genes (Fig. 3E-3G). Thus, as it has been reported recently by other groups, GCM1 is essential for EVT and STB differentiation.(Jeyarajah et al., 2022)

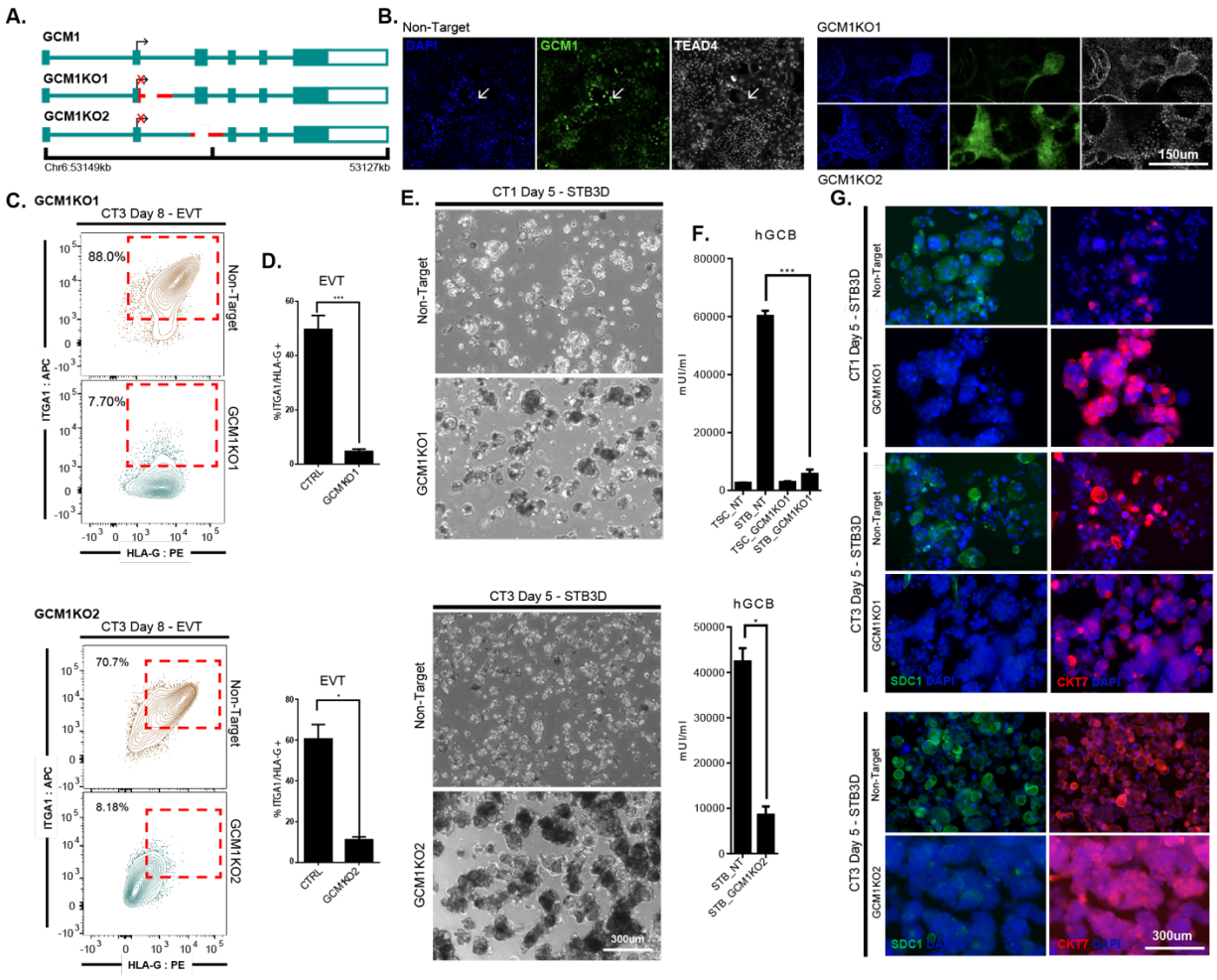

Figure 3. Observations into GCM1 deletion on TSC differentiation capacity. A. Strategies for mutation of GCM1 using a two sgRNA CRISPR approach. Lines were generated by deletion of the exon2/intron2 boundary, and by ablation of exon 3, either of which should disrupt the DBD of GCM1. **B.** Immunofluorescence indicated that NT-TSC express GCM1 at regions of high density. Specific nuclear staining for GCM1 is not observed in either KO lines. **C.** Flow cytometric analysis from EVT differentiation of GCM1KO and control (non-targeted) TSC. NT cells differentiation produce ITGA1^{hi}/HLA-G^{hi} cells whereas GCM1KO TSC do not. **D.** Bar graph plot the average measurement of ITGA1^{hi}/HLA-G^{hi} population from each differentiation condition (GCM1KO1:CT1 n=2, CT3 n=3; GCM1KO2:CT3 n=3; NT-control n=5). **E.** NT-STB3D form by the fusion of TSCs to make one syncytium and to make a fluid filled bubble. GCM1KO-STB3D do not make this bubble and instead resemble proliferating TSCs. **F.** hCGB ELISA was perform using supernatant from each condition. The average measurements of hCGB secretion confirm significantly reduce secretion from GCM1KO-STB3D samples (GCM1KO1:CT1 and CT3, n=5; GCM1KO2:CT3, n=3). **G.** STB3D differentiation show lack of SDC1 expression from GCM1KO lines.

(Image are from the several cell-lines as a representation of the experiments performed here.) * p <0.05; *** p <0.0001unpaired t test comparing each sample to the controls. mean ± SEM

3.3.4 GCM1 Regulated the Switch from WNT to NOTCH Signaling

We performed RNAseq from GCM1KO generated lines in TSC, EVT, and STB to explore the intrinsic mechanisms that are defective in GCM1KO background. PCA and correlation matrix mapping show that GCM1KO-EVT and STB cluster more closely to TSCs from which they originated (Fig. 4A, S4A, S4B), than with differentiated EVT and STB in non-targeted cells. Using the same 100 gene set from Figure 2F, we confirmed that without GCM1, TSC specific gene sets were unable to be turned off and EVT and STB-specific gene sets were not turned on (Fig. 4B, Table S3). Interestingly, some EVT and STB specific genes were already down regulated in GCM1KO-TSC and remained low when differentiated to EVT or STB (Fig. S4C, S4D, Table S3). Confirming that even low levels of GCM1 expression is continually pushing differentiation.

We performed hierarchical gene clustering of GCM1KO-EVT and GCM1KO-STB along with starting cells and differentiated control (Fig. 4C, 4D, Table S4). In the GCM1KO-EVT comparison, Cluster 1 and 4 showed genes that were downregulated in GCM1KO-EVT relative to control differentiation. Cluster 1 included the TGF-B signaling pathway, the EVT gene *NOTCH2*, and *WWTR1*, a gene essential for EVT maturation and prevention of STB cell fate.(Ray et al., 2022) Cluster 4, which consists of genes especially downregulated in GCM1KO-EVT, is enriched for WNT signaling pathway components. Cluster 2 consists of genes aberrantly activated in GCM1KO-EVT, while Cluster 3 consists of stem cell genes that are downregulated in control but not GCM1KO-EVT. Most interestingly in Cluster 2, we found an increase in *ITGA2* which is seen in the most proliferative population found at the base of the cell column (Lee et al., 2016), highlighting GCM1's role in exit of CTB/TSC lineages. Similarly in the GCM1KO-STB analysis,

we see up regulation of *ITGA2*, *NOTCH3*, and *FZD5* in Cluster 1 and 4 (higher in KO), all of which are strong TSC markers.(Arutyunyan et al., 2023; Dietrich et al., 2022; Dietrich et al., 2023) In Cluster 2 and 3 (higher in WT) *NOTCH2* is reduced, as well as P13K/pAKT signaling (Fig. 4C, 4D, Table S4).

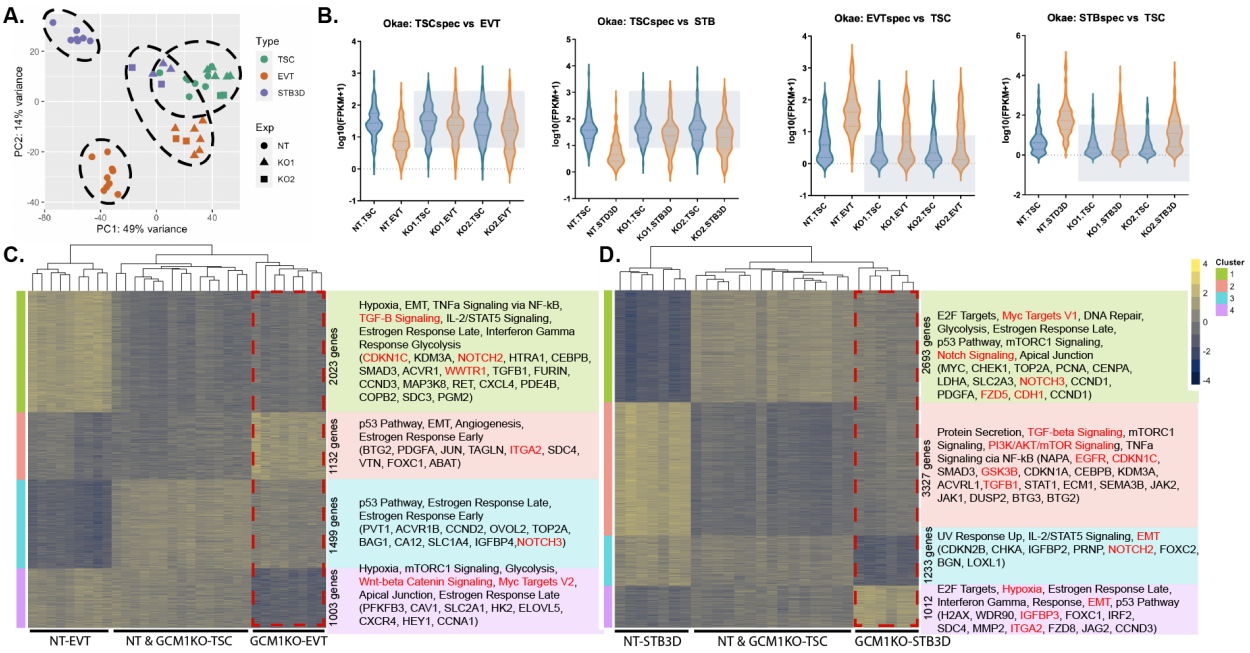

Figure 4. GCM1KO EVT and STB are deficient in cells specifc expression. A. PCA comparing NT and GCM1KO TSC, EVT, and STB. Note that GCM1KO cells cluster closer to the TSC population (GCM1KO1:CT1 n=2, CT3 n=3; GCM1KO2:CT3 n=3; NT-control n=5). **B.** Violin plot displaying Okae et al. 2018 top 100 specific genes to TSC, EVT, and STB for cells indicated. GCM1KO differentiated cell types fail to express differentiation markers and retain expression of TSC markers instead. **C.-D.** GSEA analysis of all clustering defined by heirarchical gene clustering using EnrichR (https://maayanlab.cloud/Enrichr/) reveals several mis-regulated mechanisms in GCM1KO-EVT and STB (Red: highlighting some genes of interest).

3.3.5 GCM1 Driven Activation of EVT and STB Specific Regulators

As failure to express GCM1 affects the differentiation process, we performed Chromatin Immunoprecipitation Sequencing (ChIPseq) for GCM1 from day 3 EVTs (CT3), a timepoint

conducive to successful GCM1 ChIP (Experiment performed and donated from Jeyarajah et al. 2022). We identified 2271 peaks with >4-fold enrichment over INPUT. These peaks corresponded to regions that show higher openness in EVT and STB than in TSC (Fig. 5A, Table S5). Motif analysis showed extremely strong enrichment for the motif of the GCM1 protein, with weaker enrichment for other TFs common in trophoblast (Fig. 5B). We confirmed enrichment at several known GCM1 targets e.g PGF, LMO2, and ASCL2.(Chen et al., 2022; Jeyarajah et al., 2022; Li & Roberson, 2017) One of the strongest enrichment sites in the genome was found within the CDKN1C/KCNQ1 imprinted locus, as were several smaller peaks (Fig. 5C). This significance will further be discussed below. Annotation of genes whose TSS were within 10kb of genes associated TSS show enrichment for pathways such as apical junction and TGF-B signaling (Fig. 5D). This coincides with required lateral epithelium formation for growing villus and increased TGFB signaling for EVT maturation. We further used RAD (Region Associated DEG) analysis to correlate proximity of a peak to the up and down regulated genes in various gene sets. Genes downregulated in GCM1KO cells were found in proximity to GCM1 ChIPseq peaks (Figure 5E).

ATAC-seq analysis of TSC, EVT, and STB data showed enrichment of the GCM1 motif in EVT and STB-specific regions of open chromatin (Fig. 5F, 5G, 5SB). We also observed association of EVT and STB-specific ATAC-seq peaks with genes downregulated in GCM1KOs of the corresponding cell types (Fig. 5F, 5G). Additionally, genes within 10kb of an EVT-specific open chromatin site are enriched for PI3K activation pathway, while genes within 10kb of an STB-specific site are enriched for aldosterone synthesis and secretion activation in STB which tightly correlates with each cell types of function (Fig. 5F, 5G). Lastly, strong co-enrichment of H3K27Ac with specific ATAC-seq peaks was observed in each cell type (Fig. 5H).

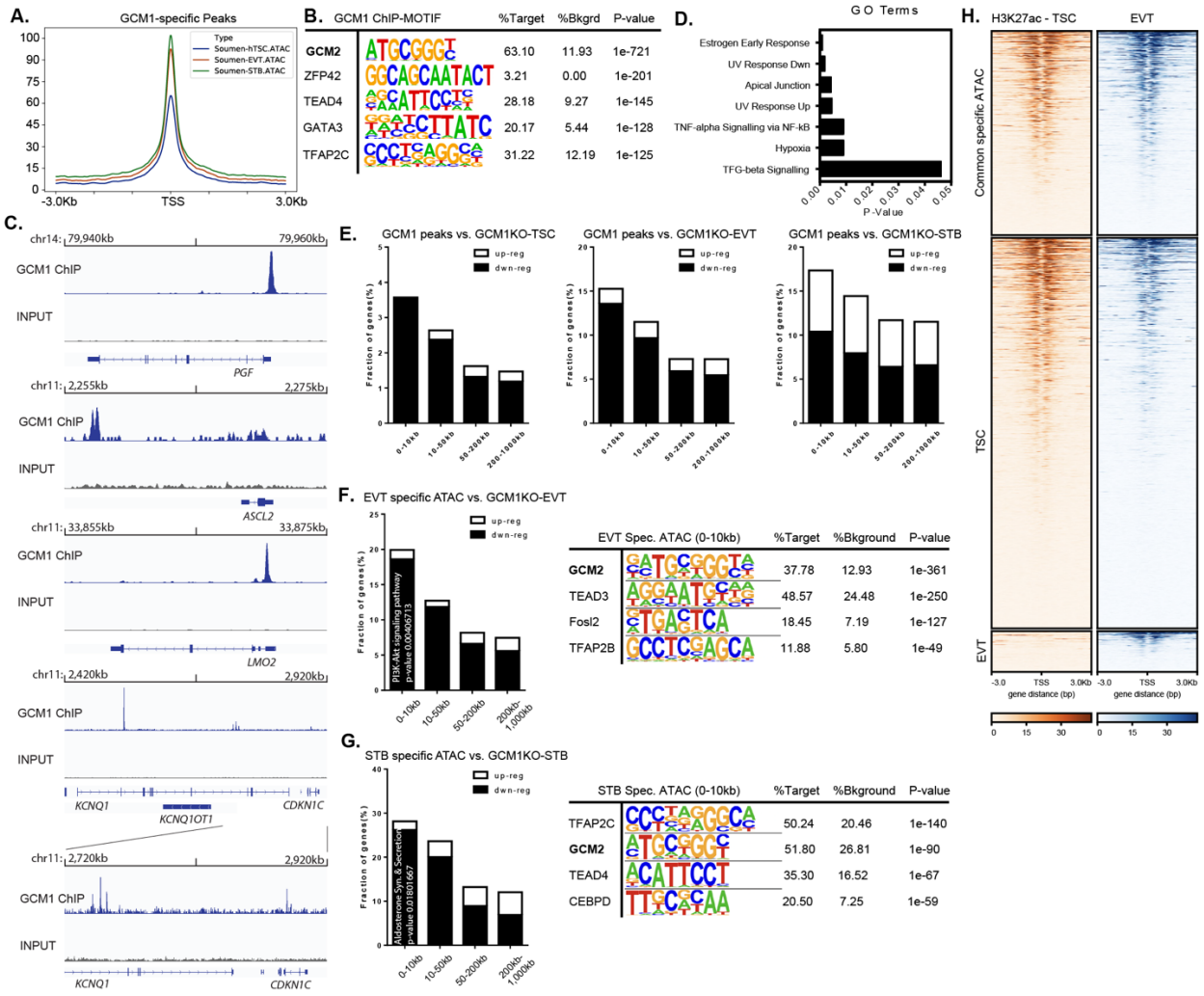

Figure 5. GCM1 ChIP and ATACseq reveal gene patterns driven by GCM1 occupancy. A. ATACseq signals for TSC, EVT, and STB show open chromatin over GCM1 peaks. Note higher enrichment over EVT and STB relative to TSC. **B.** Motif analysis of GCM1 motifs shows very strong enrichment for GCM1. **C.** Annotation of genes whose TSS were within 10kb of gene associated TSS GSEA analysis with EnrichR **D.** GCM1 enrichment of several reported targets including PGF, ASCL2, LMO2, and the KCNQ1-CDKN1C locus. **E.** RAD analysis that measures association of given DEG with given peaks set. This graph shows the special relationship of GCM1 ChIPseq peaks vs. differentially expressed genes in GCM1KO relative to control for the cell type indicated. **F.-G.** RAD (https://labw.org/rad#dashboard) of EVT and STB specific ATAC peaks in relation to GCM1KO DEGs of respective cell types. Additionally, for dysregulated genes within <10kb of a GCM1 peak, we conducted GSEA analysis and indicate top association EVT and STB specific open chromatin sites show enrichment for GCM1 (EnrichR). **H.** Published H3K27ac plotted alongside ATAC-seq data (https://www.ncbi.nlm.nih.gov/geo/query/acc.cgi?acc=GSE204722).(Varberg et al., 2023)

3.3.6 GCM1 Regulates CDKN1C and Trophoblast Overgrowth

CDKN1C ($P57^{kip2}$) is an inhibitor of cell division which binds to cyclin/CDK and blocks cell division.(Takahashi et al., 2019) CDKN1C is an imprinted gene with preferential expression from the maternal allele.(Matsuoka et al., 1995) It belongs to the 11p15.5 gene cluster containing the locus encoding for KCNQ1-KCNQ1OT1 were CDKN1C flanks its end. KCNQ1OT1, which is read in the other direction, encodes for the long-noncoding RNA (LncRNA) that self-regulates the expression of KCNQ1 and the expression of CDKN1C and therefore controls cell division.(Smilinich et al., 1999)

Full hydatidiform moles arise from androgenetic pregnancies in which all genetic material is of paternal origin, and thus placental cells in hydatidiform moles feature loss of *CDKN1C* as well as persistent trophoblastic outgrowth.(Jun et al., 2003) hTSC upregulate *CDKN1C* at high confluence, and in *CDKN1C-/-* hTSC contact inhibition is lost and these cells continue growing after hitting confluence (Fig. 6A).(Takahashi et al., 2019)

We observed *CDKN1C* downregulated in *GCM1* KO hTSC, EVT and STB (Fig. S4C), as well as several GCM1 peaks in the extended KCNQ1 imprinting cluster (Fig 5C). When we grew hTSCs to high confluence, we observed upregulation of *GCM1* and *CDKN1C* in tandem (Fig. 6A, 6B), with more modest increases in other differentiation markers (Fig. 6B). While control cells stop dividing as confluence occurs, GCM1KO cells continue to expand, similar to the reported $CDKN1C^{-/-}$ phenotype (Fig, 6C).(Takahashi et al., 2019) We observe reduced *CDKN1C* expression in hypoxia, where GCM1 is lower (Fig. 6D, S2F). *CDKN1C* still shows upregulation upon STB and EVT differentiation in GCM1 KO cells but reaches a much lower level of expression. These results collectively indicate that GCM1 acts upstream of *CDKN1C* in response to confluence and controls its expression.

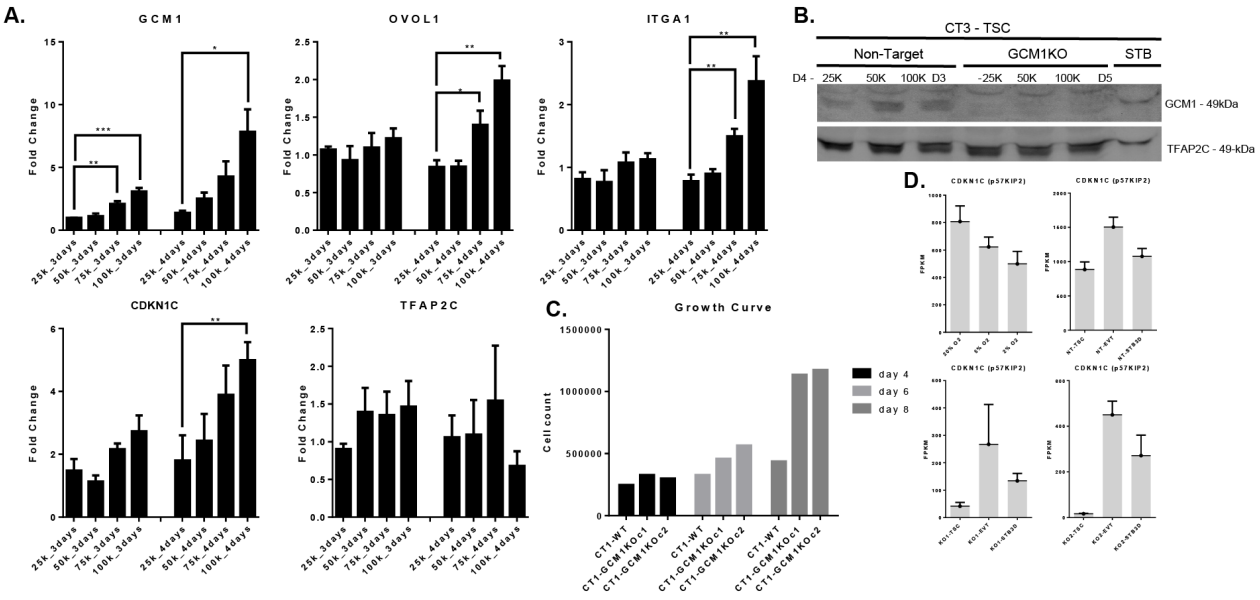

Figure 6. KCNQ1-CDKN1C-GCM1 auto-regulation of cell proliferation. A. hTSC (CT3) are plated at different increasing cell number and allowed to grow for 3 or 4 days. As hTSC proliferate, the varying cell numbers should reach confluency at different times. Gene expression for differentiation-associated genes *GCM1*, *OVOL1*, *ITGA1*, and *CDKN1C* is profiled, with *TFAP2C* as a pan-placental marker. **B.** Protein collected from the variable growth conditions show increased GCM1 in NT-GCM1 over GCM1KO-TSC. STB serving as a control for GCM1 expression. **C.** Growth of WT-hTSC and GCM1KO-TSC were monitored over 8 days. **D.** RNA-seq confirms reduced expression of *CDKN1C* hypoxia and GCM1KO cells. * p <0.05; ** p <0.001unpaired t test comparing each sample to the controls. mean ± SEM

3.3.7 Non-Conventional 3D-TSC Formation in GCM1 Reduced Background

Interestingly, when GCM1KO lines were grown to over confluency, we observed dome-like projections when cultured in TSCM and even larger domes when removing the GSK3B inhibitor CHIR99021 as a precursor to EVT formation (Fig. 7A, S7A).(Haider et al., 2022) These dome-like structure seem to have a hollow morphology. To further explore the 3-D organization of GCM1KO cells, we grew cells as 3D-TSC organoids. We followed a modified protocol from Haider and colleagues for TSC-org culture (mTOM) and EVT differentiation (mTOM without CHIR, mTOM-C), though we omitted Matrigel embedding.(Haider et al., 2022) Since, GCM1KO-

STB had the ability to perpetuate very well in 3D form (Fig. 3G), we speculated that matrigel is possibly not required for in vitro growth. GCM1KO-TSC were grown in micro-V-shape wells in mTOM and transitioned to mTOM without CHIR media (Fig.7B). Upon subsequent removal of CHIR99021 (mTOM-C) over a span of 9 days, we observed significant growth and several of these clusters even grew large hollow cavities. (Fig. 7C). DAPI/TEAD4/TFAP2C staining illustrate an empty cavity morphology in 3D-GCM1KO lines (Fig. 7C). Notably, the cells in this condition form a monolayer epithelium (Fig. 7C). 3D-control organoids with CHIR omitted lose expression of TEAD4, stem cell marker, and have lower TFAP2C to KRT7 surface ratio (Fig. 7C). Interestingly, increasing the number of cells of GCM1KO lines by 10x to undergo organoid formation, multiple monolayer protrusion of open cavity branching arises almost like villous trees (Figure 7C, right panel).(Aplin & Jones, 2021) When we further progress these 3D-GCM1KO clusters towards mature EVT formation (Okae et al. 2018 protocol), 3D-GCM1KO are unable to regulate expression to $EPCAM^{lo}$/$HLA\text{-}G^{hi}$, markers of EVT differentiation, but do show upregulation of the marker ITGB6 (Fig. 7E, S7B). Arut. et al. published data suggesting 4 subtypes of CTBs; CTB, CTB-fusing, CTB-proliferative, CTB-CCC (cell column); CTB-CCC's unique signature is that they express ITGB6.(Arutyunyan et al., 2023; Lee et al., 2018) GCM1KO cells, upon differentiation to EVT, may best resemble the $ITGB6^{hi}$, $GCM1^{lo}$ population observed in placenta (Fig. S7C).

Trophoblast organoids undergo spontaneous differentiation, forming a core of syncytiotrophoblast in the middle. We considered whether we could prevent this by reducing expression of GCM1. Previously, a published report demonstrated in CTBs that hypoxia shows inhibition of the PI3K/pAKT pathway and can lead to reduced expression of GCM1.(Chiang et al., 2009) Since treatment of LY294002 showed robust PI3K/pAKT inhibitor HTR-8/Svneo cells,

trophoblastic cell line, we proceeded to recapitulate GCM1KO phenotype with this small molecule.(Liu et al., 2023) Treatment of WT-TSCs with 2uM LY290042 reduced *GCM1* and *ITGA1* by at least half and similar dome-shape projections appeared (Fig. 7D, S7D). In 3D culture, LY290042 treatment prevented the formation of $SDC1^+$ cells in the middle of the organoid (Fig. 7F) Consistently, Treatment of LY294002 reduces expression of GCM1, ITGA1, and SDC1 (Fig. 7G). LY294002 is reported to reduce GCM1 protein levels by increasing GSK3β activity; GSK3β in turn phosphorylates GCM1 which leads to GCM1 ubiquitination and degradation. However, the GCM1-reducing effect of LY294002 was observed even in media with CHIR99021 where GSK3β is inhibited (Fig. 7G), and other WNT pathway inhibitors did not have the same effect as LY294002 (Fig. S7E, S7F). Nonetheless, the addition of LY294002 allows culture of trophoblast organoids in an undifferentiated state.

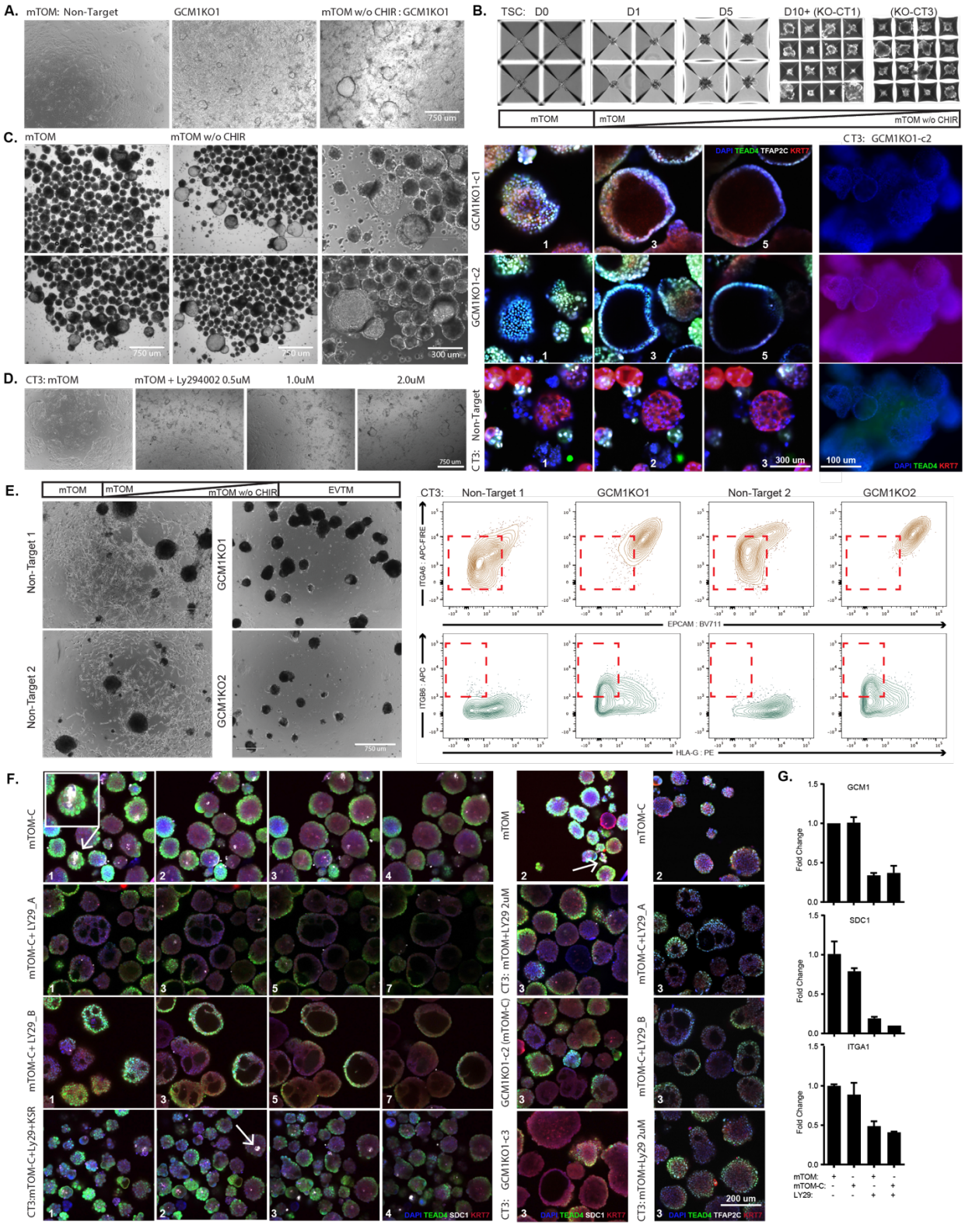
A.
mTOM: Non-Target
GCM1KO1
mTOM w/o CHIR : GCM1KO1
750 um
B.
TSC: D0
D1
D5
D10+ (KO-CT1)
(KO-CT3)
mTOM
mTOM
mTOM w/o CHIR
C.
mTOM
mTOM w/o CHIR
750 um
750 um
300 um
CT3: GCM1KO1-c2
GCM1KO1-c1
GCM1KO1-c2
CT3: Non-Target
DAPI TEAD4 TFAP2C KRT7
100 um
DAPI TEAD4 KRT7
D.
CT3: mTOM
mTOM + Ly294002 0.5uM
1.0uM
2.0uM
750 um
E.
mTOM
mTOM
mTOM w/o CHIR
EVTM
Non-Target 1
Non-Target 2
GCM1KO1
GCM1KO2
750 um
CT3:
Non-Target 1
GCM1KO1
Non-Target 2
GCM1KO2
ITGA6 : APC-FIRE
EPCAM : BV711
ITGB6 : APC
HLA-G : PE
F.
mTOM-C
mTOM-C+ LY29_A
mTOM-C+ LY29_B
CT3:mTOM-C+Ly29+KSR
DAPI TEAD4 SDC1 KRT7
mTOM
CT3: mTOM+LY29 2uM
GCM1KO1-c2 (mTOM-C)
CT3: GCM1KO1-c3
DAPI TEAD4 SDC1 KRT7
mTOM-C
mTOM-C+LY29_A
mTOM-C+LY29_B
CT3:mTOM+Ly29 2uM
200 um
DAPI TEAD4 TFAP2C KRT7
G.
GCM1
SDC1
ITGA1
Fold Change
mTOM:
mTOM-C:
LY29:

Figure 7. 3D-TSC form hollow cavities in GCM1 low expressing conditions. A. GCM1KO-TSC were grown in mTOM or mTOM without CHIR99021 (mTOM-C). Dome-like projections appeared in regions of high cell density. **B.** Schematic diagram illustrating the process of generating 3D-TSC. **C.** GCM1KO-TSC and NT-TSC were grown in the conditions illustrated in the diagram. Images and IF were observed to see morphological and phenotypical changes. **D.** WT-TSC were treated with increasing concentrations of LY294002 (LY29) and cultured to confluency. **E.** NT and GCM1KO-3D-TSC were subsequently differentiated to EVT (Okae et al. 2018 method) and flowcytometric expression profiles were observed. **F.** WT-TSC were treated over a variety of condition to discover conditions that mimic GCM1KO phenotype. GCM1KO controls were included in this experiment. Treatment of cells with LY294002 mimics GCM1KO, with growth of large epithelial bodies with no internal differentiation. KSR (Knockout serum replacement) indicate addition of serum to treatment. _A and _B indicate two separate views of the experiment. Arrow indicated SDC1 staining in white. **G.** qRT-PCR confirms LY294002 treatment effectively reduces expression of differentiation markers. (**C., F.** Number indicating section in z-stack.)

3.4 Discussion

The study of human placenta presents many challenges, but with improved methods of culturing trophoblast stem cells and the many sub-lineage derivatives, much has been uncovered about the roles of implantation, proper lineage patterning, function, and formation. Recent spatial and multi-omics analysis spanning the cascade of placenta development have shed light on the various stem cells and differentiating populations. Novel cellular mechanisms and cell-to-cell crosstalk have broadened our conception of placenta formation.(Arutyunyan et al., 2023; Liu et al., 2018; Petropoulos et al., 2016; Vento-Tormo et al., 2018) Arut. et al. 2022 recent comprehensive spatial trajectory analysis follows the lineage specific gene expression patterns and changes across the newly uncovered placental cell types. This profiling details mechanistic shifts in gene regulation that match with previous findings. The derivation of trophoblast is dependent on epidermal growth factor (EGF) and inhibition of HIPPO signaling, where Yes-associated protein (YAP) and co-factor TEA domain 4 (TEAD4) stably maintain CTB/TSC and suppress differentiation.(Meinhardt et al., 2020; Ray et al., 2022; Saha et al., 2020; Turco & Moffett, 2019)

EVT differentiation and remodeling arises from the proliferative cell column, which likely correlates to the newly identified VTC-CCC population marked by ITGB6 expression from the Arut. et al. sample set. From the VCT-CCC, EVT migrate into the decidua as interstitial EVT (iEVT) and others as endovascular EVT (eEVT) for vascular reconstruction to anchor the placenta and allow for sufficient blood flow through the arteries.(Arutyunyan et al., 2023; Haider et al., 2016; Pijnenborg et al., 1983; Pijnenborg et al., 1980; Pollheimer et al., 2018; Velicky et al., 2018; Zhou et al., 1997) Arising from VCT-fusing epithelium, STB fusion creates multinucleated epithelial bi-layer over VCT-fusing cells to form the placental barrier and be a site for hormone secretion.(Aplin & Jones, 2021; Hemberger et al., 2020; Knöfler et al., 2019) With what we know about the composition of cells that constitute the placental villus, we need to expand our knowledge of regulatory mechanism monitoring this process.

It has been well established that WNT activation is required for the maintenance of TSC, and NOTCH1/2 signaling drives EVT lineages specification.(Chang et al., 2018; Dietrich et al., 2022; Haider et al., 2016; Haider et al., 2018; Haider et al., 2014; Jeyarajah et al., 2022) However, even less has been understood about the mechanism of STB fusion. Yet, one TF remains the pinpoint of differentiation, the expression of GCM1. This gene seems to be the root at which differentiation commences to either the EVT or STB lineage. Even more so, changes in oxygen levels have been identified as major contributors to the regulation of GCM1 and this may have several links to poor prognosis in preeclampsia.(Horii et al., 2016; Wakeland et al., 2017; Wang et al., 2022a) Several signaling pathways seem to be dysregulated in low oxygen via the low expression of GCM1 such as WNT and NOTCH signaling that warrants further investigation.(Chiang et al., 2009; Jeyarajah et al., 2022) In our present data, we observe regulation of GCM1 through oxygen tension, its specific dysfunction in differentiation to placental lineages

, and it's possible context for branching morphology. The rate of oxygen diffusion that crosses the endometrial layer into placental may have an evolutionary role in the regulation of GCM1 for these purposes of regulating proper placental formation.(Carter, 2009) With GCM1 ablation, since neither EVT nor STB differentiation occurs, dysregulation of the NOTCH pathway seems to be a major target. NOTCH1 and NOTCH2 do not express in GCM1KO-EVT and NOTCH3 is not properly down regulated in GCM1KO-STB. When accounting for genes sensitive to oxygen regulation, such as GCM1, mechanisms defective during any process of placentation may be the root cause of severe pregnancy disorders that include early-onset preeclampsia, fetal growth restriction, placental accreta, even stillbirth.(Brosens et al., 2011)

TSC-org derived from human placenta collected over several gestational stages have the consistent feature that STB differentiation occurs inside the organoid.(Haider et al., 2018; Sheridan et al., 2021; Turco et al., 2018; Yang et al., 2022) This may reflect higher pressure inside the organoid, or lack of access to EGF, but this organization is inverted with respect to the bilayer formation of chorionic villus.(Enders & Blankenship, 1999) Yang et al. 2024 and Hori et al. 2024 have both observed the removal of the ECM component allow reorganization of the STB layer on the outside of the TSC-org. But as it is understood, the chorionic villus (villous tree) if formed by a epithelial bilayer that is lined by VCT and VCT-fusing on the inside and STB lining the outside strengthening the placental barrier.(Baines & Renaud, 2017; Hamilton & Boyd, 1960; Hemberger et al., 2020; Knöfler et al., 2019; Turco & Moffett, 2019) We suggest the potential GCM1 disfunction in reduced WNT activation (removal of CHIR99021) trap VCT/TSC in the VCT-CCC stage that express ITGB6 upon differentiation of EVT.(Arutyunyan et al., 2023; Lee et al., 2018) 3D-TSC in the presence of LY294002 (PI3K inhibitor) in media conditions containing CHIR99021 (WNT activator) and A8301 (TGFB inhibitor) maintain stemness without any

indication of differentiation. When the WNT activator is removed, cavity formation is observed, again without any indication of differentiation. While knowledge of the placental lineage has expanded, the growth and formation of the villous tree is still relatively unknown. Here, we demonstrate a potential pathway in which we can culture TSC-org then generated 3D-TSC with cavities simulating the epithelial lumen of a villous tree. Furthermore, by culturing cells in LY294002, it may be possible to maintain cells in an undifferentiated state, then remove the inhibitor and allow differentiation to occur. As this window from implantation to the primitive villus formation is still a black box, this system gives a possible view of 3D-villus formation.

3.5 Experimental Procedures

Cell Culture-Maintenance of TSC: CT1 and CT3 lines were generously provide from Dr. Arima's lab in Japan. TSC were cultured in TSC basal media containing DMEM F-12 (GIBCO), 1x ITS-X (GIBCO), 0.3% BSA (WISENT), 1% Penicillin/Streptomyocin (GIBCO), 1% ESC qualified Fetal Bovine Serum (GIBCO), 0.1mM β-mercaptoethanol (GIBCO), 15ug/ml L-ascorbic acid (SIGMA), and 50ng/ml recombinant hEGF (GIBCO). To this, made fresh, 0.75mM valporic acid, 2uM CHIR99021 (CaymenChem), 0.5uM A8301 (CaymenChem), 1uM SB431542 (CaymenChem), and 5μM Y27632 (CaymenChem) was added to make TSCMedia. TSC were dissociated using TRYPLE (GIBCO) diluted with PBS to 30% and incubated at 37C for 10 min. Deactivation of TRYPLE was done by using 1:1 vol of 0.5mg/ml Soybean trypsin inhibitor (GIBCO) diluted in PBS. For experiments performed in figure 1-2, TSC were passaged on to 5ug/ml of Collagen IV (Corning) coated plates, but due to product availability, TSC from experiment in figure 3-6 were passaged onto Laminin 511(SIGMA) coated plates.

Cell Culture-Differentiation of TSC to EVT: TSC were converted to EVT using a modified TSC basal media containing DMEM F-12 (GIBCO), 1x ITS-X (GIBCO), 0.3% BSA (WISENT), 1% Penicillin/Streptomyocin, and 0.1mM β-mercaptoethanol (GIBCO). For day 1-2, TSC were passage onto 1ug/ml Collagen IV coated plates in mod. TSC basal with added 5% Knock-serum replacement (GIBCO), 5uM Y27632 (CaymenChem), 3uM A8301 (CaymenChem), 100ng/ml NRG1 (NEB) and 2% GFR-Matrigel (Corning) while the media is still cold. Day 3-5, the media is change to the previously mention ETVM but this time without NRG1 and reduction to 0.5% GFR-Matrigel. Day6-8, the media is change to the previously mention ETVM but this time without

NRG1, KSR, and reduction to 0.5% GFR-Matrigel. At the end of day 8, differentiated EVT can be assess by Flowcytometry.

Cell Culture-Differentiation of TSC to STB: TSC were converted to STB using a modified TSC basal media containing DMEM F-12 (GIBCO), 1x ITS-X (GIBCO), 0.3% BSA (WISENT), 1% Penicillin/Streptomyocin, and 0.1mM β-mercaptoethanol (GIBCO). For day 1-2, TSC were passage on to suspension plate (Starsted) in TSC basal media containing 5uM Y27632, 2uM Forskolin (CaymenChem), 5% KSR (GIBCO), and 50ng/ml recombinant hEGF. On day 3, cell clustered were collect and pulse-spin for 30sec to separate single cell from STB fusion-clusters and replate in STBMedia mentioned above. At day 5, STB-3D are ready to be assessed by immunofluorescence and/or hCG- ELISA.

Cell Culture-3D-TSC and EVT differentiation: 3D-TSC (TB-ORG) were cultured on a modification based on Okae et al. 2018 and Haider et al. 2022 publications. Our modified-TOM (mTOM) media contains DMEM F-12 (GIBCO), 10mM Hepes (GIBCO), 1x ITS-X (GIBCO), 2mM GlutaMax (GIBCO), 1x Penn/Strep (GIBCO), 0.2% ESC-FBS (GIBCO), 50ng/ml rhEGF (Invitrogen), 3uM CHIR99021 (Caymen Chem.), 2uM A8301 (Caymen Chem.), and 5uM Y27632 (Caymen Chem.) Instead of Matrigel embedding, micro-V-shape wells (AggreWell 400, Stemcell Tech) were used to generate organoids. ~50,000 cells were resuspended in 1ml mTOM per 24 well and centrifuged in a plate spinner for 5 min at 1000 rpm to collect cells to the bottom at ~100 cells per V-shape well (Fig. 7B for reference). After 24 hours, 500ul of media is gently removed and either mTOM is replaced or mTOM without CHIR99021 (mTOM-C) for CTB-CCC/early-EVT formation was replaced every other day over a ~10-day period. For LY294002 treat, treatment up

to 14 days may be required to physically see by microscopy cavity formation. For EVT maturation, uses the protocol described above from Okae et al. 2018 described previously above.

Generation of CRISPR Knockout lines by Nucleofection: CRISPR guides were design using IDT- Custom Alt-R™ CRISPR-Cas9 guide RNA program. sgRNA guides targeting a small region of nucleotide just after the ATG-start site in exon 2 and intron 2-3 (sgRNA1- UCU UCA GAA UCA AAG UCG UC and sgRNA2- ACU AUU AAC AUG CGG AGA CC, guide design was done with assistance from Ishtiaque Hossain). Additional deletion of exon 3 were design (sgRNA3- GAG CGC UGC UCA GAU AGC GA and sgRNA4- AGA CCU AAG AGC AAU CAG UG). Cas9-sgRNA ribonucleoprotein complexes were generate from sgRNA and Cas9 synthesized by Synthego. In brief, 75pmol of each individual sgRNA is complexed with 10pmol of Cas9 in Cas9 annealing buffer (NEB) for 10min. In the meantime, TSC are dissociated with 30% TRYPLE and reconstituted in PBS to a concentration of 1 x 10^5 cell/ul. Pre-complexed RNPs sgRNA1 and sgRNA2 are combined together with 10ul of cell solution and 20ul of P3 solution (LONZA) and transferred to a cuvette to be nucleofected in an Amaxa 4D nucleofector (Lonza) with pulse code CA137. Immediately after 150ul of TSCM media is added to the cuvette to neutralize the reaction and transfer cell to a freshly prepared 10cm plate coated with Lam-511 and TSCM for generating single clones. 2mg/ml Collagenase V solution was used dissociate colonies to pick single clones and deletions were confirmed by genotyping (GCM1KO1: Forward-TTGTATGAGGACTTGTGCATAACAA, Reverse- GCCATTGGTTACAGATGACAAC, GCM1KO2: Forward-ATGGAACTCACAGGGGCTAT and Reverse-TAACAGGAGCCTTCAGTCCA).

Chromatin immunoprecipitation: Cell samples are fixed with 0.66% paraformaldehyde (FisherSci) diluted with PBS and incubated on a rotator for 10 minutes at room temperature. Samples are quenched by adding glycine to a final concentration of 0.125M with continued rotation for another 10 minutes at room temperature then wash with cold PBS 2x and replaced with PBS + 1mM EDTA + protease inhibitor (Roche)before collection with a cell scrapper. Cell pellets were centrifuged at 13200 rpm for 5 mins. Nuclear lysis extraction begins with 10 min incubation on a rotator in nuclear lysis buffer (50mM HEPES pH 7.8, 0.5% Triton X-100, 1mM EDTA, 0.5mM EGTA, 140 mM NaCl, 10% glycerol and 1% NP-40). Nuclear pellets are collected by centrifugation at 13200 rpm for 5 minutes at 4°C. Nuclei are resuspended in nuclear wash buffer (10mM Tris-HCl pH 8.0, 200mM NaCl, 1mM EDTA, and 0.5mM EGTA) and then rotated 5 minutes at 4°C the repeated twice. Nuclear pellets are then resuspended in SDS lysis buffer (50mM Tris-HCl pH 8, 10mM EDTA, 1% SDS, and 1% Triton X-100). Nuclei samples are transferred to a 1ml tube (Bioruptor) and keep cold before sonication. Sonication was performed using the Diagenode Bioruptor sonicator (settings: 30sec on, 30 sec off, 30-35 cycles). Dilute the sonicate by 10-fold with Dilution buffer (25mM Tris-HCl pH 8, 150 mM NaCl, 3mM EDTA, and 1% Triton X-100). Pre-washed Protein G Sepharose beads (SIGMA, P3296-5ml) are prepared by washing them three times with dilution buffer. A pre-clearing step is performed by using 40µl of pre-washed beads combined sonicated sample. This rotated for 1hrs at 4°C then centrifuged at 1000xg for 1 min. Sticky-chromatin is remove by the beads and the supernatant is retained for the IP. 2ug of GCM1(HPA001343) antibody is added to each pre-cleared sample and then rotated overnight at 4°C. The next day, pre-washed Protein G Sepharose beads are added to the ChIP samples and rotated 2 hours at 4°C. The beads washed with 3 buffer: DB150 (25mM Tris-HCl pH 8.0, 150mM NaCl, 3mM EDTA, 1% Triton X-100, and 0.05% SDS), DB500 (25mM Tris-HCl pH

8.0, 500mM NaCl, 3mM EDTA, 1% Triton X-100, and 0.05% SDS), Buffer III (10mM Tris-HCl pH 8.0, 250mM LiCl, 1% Sodium Deoxycholate, 1% NP-40, and 1mM EDTA, and lastly TE buffer (10mM Tris-HCl pH 8.0, 1mM EDTA). DNA is eluted for 15 min on shaker rotating at 1000rpm with 200ul elution buffer (100 mM NaHCO3, and 1% SDS). 16ul of 5M NaCl is added to each sample and further incubated at 65C overnight for decrosslinking. Ethanol precipitation is performed to collect ChIP material, and further purification was performed with Geneaid Gel/PCR cleanup protocol. Purified DNA fragments passed to sequencing library preparation.

RNA isolation: Total RNA isolation used manufacturing protocol indicated by Sigma-Aldrich RNAzol^{RT} R4533. Qubit™ RNA BR Assay kit (Q10211) was used to accurately measure RNA concentration.

Library preparation: For RNA library synthesis, in brief, purified mRNA was cleaned using the NEBNext Poly(A) mRNA Magnetic Isolation Module kit (NEB E7490) and final library generation was created with the NEBNext® Ultra RNA Library Prep Kit for Illumina® (NEB E7530) following manufacturing instructions. Barcoding came from TruSeq Unique Dual Indexes (Illumina, San Diego, CA) Qubit™ 1x dsDNA HS Assay kit (Q33231) was used to measure synthesis of the library.

Sequencing Analysis: For RNA and ChIP/ATAC sequencing analysis, Genpipes 4.3.2 (https://bitbucket.org/mugqic/genpipes) provided the pipeline for basic sequencing processing. In brief for RNAseq, sequencing quality and adaptor removal was trimmed with trimmomatic (v0.36). Trimmed fastq files alignment was performed with STAR aligner (v2.7.8a) using

hg38/GRCh38 (ensembl v104). Picard (v2.9.0) was then used merged, mark duplicates, identify unique read, and sort .bam files proceeding alignment. Read counts were collected using HTseq-count and StringTie (v1.3.5). Differentially expressed gene (DEG) comparison was performed with DESeq2 package on RStudio (R v4.3.1). Correlation matrix, hierarchal gene cluster analysis, and PCA were generated in R. Gene pathway analysis were performed on ConsensusPathwayDB and EnrichR. For ChIPSeq and ATACseq, in brief, raw fastq files trimmed using trimmomatic (v.0.36). Then qualified fastq reads were mapped with BWA (v.0.7.17) with post processing with sambamda (v0.8.1) to merge replicates, mark and filter duplicates, and remove blacklist regions. Peak calling and differential-bind was performed with MACS2 (v2.2.7.1). Gene annotations and motif analysis used with Homer (v4.11). Bam to bigwig bamCoverage from deepTools (v3.5.1) was used to generate the tracks for viewing on IGV (v2.9.4).

hCG ELISA: hCG secretion was measured using an hCG AccuBind ELISA (Monobind) according to manufacturer instructions.

Flow cytometry: Dissociate single cells are first washed with 1% KSR-PBS solution. Cell samples are incubated with fluorescently conjugated antibodies for 15min at room temperature. Post-incubation, the sample are wash once with 1% KSR-PBS and then resuspended in 1% KSR-PBS containing DAPI nuclear counterstain to identify live or dead cells. Data acquisition was preformed using the LSR Fortessa and data analysis was performed on FlowJo v10.

Western blot: Dissociated single cell samples are washed with cold PBS and lysed with laemmli buffer without blue dye and boiled at 95C for 5 min. Protein concentration was determined using

standard Bradford assay. Standard Bio-RAD SDS-PAGE system was used to separate protein and transfer it to PVDF membrane (Millipore). Membranes blocking, primary and secondary antibody incubations are diluted in Odyssey Blocking buffer (LICOR). Infrared conjugated secondary antibodies are using for detection and visualization of the protein of interest on the membrane with the LICOR-Odyssey Imager. GCM1 antibody (ab187860-C-term)

Immunofluorescence: Glass coverslips are precoated with 5ug/ml Collagen IV (CORNING) overnight before cell attachment. Cells are grown for a determined amount of time for its corresponding experiment. Coverslips are fixed with 4% PFA for 20 min. at room temperature. PFA solution is washed 3 times with PBS before permeabilization with permeabilization buffer (PBS + 5% donkey serum + 0.1% Trition-X100) for 30 min. Primary and secondary antibody are diluted in permeabilization buffer and incubated for 1-2 hours each process. Coverslips are washed with PBS containing DAPI nuclear counterstain and mounted on to glass slide using Prolong gold (Invitrogen). Imaging analysis is performed using the Axiovert (Zeiss).

3.6 Author Contributions

J.K.C., S.Y.K., J.S., J.G., and J.Z. conducted the experiments. J.K.C. conducted the bioinformatic analysis. S.J.R. provided the GCM1 ChIP which we prepared for sequencing and S.P. provided the ATAC-seq data which we analyzed. S.J.R., S.P., and W.A.P. supervised the experiments and analysis.

3.7 Acknowledgments

We thank the Goodman Cancer Research Center Flow Cytometry core, the SickKids Center for Applied Genomics Facility, the La Jolla Institute for Allergy and Immunology

Sequencing Core, and the Canada Michael Smith Genome Sciences Center at BC Cancer for their dedicated service. We thank the Stephen Renaud (UWO) and Soumen Paul (KU) labs for providing the GCM1 ChIP samples and access to placental ATACseq data. This work was funded by the New Frontiers in Research Fund (NFRF) grant NFRFE-2018-00883 and the Canadian Institutes of Health Research (CIHR) project grant PJT-166169 to W.A.P. J.K.C. was supported by a Fonds de recherche Santé Québec graduate fellowship and studentships from the McGill University Faculty of Medicine.

3.8 Supplemental Information

Reduction of GCM1 Expression by Hypoxia or PI3K Pathway Inhibition Prevents Spontaneous Differentiation of Trophoblast Stem Cells

Jessica Cinkornpumin et al.

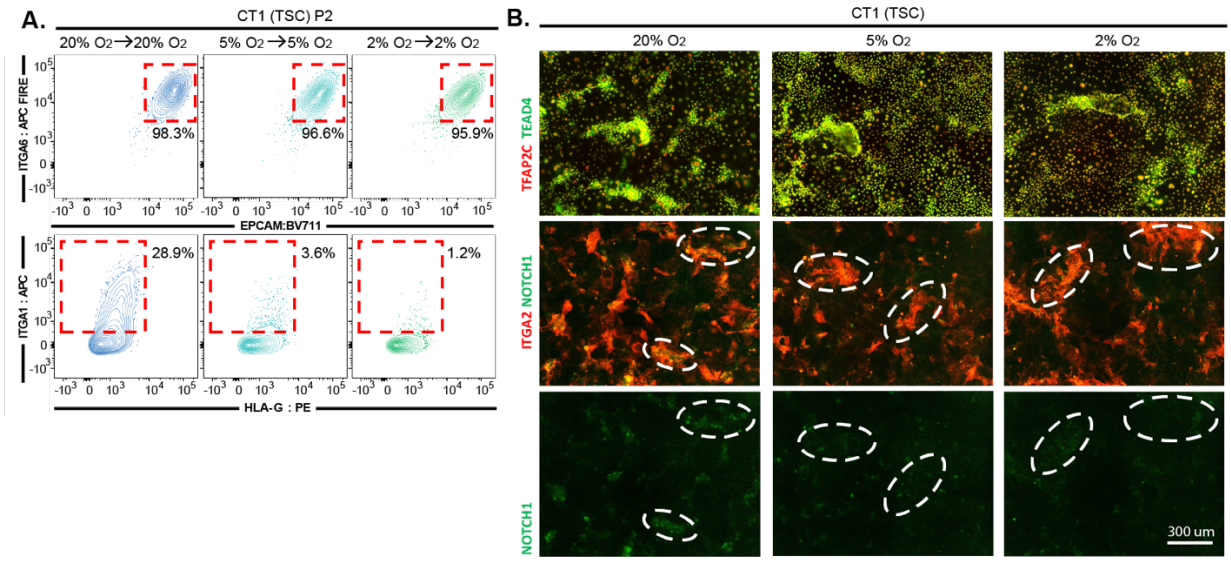

Figure S1. Continued culture in low oxygen conditions reveal reduced differentiation. A. Trophoblast stem cells shown in 1A were passaged and cultured for additional 72hrs in varying levels of oxygen (20%, 5%, 2% O_2). Continued low oxygen tension causes further reduction of ITGA1+ cell population. B. TSC in the varying oxygen conditions were grown to over maximum confluency. At region where overgrowth cause increase cell-to-cell contact and cell pile-up, spontaneous nuclear NOTCH1 signal was detect. In the low oxygen cultures, NOTCH1 expression was not detected. TFAP2C, TEAD4, ITGA2 are markers of TSC population.

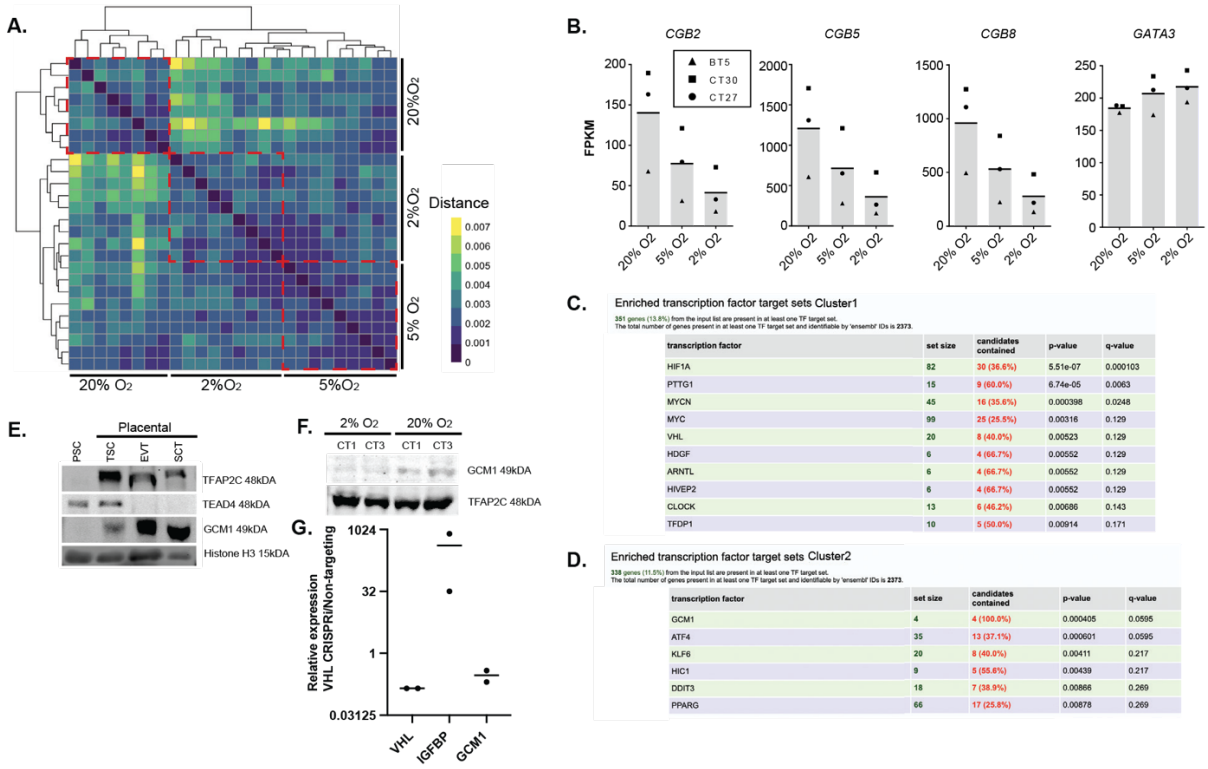

Figure S2. RNAseq of TSC in ambient oxygen versus hypoxia find oxygen sensitive genes. A. Correlation matrix showing sample clustering of similar TSC culture conditions (3 cell lines, n=3 for each line in each condition) **B.** Bar graph of specific genes of interest using averaged FPKM of each cell type from the 3 replicates. **C., D.** ConsensusPathwayDB analysis of Cluster 1 and Cluster 2 identifying TF target with significance from each cluster. **E.** Western blot compare pluripotent stem cell (PSC) that don't expression placental markers, with TSC and differentiated EVT and STB to highlight specific expression patterns. Histone H3 and TFAP2C serve as loading controls. **F.** Western blot for GCM1 in 2 cell lines grown in 2% and 20% O_2. TFAP2C is the loading control. **G.** TSC were subject to CRISPRi targeted degradation of VHL. VHL expression and GCM1 expression are reduced, while the known hypoxia target IGFBP3 is dramatically upregulated.

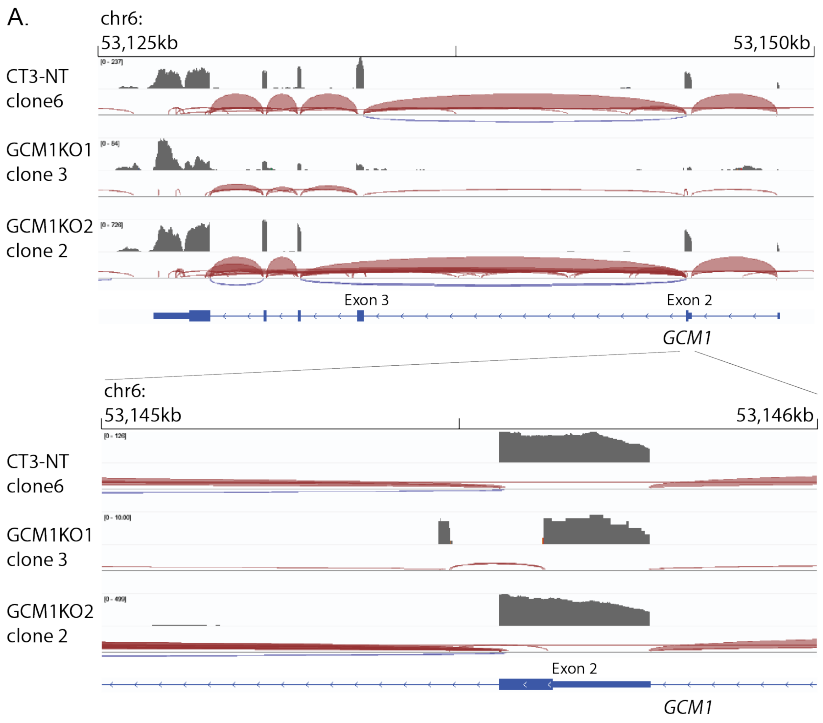

Figure S3. Sashimi plot of *GCM1* CRISPR deletion in TSC. A. Sashimi plot across the genomic region of *GCM1*. Representative clones were chosen. Normal splicing is observed from NT line. GCM1KO1 (from right to left) show a deletion at the distal tip of exon2 but an alternative slice site forming just after. GCM1KO2 shows the complete skipping of exon 3.

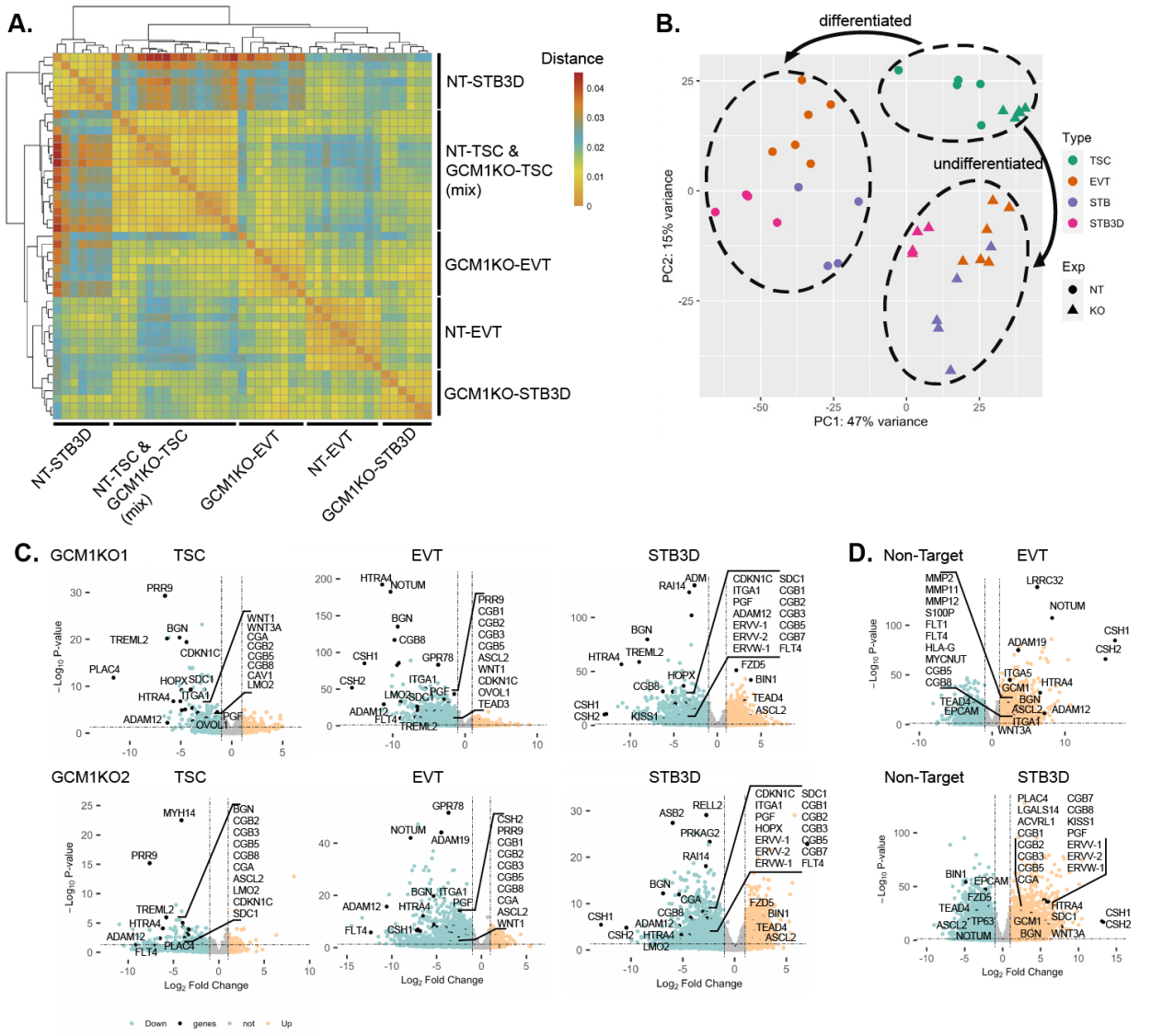

Figure S4. GCM1KO EVT and STB are deficient in cells specifc expression. A. Correlation heatmap show sample type clusting patterns. **B.** PCA comparision including STB2D comparison that was remove from Fig. 4A-4D as it seemed to have a strong pull on the downstream analysis. **C.-D.**Volcano plots of each comparison from GCM1KO and NT lines.

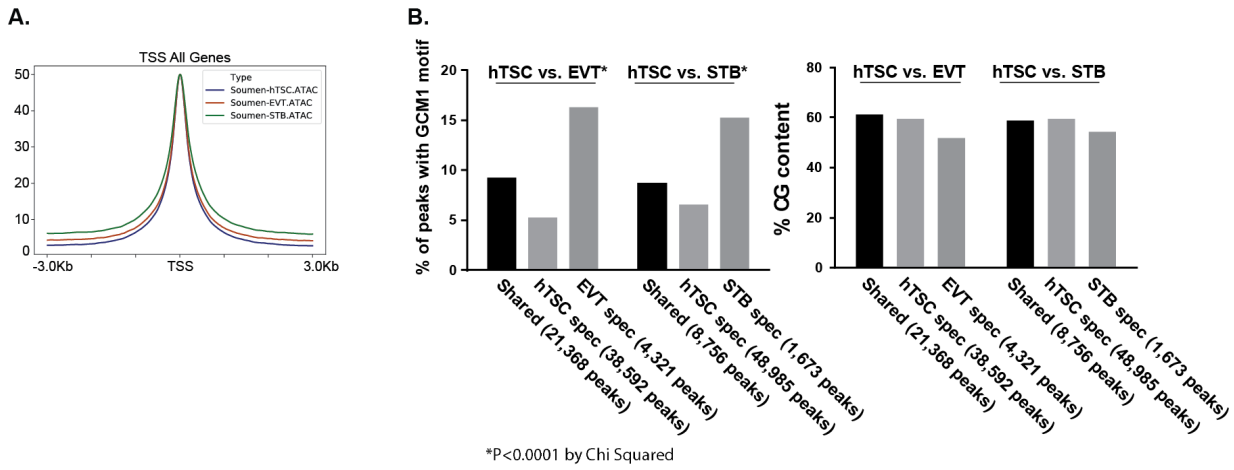

Figure S5. ATACseq show increased GCM1 motif occupancy in EVT and STB specific peaks. A. ATACseq metaplot over all genes showing normalization over TSS. **B.** GCM1 motif % enrichment found in our analysis of cell specific and shared ATAC peak sets.

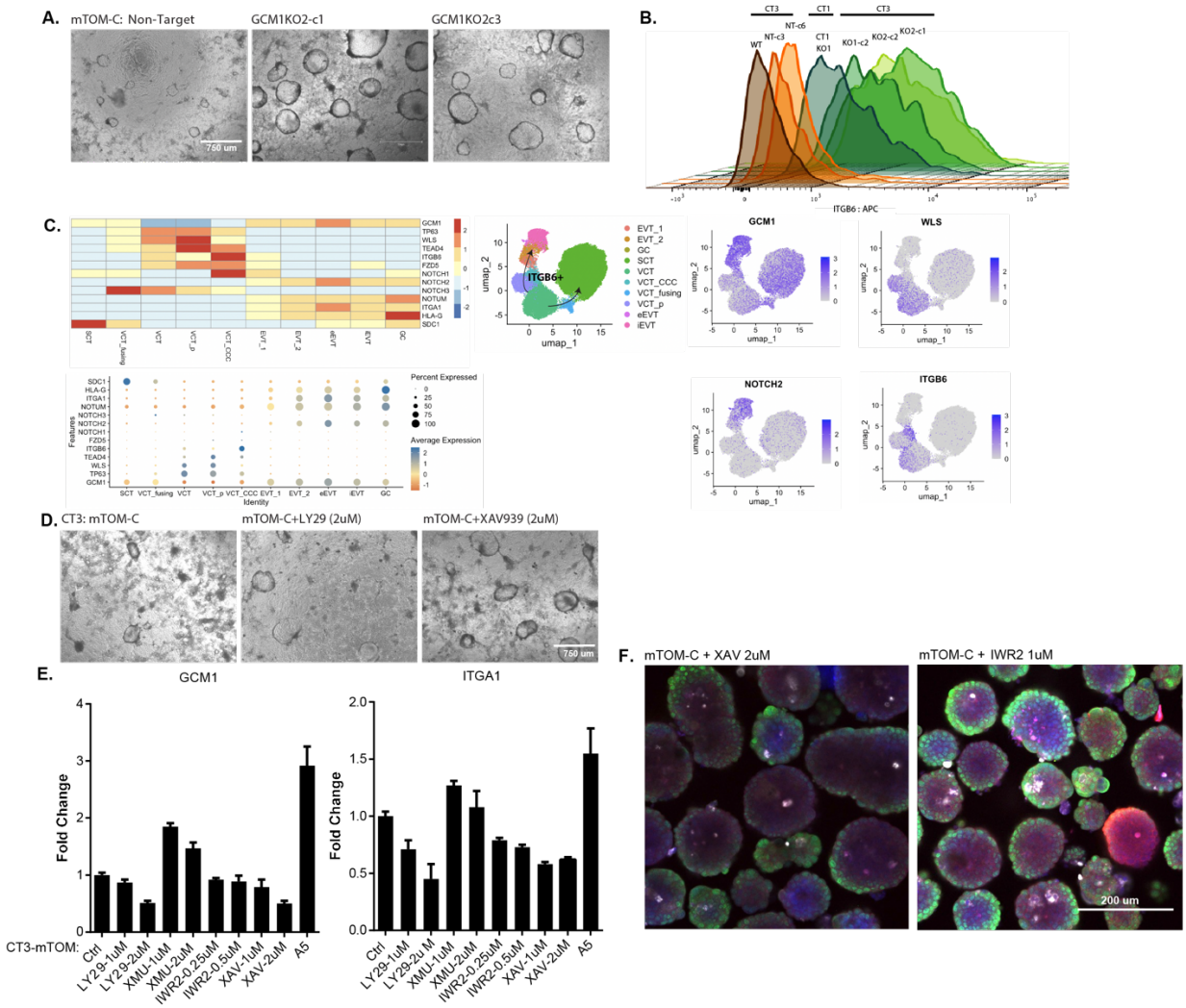

Figure S7. 3D-TSC characterization in *GCM1* low expressing conditions. A. GCM1KO2-TSC were grown in mTOM without CHIR99021 (mTOM-C). Dome-like projections appeared in regions of high cell density. **B.** ITGB6 expression over several lines in histogram display**. C.** Reanalysis of Arut. et al. 2022 single RNAseq profiling the several subtypes found in early villus of the placenta. *GCM1*, *WLS*, *NOTCH2*, and *ITGB6* marking regions of population division. Path of differentiation is indicated. **D.** LY294002 (LY29) and XAV939 (XAV) treatment for 2D hTSCs grown in mTOM-C differentiation media. **E.** qRT-PCR for differentiation markers hTSC grown with mTOM and LY294002, an MST-1 inhibitor (XMU-MP-1) and tankyrase inhibitors (IWR2, XAV939). Note the strongest effect was observed for LY294002 treatment. **F.** XAV939 and IWR2 do not suppress differentiation in 3D trophoblast organoids.

3.9 Supplemental Table (will be available upon publication)

Table S1. FPKM, DEG (differentially expressed gene) analysis, z-score cluster analysis, and GSEA of all samples. Related to Figure 2.

Table S2. Okae et al. 2018 list of 100 specific cell type genes corresponding to FPKM of all samples. Related to Figure 2.

Table S3. FPKM and Okae et al. 2018 list of 100 specific cell type genes corresponding to FPKM of all samples. Related to Figure 4.

Table S4. z-score cluster analysis and EnrichR GSEA analysis. Related to Figure 4.

Table S5. Homer annotation of peaks with EnrichR GSEA analysis. Related to Figure 5.

CHAPTER 4: DISCUSSION

4.1 The advances from and beyond trophoblast stem cells

The human naive pluripotent stem cells can generate cultures containing the three primary blastocyst lineages. These findings have since been corroborated and expanded upon by a number of groups, including one report that shows that cells of the human epiblast have the lineage plasticity capability to differentiate trophoblast.(G. Guo et al., 2021; Sathyanarayanan et al., 2022) Prior to this research project, researchers primarily attempted to design directed differentiation methods for trophoblast lineages with varying results. Previously, BMP4 treatment has been used to induce hESC differentiation into trophoblast-like cells.(Xu et al., 2002) However, this model produced mixed cultures that express trophoblast, mesodermal, and vascular endothelial cell markers. This suggests that the BMP4 induction process is not specific to the trophoblast lineage, but instead may drive hESC differentiation into either trophoblast-like or mesodermal-like cells.(Bernardo et al., 2011) Subsequently, with the establishment of 2D self-renewing human TSCs from both blastocysts and first trimester CTB preparation, derivation of hTSCs from hESC seem possible.

In Chapter 2, primed hESC reverted to a naive state were observed to have a transcriptional and epigenetic signature that resembled preimplantation epiblast. This state proved ideal for the derivation of hTSC from hESC, termed transdifferentiated human TSC (tdhTSC). Our naïve-hESC derived tdhTSC gained a trophoblast-like methylome, expressed many trophoblast-specific markers, had strong proliferative capacity, and could differentiate to the other two main placental lineages. Although naïve culture results in widespread imprint erasure, few imprinted genes (*PEG3*, *ZFAT* and *PROSER2-AS1*) remained hypermethylated. This signature was already present at the prime state of this line and was possibly a result of incomplete naïve reversion or an

epigenetic memory retained in this cell line.(Cinkornpumin et al., 2020) Considering this caveat, even though we have established a system for modeling trophoblast specification, it is essential to perform full characterization of tdhTSC. This will be especially important if used for the purpose of modeling placental diseases that harbor an epigenetic defect. This manuscript is currently published in *Stem Cell Reports* in the July 2020 issue. (https://doi.org/10.1016/j.stemcr.2020.06.003).

Since this publication, several protocols have become readily available. Dong et al. 2020 reported a similar outcome and observed pure hTSC lines after 5-10 passages of naive cells in hTSC medium.(Dong et al., 2020) Similarly, Io et al. (Io et al., 2021) and Guo et al. were able to isolate hTSC from a culture of naïve hESC. Guo et al. additionally used live-cell tracking to confirm that naive hESC transform into trophectoderm and express markers of early trophectoderm, including a short burst of *CDX2* expression before converting into hTSC.(Ge Guo et al., 2021) Since then, trophoblast stem cells have been generated from a number of different sources that had previously been considered less than ideal. Two teams have developed a protocol to derive hTSC from primed hPSC that are similar to hTSC derived from naive hPSC.(Dong et al., 2020; Soncin et al., 2022; Wei et al., 2021) Soncin et al. derived TSCs from primed hPSCs with a modified BMP4 protocol that had originally differentiated into a mixed culture of trophoblast and mesoderm cells. By adding the WNT inhibitor IWP2 and a second step with a recently developed culture medium, they were able to convert primed hPSCs into self-renewing CTBs that resemble the transition period from hPSC and the final trophoblast lineages observed in their naive hPSC counterparts.(Soncin et al., 2022) Finally, induced trophoblast-like stem cells (iTSCs) have even been generated from villous CTB in term placentas (Bai et al., 2021) and adult somatic human fibroblasts as well.(Tan et al., 2022)

Beyond this, developing a reliable model of placental development is an important step to understanding why pregnancies fail to progress during the first 2 weeks following fertilization.(Macklon et al., 2002; Weatherbee et al., 2023) Studying this has been difficult as early approaches primarily relied on short-term primary cell cultures and tissue/organ explants that are challenging to establish and manipulate and are often difficult to access. Alternatively, immortalized or transformed cell lines fail to recapitulate cell spatial complexity and heterogeneity, and are frequently karyotypically abnormal, lack genetic diversity, and do not represent states of cell development.(Adey et al., 2013; Haider & Beristain, 2023; Lee et al., 2016) After the establishment of naïve hESC conversion to trophoblast, teams began developing 3D blastoid models: self-assembling blastocyst-like structures consisting of trophectoderm (placenta) and inner cell mass (embryonic epiblast and the yolk sac precursor hypoblast).(Kagawa et al., 2022; Rossant & Tam, 2022; Weatherbee et al., 2023; Yu et al., 2021) In generating this integrated structure of epiblast-, hypoblast-, and trophectoderm-like lineages, a variety of cell types have been used to develop self-assembling organoids, ranging from the 8-cell stage (8CLCs), naive hPSCs, primed hPSCs, hEPSC, and fibroblasts.(Liu & Polo, 2024) To generate these blastocyst-like structures, most teams are taking a similar approach, but utilizing different starting cell types and media formulations. These methods frequently include a multi-step process in which the cell type is allowed to aggregate and self-organize under specific media conditions or one lineage is induced separately before aggregating under new conditions and eventually self-organizing.(Liu & Polo, 2024) Kagawa et al. showed that culturing naive hPSC in PXGL medium formed blastocyst-like structures that possessed all three lineages of the blastocyst stage after inhibition of Hippo, TGF-ß, and ERK pathways. Importantly, while other models represent cells from later developmental stages, Kagawa and colleagues were able to confirm that their blastocyst-like

structures followed a similar developmental timeline to natural human blastocyst stages. TE specification also mimicked human blastocyst dependency on atypical protein kinase-c (aPKC), Hippo pathway inhibition, and the ability of YAP1 to bind with TEAD transcription factors after nuclear translocation. This is a critical verification as it allows confident use of this model to study aspects of implantation that may affect pregnancy complications.(Kagawa et al., 2022) Weatherbee et al. developed a novel method of generating a post-implantation stage human embryoid containing embryonic and extraembryonic tissues. In this model, wild-type ESC were allowed to aggregate with cells induced to overexpress extraembryonic factors that were observed to drive ESC towards hypoblast or trophectoderm lineages. This allowed the generation of embryo-like structures without the need for exogenous factors that could affect tissue-tissue crosstalk. Additionally, by creating a modular system of inducible genetic factors, specific interaction of TFs between different lineages can now be studied. SOX17 was identified to have an inhibitory role in the specification of anterior hypoblast-like cells.(Weatherbee et al., 2023) With the variety of 3D-modelling methods available, key questions about why pregnancies may fail at pre- and post-implantation stages can be more thoroughly studied.

The most exciting develop in embryonic modeling has come from mouse research, in which synthetic mouse embryos were grown to day 8.5. At this stage, embryos have gone beyond gastrulation and begun organogenesis. Interestingly, while these embryos self-organized to have body patterning, neural tube, gut tube and heart development, Tarazi et al. mentions heterogeneity of extraembryonic tissues arising from these growth conditions and that quality of TSC was essential to the success of these synthetic embryos.(Amadei et al., 2022; Lau et al., 2023; Lau et al., 2022; Tarazi et al., 2022) This limitation suggests that the trophectoderm is an essential component of implantation, embryo development, and overall embryo survival.

Similar to the blastocyst, 3D-modeling of placentation would significantly improve the tools at hand to better understand human developmental processes. Our primary understanding of 3D-TSC was originally accomplished by establishing long-term regenerative trophoblast cultures from CTB of first trimester chorionic villus.(Haider et al., 2018; Turco et al., 2018) However, these organoids had limited cellular sources and an inverted orientation of TSC covered by a layer of STB. Now, hTSCs derived from naïve-hPSC and other sources are shown to self-organize into self-renewing 3D trophoblast organoids similar to primary trophoblast organoids.(Karvas et al., 2022) The inverted orientation of 3D trophoblast organoids was also potentially corrected by two teams, with large syncytial structures observed on the outside of the organoid that secrete the STB-associated hormone, hCGB.(Hori et al., 2024; Yang et al., 2024) Combined with our research in Chapter 2, 3D organoids could help expand our knowledge of regulatory networks that control the gradual increased from ~2% to 8% over the course of placentation during the 1st trimester. In Chapter 3, we studied GCM1, an oxygen sensitive transcription factor known to be involved in hTSC differentiation towards other trophoblast lineages. Its importance in trophoblast stemness and differentiation was suggested by previous studies based on its potential role in modulating WNT and NOTCH signaling during differentiation.(Jeyarajah et al., 2022; Wang et al., 2022b) Later, patterning of its expression across the placental lineages indicated several key branch points where GCM1 expression coincides with critical gene profile changes observed in EVT and STB derivatives.(Arutyunyan et al., 2023) In our studies, in reduced WNT activation and maintained EGF signaling conditions, GCM1 reduced background TSC seemingly generated a hollow open cavity that resembled the hollow cavity of a villous tree.(Aplin & Jones, 2021) This data is concordant with reports of a subpopulation of double positive GCM1 and TP63 (WNT-dependent TSC stemness factor) found both at the proximal cell column and within the villous CTB. They

are thought to be a transition state between stem-like CTB to differentiated lineages.(Wang et al., 2022b) Yet it is unclear whether the Ki67 proliferative population also found in the same place are the same double positive cells and how they contribute to villus structural growth.(Lee et al., 2018) While this mechanism cannot be confirmed as villous tree formation, the 3D-TSC model we developed will provide an avenue to study the structure and function of the placental barrier that has previously been unattainable.

4.2 Contributions to original knowledge

The research proposal for this thesis focused on uncovering a method of deriving human trophoblast stem cell in vivo and to further look at how these cells regulate cell fate decisions into their designated lineage. In Chapter 2, we demonstrated the removal of a prime ESC-specific signature in naïve stem cell culture that allowed for the sufficient reprogramming of the cell into tdTSC. While a number of groups reported corresponding findings throughout 2020 and 2021, we conducted a rigorous transcriptional and epigenetic comparison to placental hTSCs and demonstrated high, if imperfect, similarity. This discovery paved a path to modeling the earliest window of development before and after implantation, as well as later advances in blastoid culture. Secondly, our studies of GCM1 transcription factor in the context of oxygen sensitivity potentially provides a view of early placentation. Low oxygen, where GCM1 expression is also low, is known to perpetuate TSC even in areas and processes that have high cell-to-cell contact, such as rapid expansion into the endometrium. Our observation that GCM1 is implicated in regulating the KCNQ1-CDKN1C locus and contact inhibition is therefore important, as it could play a role in that function. Additionally, GCM1KO organoids resemble the hollow cavity formation similarly found in placental villus, suggesting that proper GCM1 regulation might be important for placental villus growth.

REFERENCES

Aboagye-Mathiesen, G., Laugesen, J., Zdravkovic, M., & Ebbesen, P. (1996). Isolation and characterization of human placental trophoblast subpopulations from first-trimester chorionic villi. *Clin Diagn Lab Immunol*, *3*(1), 14-22. https://doi.org/10.1128/cdli.3.1.14-22.1996

Adey, A., Burton, J. N., Kitzman, J. O., Hiatt, J. B., Lewis, A. P., Martin, B. K., Qiu, R., Lee, C., & Shendure, J. (2013). The haplotype-resolved genome and epigenome of the aneuploid HeLa cancer cell line. *Nature*, *500*(7461), 207-211. https://doi.org/10.1038/nature12064

Alarcon, V. B., & Marikawa, Y. (2022). Trophectoderm formation: regulation of morphogenesis and gene expressions by RHO, ROCK, cell polarity, and HIPPO signaling. *Reproduction*, *164*(4), R75-r86. https://doi.org/10.1530/rep-21-0478

Alison, R. H., Lewis, D. J., & Montgomery, C. A. (1987). Ovarian choriocarcinoma in the mouse. *Vet Pathol*, *24*(3), 226-230. https://doi.org/10.1177/030098588702400305

Alsat, E., Wyplosz, P., Malassiné, A., Guibourdenche, J., Porquet, D., Nessmann, C., & Evain-Brion, D. (1996). Hypoxia impairs cell fusion and differentiation process in human cytotrophoblast, in vitro. *J Cell Physiol*, *168*(2), 346-353. https://doi.org/10.1002/(sici)1097-4652(199608)168:2<346::Aid-jcp13>3.0.Co;2-1

Amadei, G., Handford, C. E., Qiu, C., De Jonghe, J., Greenfeld, H., Tran, M., Martin, B. K., Chen, D. Y., Aguilera-Castrejon, A., Hanna, J. H., Elowitz, M. B., Hollfelder, F., Shendure, J., Glover, D. M., & Zernicka-Goetz, M. (2022). Embryo model completes gastrulation to neurulation and organogenesis. *Nature*, *610*(7930), 143-153. https://doi.org/10.1038/s41586-022-05246-3

Amita, M., Adachi, K., Alexenko, A. P., Sinha, S., Schust, D. J., Schulz, L. C., Roberts, R. M., & Ezashi, T. (2013). Complete and unidirectional conversion of human embryonic stem cells to trophoblast by BMP4. *Proc Natl Acad Sci U S A*, *110*(13), E1212-1221. https://doi.org/10.1073/pnas.1303094110

Ananth, C. V., & Vintzileos, A. M. (2006). Maternal-fetal conditions necessitating a medical intervention resulting in preterm birth. *Am J Obstet Gynecol*, *195*(6), 1557-1563. https://doi.org/10.1016/j.ajog.2006.05.021

Aplin, J. D., & Jones, C. J. P. (2021). Cell dynamics in human villous trophoblast. *Hum Reprod Update*, *27*(5), 904-922. https://doi.org/10.1093/humupd/dmab015

Armistead, B., Kadam, L., Siegwald, E., McCarthy, F. P., Kingdom, J. C., Kohan-Ghadr, H. R., & Drewlo, S. (2021). Induction of the PPARγ (Peroxisome Proliferator-Activated Receptor γ)-GCM1 (Glial Cell Missing 1) Syncytialization Axis Reduces sFLT1 (Soluble fms-Like Tyrosine Kinase 1) in the Preeclamptic Placenta. *Hypertension*, *78*(1), 230-240. https://doi.org/10.1161/hypertensionaha.121.17267

Arutyunyan, A., Roberts, K., Troulé, K., Wong, F. C. K., Sheridan, M. A., Kats, I., Garcia-Alonso, L., Velten, B., Hoo, R., Ruiz-Morales, E. R., Sancho-Serra, C., Shilts, J., Handfield, L. F., Marconato, L., Tuck, E., Gardner, L., Mazzeo, C. I., Li, Q., Kelava, I., . . . Vento-Tormo, R. (2023). Spatial multiomics map of trophoblast development in early pregnancy. *Nature*, *616*(7955), 143-151. https://doi.org/10.1038/s41586-023-05869-0

Baczyk, D., Drewlo, S., Proctor, L., Dunk, C., Lye, S., & Kingdom, J. (2009). Glial cell missing-1 transcription factor is required for the differentiation of the human trophoblast. *Cell Death Differ*, *16*(5), 719-727. https://doi.org/10.1038/cdd.2009.1

Baczyk, D., Satkunaratnam, A., Nait-Oumesmar, B., Huppertz, B., Cross, J. C., & Kingdom, J. C. (2004). Complex patterns of GCM1 mRNA and protein in villous and extravillous trophoblast cells of the human placenta. *Placenta*, *25*(6), 553-559. https://doi.org/10.1016/j.placenta.2003.12.004

Bai, T., Peng, C. Y., Aneas, I., Sakabe, N., Requena, D. F., Billstrand, C., Nobrega, M., Ober, C., Parast, M., & Kessler, J. A. (2021). Establishment of human induced trophoblast stem-like cells from term villous cytotrophoblasts. *Stem Cell Res*, *56*, 102507. https://doi.org/10.1016/j.scr.2021.102507

Baines, K. J., & Renaud, S. J. (2017). Transcription Factors That Regulate Trophoblast Development and Function. *Prog Mol Biol Transl Sci*, *145*, 39-88. https://doi.org/10.1016/bs.pmbts.2016.12.003

Barak, Y., Nelson, M. C., Ong, E. S., Jones, Y. Z., Ruiz-Lozano, P., Chien, K. R., Koder, A., & Evans, R. M. (1999). PPAR gamma is required for placental, cardiac, and adipose tissue development. *Mol Cell*, *4*(4), 585-595. https://doi.org/10.1016/s1097-2765(00)80209-9

Barbaux, S., Gascoin-Lachambre, G., Buffat, C., Monnier, P., Mondon, F., Tonanny, M. B., Pinard, A., Auer, J., Bessières, B., Barlier, A., Jacques, S., Simeoni, U., Dandolo, L., Letourneur, F., Jammes, H., & Vaiman, D. (2012). A genome-wide approach reveals

novel imprinted genes expressed in the human placenta. *Epigenetics*, *7*(9), 1079-1090. https://doi.org/10.4161/epi.21495

Bernardo, A. S., Faial, T., Gardner, L., Niakan, K. K., Ortmann, D., Senner, C. E., Callery, E. M., Trotter, M. W., Hemberger, M., Smith, J. C., Bardwell, L., Moffett, A., & Pedersen, R. A. (2011). BRACHYURY and CDX2 mediate BMP-induced differentiation of human and mouse pluripotent stem cells into embryonic and extraembryonic lineages. *Cell Stem Cell*, *9*(2), 144-155. https://doi.org/10.1016/j.stem.2011.06.015

Blakeley, P., Fogarty, N. M., del Valle, I., Wamaitha, S. E., Hu, T. X., Elder, K., Snell, P., Christie, L., Robson, P., & Niakan, K. K. (2015). Defining the three cell lineages of the human blastocyst by single-cell RNA-seq. *Development*, *142*(18), 3151-3165. https://doi.org/10.1242/dev.123547

Brosens, I., Pijnenborg, R., Vercruysse, L., & Romero, R. (2011). The "Great Obstetrical Syndromes" are associated with disorders of deep placentation. *Am J Obstet Gynecol*, *204*(3), 193-201. https://doi.org/10.1016/j.ajog.2010.08.009

Bulmer, J. N., Innes, B. A., Robson, S. C., & Lash, G. E. (2020). Transient loss of endothelial cells in human spiral artery remodelling during early pregnancy: Challenging the dogma. *Placenta*, *101*, 230-233. https://doi.org/10.1016/j.placenta.2020.10.003

Burton, G. J., Charnock-Jones, D. S., & Jauniaux, E. (2009). Regulation of vascular growth and function in the human placenta. *Reproduction*, *138*(6), 895-902. https://doi.org/10.1530/rep-09-0092

Burton, G. J., Cindrova-Davies, T., Yung, H. W., & Jauniaux, E. (2021). HYPOXIA AND REPRODUCTIVE HEALTH: Oxygen and development of the human placenta. *Reproduction*, *161*(1), F53-f65. https://doi.org/10.1530/rep-20-0153

Burton, G. J., & Fowden, A. L. (2015). The placenta: a multifaceted, transient organ. *Philos Trans R Soc Lond B Biol Sci*, *370*(1663), 20140066. https://doi.org/10.1098/rstb.2014.0066

Burton, G. J., & Jauniaux, E. (2017). The cytotrophoblastic shell and complications of pregnancy. *Placenta*, *60*, 134-139. https://doi.org/10.1016/j.placenta.2017.06.007

Cambuli, F., Murray, A., Dean, W., Dudzinska, D., Krueger, F., Andrews, S., Senner, C. E., Cook, S. J., & Hemberger, M. (2014). Epigenetic memory of the first cell fate decision

prevents complete ES cell reprogramming into trophoblast. *Nature Communications*, *5*(1), 5538. https://doi.org/10.1038/ncomms6538

Carter, A. M. (2007). Animal models of human placentation--a review. *Placenta*, *28 Suppl A*, S41-47. https://doi.org/10.1016/j.placenta.2006.11.002

Carter, A. M. (2009). Evolution of factors affecting placental oxygen transfer. *Placenta*, *30 Suppl A*, S19-25. https://doi.org/10.1016/j.placenta.2008.11.006

Chang, C. W., Wakeland, A. K., & Parast, M. M. (2018). Trophoblast lineage specification, differentiation and their regulation by oxygen tension. *J Endocrinol*, *236*(1), R43-r56. https://doi.org/10.1530/joe-17-0402

Chazaud, C., & Yamanaka, Y. (2016). Lineage specification in the mouse preimplantation embryo. *Development*, *143*(7), 1063-1074. https://doi.org/10.1242/dev.128314

Chen, H. C., Hodgen, G. D., Matsuura, S., Lin, L. J., Gross, E., Reichert, L. E., Jr., Birken, S., Canfield, R. E., & Ross, G. T. (1976). Evidence for a gonadotropin from nonpregnant subjects that has physical, immunological, and biological similarities to human chorionic gonadotropin. *Proc Natl Acad Sci U S A*, *73*(8), 2885-2889. https://doi.org/10.1073/pnas.73.8.2885

Chen, J., Yue, C., Xu, J., Zhan, Y., Zhao, H., Li, Y., & Ye, Y. (2019). Downregulation of receptor tyrosine kinase-like orphan receptor 1 in preeclampsia placenta inhibits human trophoblast cell proliferation, migration, and invasion by PI3K/AKT/mTOR pathway accommodation. *Placenta*, *82*, 17-24. https://doi.org/10.1016/j.placenta.2019.05.002

Chen, Y., Meng, Y., Yu, Y., Li, W., Shen, Y., Li, S., Chang, Y., & Sun, W. (2022). LMO2 plays differential roles in trophoblast subtypes and is associated with preeclampsia. *Biochem Biophys Res Commun*, *604*, 43-50. https://doi.org/10.1016/j.bbrc.2022.03.033

Chiang, M. H., Liang, F. Y., Chen, C. P., Chang, C. W., Cheong, M. L., Wang, L. J., Liang, C. Y., Lin, F. Y., Chou, C. C., & Chen, H. (2009). Mechanism of hypoxia-induced GCM1 degradation: implications for the pathogenesis of preeclampsia. *J Biol Chem*, *284*(26), 17411-17419. https://doi.org/10.1074/jbc.M109.016170

Chiu, Y. H., & Chen, H. (2016). GATA3 inhibits GCM1 activity and trophoblast cell invasion. *Sci Rep*, *6*, 21630. https://doi.org/10.1038/srep21630

Cinkornpumin, J. K., Kwon, S. Y., Guo, Y., Hossain, I., Sirois, J., Russett, C. S., Tseng, H. W., Okae, H., Arima, T., Duchaine, T. F., Liu, W., & Pastor, W. A. (2020). Naive Human

Embryonic Stem Cells Can Give Rise to Cells with a Trophoblast-like Transcriptome and Methylome. *Stem Cell Reports*, *15*(1), 198-213. https://doi.org/10.1016/j.stemcr.2020.06.003

Cokus, S. J., Feng, S., Zhang, X., Chen, Z., Merriman, B., Haudenschild, C. D., Pradhan, S., Nelson, S. F., Pellegrini, M., & Jacobsen, S. E. (2008). Shotgun bisulphite sequencing of the Arabidopsis genome reveals DNA methylation patterning. *Nature*, *452*(7184), 215-219. https://doi.org/10.1038/nature06745

Corvinus, F. M., Fitzgerald, J. S., Friedrich, K., & Markert, U. R. (2003). Evidence for a correlation between trophoblast invasiveness and STAT3 activity. *Am J Reprod Immunol*, *50*(4), 316-321. https://doi.org/10.1034/j.1600-0897.2003.00099.x

Cowden Dahl, K. D., Fryer, B. H., Mack, F. A., Compernolle, V., Maltepe, E., Adelman, D. M., Carmeliet, P., & Simon, M. C. (2005). Hypoxia-inducible factors 1alpha and 2alpha regulate trophoblast differentiation. *Mol Cell Biol*, *25*(23), 10479-10491. https://doi.org/10.1128/MCB.25.23.10479-10491.2005

Damsky, C. H., Fitzgerald, M. L., & Fisher, S. J. (1992). Distribution patterns of extracellular matrix components and adhesion receptors are intricately modulated during first trimester cytotrophoblast differentiation along the invasive pathway, in vivo. *J Clin Invest*, *89*(1), 210-222. https://doi.org/10.1172/jci115565

De Paepe, C., Cauffman, G., Verloes, A., Sterckx, J., Devroey, P., Tournaye, H., Liebaers, I., & Van de Velde, H. (2013). Human trophectoderm cells are not yet committed. *Hum Reprod*, *28*(3), 740-749. https://doi.org/10.1093/humrep/des432

Dietrich, B., Haider, S., Meinhardt, G., Pollheimer, J., & Knofler, M. (2022). WNT and NOTCH signaling in human trophoblast development and differentiation. *Cell Mol Life Sci*, *79*(6), 292. https://doi.org/10.1007/s00018-022-04285-3

Dietrich, B., Kunihs, V., Lackner, A. I., Meinhardt, G., Koo, B. K., Pollheimer, J., Haider, S., & Knofler, M. (2023). NOTCH3 signalling controls human trophoblast stem cell expansion and differentiation. *Development*, *150*(22). https://doi.org/10.1242/dev.202152

Dong, C., Beltcheva, M., Gontarz, P., Zhang, B., Popli, P., Fischer, L. A., Khan, S. A., Park, K. M., Yoon, E. J., Xing, X., Kommagani, R., Wang, T., Solnica-Krezel, L., & Theunissen, T. W. (2020). Derivation of trophoblast stem cells from naïve human pluripotent stem cells. *Elife*, *9*. https://doi.org/10.7554/eLife.52504

Enders, A. C., & Blankenship, T. N. (1999). Comparative placental structure. *Adv Drug Deliv Rev*, *38*(1), 3-15. https://doi.org/10.1016/s0169-409x(99)00003-4

Fisher, S. J. (2015). Why is placentation abnormal in preeclampsia? *Am J Obstet Gynecol*, *213*(4 Suppl), S115-122. https://doi.org/10.1016/j.ajog.2015.08.042

Fitzgerald, J. S., Tsareva, S. A., Poehlmann, T. G., Berod, L., Meissner, A., Corvinus, F. M., Wiederanders, B., Pfitzner, E., Markert, U. R., & Friedrich, K. (2005). Leukemia inhibitory factor triggers activation of signal transducer and activator of transcription 3, proliferation, invasiveness, and altered protease expression in choriocarcinoma cells. *Int J Biochem Cell Biol*, *37*(11), 2284-2296. https://doi.org/10.1016/j.biocel.2005.02.025

Gao, X., Nowak-Imialek, M., Chen, X., Chen, D., Herrmann, D., Ruan, D., Chen, A. C. H., Eckersley-Maslin, M. A., Ahmad, S., Lee, Y. L., Kobayashi, T., Ryan, D., Zhong, J., Zhu, J., Wu, J., Lan, G., Petkov, S., Yang, J., Antunes, L., . . . Liu, P. (2019). Establishment of porcine and human expanded potential stem cells. *Nat Cell Biol*, *21*(6), 687-699. https://doi.org/10.1038/s41556-019-0333-2

Genbacev, O., Zhou, Y., Ludlow, J. W., & Fisher, S. J. (1997). Regulation of human placental development by oxygen tension. *Science*, *277*(5332), 1669-1672. https://doi.org/10.1126/science.277.5332.1669

Georgiades, P., Ferguson-Smith, A. C., & Burton, G. J. (2002). Comparative developmental anatomy of the murine and human definitive placentae. *Placenta*, *23*(1), 3-19. https://doi.org/10.1053/plac.2001.0738

Gerbaud, P., & Pidoux, G. (2015). Review: An overview of molecular events occurring in human trophoblast fusion. *Placenta*, *36 Suppl 1*, S35-42. https://doi.org/10.1016/j.placenta.2014.12.015

Gerri, C., McCarthy, A., Alanis-Lobato, G., Demtschenko, A., Bruneau, A., Loubersac, S., Fogarty, N. M. E., Hampshire, D., Elder, K., Snell, P., Christie, L., David, L., Van de Velde, H., Fouladi-Nashta, A. A., & Niakan, K. K. (2020). Initiation of a conserved trophectoderm program in human, cow and mouse embryos. *Nature*, *587*(7834), 443-447. https://doi.org/10.1038/s41586-020-2759-x

Gnarra, J. R., Ward, J. M., Porter, F. D., Wagner, J. R., Devor, D. E., Grinberg, A., Emmert-Buck, M. R., Westphal, H., Klausner, R. D., & Linehan, W. M. (1997). Defective

placental vasculogenesis causes embryonic lethality in VHL-deficient mice. *Proc Natl Acad Sci U S A*, *94*(17), 9102-9107. https://doi.org/10.1073/pnas.94.17.9102

Guo, G., Stirparo, G. G., Strawbridge, S. E., Spindlow, D., Yang, J., Clarke, J., Dattani, A., Yanagida, A., Li, M. A., Myers, S., Ozel, B. N., Nichols, J., & Smith, A. (2021). Human naive epiblast cells possess unrestricted lineage potential. *Cell Stem Cell*, *28*(6), 1040-1056 e1046. https://doi.org/10.1016/j.stem.2021.02.025

Guo, G., Stirparo, G. G., Strawbridge, S. E., Spindlow, D., Yang, J., Clarke, J., Dattani, A., Yanagida, A., Li, M. A., Myers, S., Özel, B. N., Nichols, J., & Smith, A. (2021). Human naive epiblast cells possess unrestricted lineage potential. *Cell Stem Cell*, *28*(6), 1040-1056.e1046. https://doi.org/https://doi.org/10.1016/j.stem.2021.02.025

Guo, G., von Meyenn, F., Rostovskaya, M., Clarke, J., Dietmann, S., Baker, D., Sahakyan, A., Myers, S., Bertone, P., Reik, W., Plath, K., & Smith, A. (2017). Epigenetic resetting of human pluripotency. *Development*, *144*(15), 2748-2763. https://doi.org/10.1242/dev.146811

Haider, S., & Beristain, A. G. (2023). Human organoid systems in modeling reproductive tissue development, function, and disease. *Hum Reprod*, *38*(8), 1449-1463. https://doi.org/10.1093/humrep/dead085

Haider, S., Lackner, A. I., Dietrich, B., Kunihs, V., Haslinger, P., Meinhardt, G., Maxian, T., Saleh, L., Fiala, C., Pollheimer, J., Latos, P. A., & Knofler, M. (2022). Transforming growth factor-beta signaling governs the differentiation program of extravillous trophoblasts in the developing human placenta. *Proc Natl Acad Sci U S A*, *119*(28), e2120667119. https://doi.org/10.1073/pnas.2120667119

Haider, S., Meinhardt, G., Saleh, L., Fiala, C., Pollheimer, J., & Knöfler, M. (2016). Notch1 controls development of the extravillous trophoblast lineage in the human placenta. *Proc Natl Acad Sci U S A*, *113*(48), E7710-e7719. https://doi.org/10.1073/pnas.1612335113

Haider, S., Meinhardt, G., Saleh, L., Kunihs, V., Gamperl, M., Kaindl, U., Ellinger, A., Burkard, T. R., Fiala, C., Pollheimer, J., Mendjan, S., Latos, P. A., & Knöfler, M. (2018). Self-Renewing Trophoblast Organoids Recapitulate the Developmental Program of the Early Human Placenta. *Stem Cell Reports*, *11*(2), 537-551. https://doi.org/10.1016/j.stemcr.2018.07.004

Haider, S., Meinhardt, G., Velicky, P., Otti, G. R., Whitley, G., Fiala, C., Pollheimer, J., & Knöfler, M. (2014). Notch signaling plays a critical role in motility and differentiation of human first-trimester cytotrophoblasts. *Endocrinology*, *155*(1), 263-274. https://doi.org/10.1210/en.2013-1455

Hamada, H., Okae, H., Toh, H., Chiba, H., Hiura, H., Shirane, K., Sato, T., Suyama, M., Yaegashi, N., Sasaki, H., & Arima, T. (2016). Allele-Specific Methylome and Transcriptome Analysis Reveals Widespread Imprinting in the Human Placenta. *Am J Hum Genet*, *99*(5), 1045-1058. https://doi.org/10.1016/j.ajhg.2016.08.021

Hamilton, W. J., & Boyd, J. D. (1960). Development of the human placenta in the first three months of gestation. *J Anat*, *94*(Pt 3), 297-328. https://www.ncbi.nlm.nih.gov/pubmed/14399291

Hemberger, M., Hanna, C. W., & Dean, W. (2020). Mechanisms of early placental development in mouse and humans. *Nat Rev Genet*, *21*(1), 27-43. https://doi.org/10.1038/s41576-019-0169-4

Hemberger, M., Udayashankar, R., Tesar, P., Moore, H., & Burton, G. J. (2010). ELF5-enforced transcriptional networks define an epigenetically regulated trophoblast stem cell compartment in the human placenta. *Hum Mol Genet*, *19*(12), 2456-2467. https://doi.org/10.1093/hmg/ddq128

Hertig, A. T., Rock, J., & Adams, E. C. (1956). A description of 34 human ova within the first 17 days of development. *Am J Anat*, *98*(3), 435-493. https://doi.org/10.1002/aja.1000980306

Home, P., Kumar, R. P., Ganguly, A., Saha, B., Milano-Foster, J., Bhattacharya, B., Ray, S., Gunewardena, S., Paul, A., Camper, S. A., Fields, P. E., & Paul, S. (2017). Genetic redundancy of GATA factors in the extraembryonic trophoblast lineage ensures the progression of preimplantation and postimplantation mammalian development. *Development*, *144*(5), 876-888. https://doi.org/10.1242/dev.145318

Home, P., Saha, B., Ray, S., Dutta, D., Gunewardena, S., Yoo, B., Pal, A., Vivian, J. L., Larson, M., Petroff, M., Gallagher, P. G., Schulz, V. P., White, K. L., Golos, T. G., Behr, B., & Paul, S. (2012). Altered subcellular localization of transcription factor TEAD4 regulates first mammalian cell lineage commitment. *Proc Natl Acad Sci U S A*, *109*(19), 7362-7367. https://doi.org/10.1073/pnas.1201595109

Hori, T., Okae, H., Shibata, S., Kobayashi, N., Kobayashi, E. H., Oike, A., Sekiya, A., Arima, T., & Kaji, H. (2024). Trophoblast stem cell-based organoid models of the human placental barrier. *Nat Commun*, *15*(1), 962. https://doi.org/10.1038/s41467-024-45279-y

Horii, M., Li, Y., Wakeland, A. K., Pizzo, D. P., Nelson, K. K., Sabatini, K., Laurent, L. C., Liu, Y., & Parast, M. M. (2016). Human pluripotent stem cells as a model of trophoblast differentiation in both normal development and disease. *Proc Natl Acad Sci U S A*, *113*(27), E3882-3891. https://doi.org/10.1073/pnas.1604747113

Hornbachner, R., Lackner, A., Papuchova, H., Haider, S., Knöfler, M., Mechtler, K., & Latos, P. A. (2021). MSX2 safeguards syncytiotrophoblast fate of human trophoblast stem cells. *Proc Natl Acad Sci U S A*, *118*(37). https://doi.org/10.1073/pnas.2105130118

Hunkapiller, N. M., Gasperowicz, M., Kapidzic, M., Plaks, V., Maltepe, E., Kitajewski, J., Cross, J. C., & Fisher, S. J. (2011). A role for Notch signaling in trophoblast endovascular invasion and in the pathogenesis of pre-eclampsia. *Development*, *138*(14), 2987-2998. https://doi.org/10.1242/dev.066589

Huppertz, B. (2007). The feto-maternal interface: setting the stage for potential immune interactions. *Semin Immunopathol*, *29*(2), 83-94. https://doi.org/10.1007/s00281-007-0070-7

Hustin, J., Jauniaux, E., & Schaaps, J. P. (1990). Histological study of the materno-embryonic interface in spontaneous abortion. *Placenta*, *11*(6), 477-486. https://doi.org/10.1016/s0143-4004(05)80193-6

Io, S., Kabata, M., Iemura, Y., Semi, K., Morone, N., Minagawa, A., Wang, B., Okamoto, I., Nakamura, T., Kojima, Y., Iwatani, C., Tsuchiya, H., Kaswandy, B., Kondoh, E., Kaneko, S., Woltjen, K., Saitou, M., Yamamoto, T., Mandai, M., & Takashima, Y. (2021). Capturing human trophoblast development with naive pluripotent stem cells in vitro. *Cell Stem Cell*, *28*(6), 1023-1039.e1013. https://doi.org/10.1016/j.stem.2021.03.013

James, J. L., Carter, A. M., & Chamley, L. W. (2012). Human placentation from nidation to 5 weeks of gestation. Part I: What do we know about formative placental development following implantation? *Placenta*, *33*(5), 327-334. https://doi.org/10.1016/j.placenta.2012.01.020

James, J. L., Saghian, R., Perwick, R., & Clark, A. R. (2018). Trophoblast plugs: impact on utero-placental haemodynamics and spiral artery remodelling. *Hum Reprod*, *33*(8), 1430-1441. https://doi.org/10.1093/humrep/dey225

James, J. L., Stone, P. R., & Chamley, L. W. (2005). Cytotrophoblast differentiation in the first trimester of pregnancy: evidence for separate progenitors of extravillous trophoblasts and syncytiotrophoblast. *Reproduction*, *130*(1), 95-103. https://doi.org/10.1530/rep.1.00723

James, J. L., Stone, P. R., & Chamley, L. W. (2007). The isolation and characterization of a population of extravillous trophoblast progenitors from first trimester human placenta. *Hum Reprod*, *22*(8), 2111-2119. https://doi.org/10.1093/humrep/dem144

Jaremek, A., Jeyarajah, M. J., Jaju Bhattad, G., & Renaud, S. J. (2021). Omics Approaches to Study Formation and Function of Human Placental Syncytiotrophoblast. *Front Cell Dev Biol*, *9*, 674162. https://doi.org/10.3389/fcell.2021.674162

Jauniaux, E., Gulbis, B., & Burton, G. J. (2003). The human first trimester gestational sac limits rather than facilitates oxygen transfer to the foetus--a review. *Placenta*, *24 Suppl A*, S86-93. https://doi.org/10.1053/plac.2002.0932

Jauniaux, E., Watson, A., & Burton, G. (2001). Evaluation of respiratory gases and acid-base gradients in human fetal fluids and uteroplacental tissue between 7 and 16 weeks' gestation. *Am J Obstet Gynecol*, *184*(5), 998-1003. https://doi.org/10.1067/mob.2001.111935

Jeyarajah, M. J., Jaju Bhattad, G., Kelly, R. D., Baines, K. J., Jaremek, A., Yang, F. P., Okae, H., Arima, T., Dumeaux, V., & Renaud, S. J. (2022). The multifaceted role of GCM1 during trophoblast differentiation in the human placenta. *Proc Natl Acad Sci U S A*, *119*(49), e2203071119. https://doi.org/10.1073/pnas.2203071119

Jiang, B., Kamat, A., & Mendelson, C. R. (2000). Hypoxia prevents induction of aromatase expression in human trophoblast cells in culture: potential inhibitory role of the hypoxia-inducible transcription factor Mash-2 (mammalian achaete-scute homologous protein-2). *Mol Endocrinol*, *14*(10), 1661-1673. https://doi.org/10.1210/mend.14.10.0539

Jun, S. Y., Ro, J. Y., & Kim, K. R. (2003). p57kip2 is useful in the classification and differential diagnosis of complete and partial hydatidiform moles. *Histopathology*, *43*(1), 17-25. https://doi.org/10.1046/j.1365-2559.2003.01667.x

Kagawa, H., Javali, A., Khoei, H. H., Sommer, T. M., Sestini, G., Novatchkova, M., Scholte Op Reimer, Y., Castel, G., Bruneau, A., Maenhoudt, N., Lammers, J., Loubersac, S., Freour, T., Vankelecom, H., David, L., & Rivron, N. (2022). Human blastoids model blastocyst development and implantation. *Nature*, *601*(7894), 600-605. https://doi.org/10.1038/s41586-021-04267-8

Karvas, R. M., Khan, S. A., Verma, S., Yin, Y., Kulkarni, D., Dong, C., Park, K. M., Chew, B., Sane, E., Fischer, L. A., Kumar, D., Ma, L., Boon, A. C. M., Dietmann, S., Mysorekar, I. U., & Theunissen, T. W. (2022). Stem-cell-derived trophoblast organoids model human placental development and susceptibility to emerging pathogens. *Cell Stem Cell*, *29*(5), 810-825.e818. https://doi.org/10.1016/j.stem.2022.04.004

Khong, T. Y., De Wolf, F., Robertson, W. B., & Brosens, I. (1986). Inadequate maternal vascular response to placentation in pregnancies complicated by pre-eclampsia and by small-for-gestational age infants. *Br J Obstet Gynaecol*, *93*(10), 1049-1059. https://doi.org/10.1111/j.1471-0528.1986.tb07830.x

Knöfler, M., Haider, S., Saleh, L., Pollheimer, J., Gamage, T., & James, J. (2019). Human placenta and trophoblast development: key molecular mechanisms and model systems. *Cell Mol Life Sci*, *76*(18), 3479-3496. https://doi.org/10.1007/s00018-019-03104-6

Knofler, M., & Pollheimer, J. (2013). Human placental trophoblast invasion and differentiation: a particular focus on Wnt signaling. *Front Genet*, *4*, 190. https://doi.org/10.3389/fgene.2013.00190

Knöfler, M., Vasicek, R., & Schreiber, M. (2001). Key Regulatory Transcription Factors Involved in Placental Trophoblast Development—A Review. *Placenta*, *22*, S83-S92. https://doi.org/https://doi.org/10.1053/plac.2001.0648

Kozak, K. R., Abbott, B., & Hankinson, O. (1997). ARNT-deficient mice and placental differentiation. *Dev Biol*, *191*(2), 297-305. https://doi.org/10.1006/dbio.1997.8758

Kunath, T., Yamanaka, Y., Detmar, J., MacPhee, D., Caniggia, I., Rossant, J., & Jurisicova, A. (2014). Developmental differences in the expression of FGF receptors between human and mouse embryos. *Placenta*, *35*(12), 1079-1088. https://doi.org/10.1016/j.placenta.2014.09.008

Latos, P. A., & Hemberger, M. (2014). Review: the transcriptional and signalling networks of mouse trophoblast stem cells. *Placenta*, *35 Suppl*, S81-85. https://doi.org/10.1016/j.placenta.2013.10.013

Lau, K. Y. C., Amadei, G., & Zernicka-Goetz, M. (2023). Assembly of complete mouse embryo models from embryonic and induced stem cell types in vitro. *Nat Protoc*, *18*(12), 3662-3689. https://doi.org/10.1038/s41596-023-00891-y

Lau, K. Y. C., Rubinstein, H., Gantner, C. W., Hadas, R., Amadei, G., Stelzer, Y., & Zernicka-Goetz, M. (2022). Mouse embryo model derived exclusively from embryonic stem cells undergoes neurulation and heart development. *Cell Stem Cell*, *29*(10), 1445-1458 e1448. https://doi.org/10.1016/j.stem.2022.08.013

Lee, C. Q., Gardner, L., Turco, M., Zhao, N., Murray, M. J., Coleman, N., Rossant, J., Hemberger, M., & Moffett, A. (2016). What Is Trophoblast? A Combination of Criteria Define Human First-Trimester Trophoblast. *Stem Cell Reports*, *6*(2), 257-272. https://doi.org/10.1016/j.stemcr.2016.01.006

Lee, C. Q. E., Turco, M. Y., Gardner, L., Simons, B. D., Hemberger, M., & Moffett, A. (2018). Integrin α2 marks a niche of trophoblast progenitor cells in first trimester human placenta. *Development*, *145*(16). https://doi.org/10.1242/dev.162305

Leng, L., Ma, J., Lv, L., Wang, W., Gao, D., Zhu, Y., & Wu, Z. (2020). Both Wnt signaling and epidermal stem cell-derived extracellular vesicles are involved in epidermal cell growth. *Stem Cell Res Ther*, *11*(1), 415. https://doi.org/10.1186/s13287-020-01933-y

Li, S., & Roberson, M. S. (2017). Dlx3 and GCM-1 functionally coordinate the regulation of placental growth factor in human trophoblast-derived cells. *J Cell Physiol*, *232*(10), 2900-2914. https://doi.org/10.1002/jcp.25752

Li, Y., Moretto-Zita, M., Leon-Garcia, S., & Parast, M. M. (2014). p63 inhibits extravillous trophoblast migration and maintains cells in a cytotrophoblast stem cell-like state. *Am J Pathol*, *184*(12), 3332-3343. https://doi.org/10.1016/j.ajpath.2014.08.006

Li, Z., Kurosawa, O., & Iwata, H. (2019). Establishment of human trophoblast stem cells from human induced pluripotent stem cell-derived cystic cells under micromesh culture. *Stem Cell Res Ther*, *10*(1), 245. https://doi.org/10.1186/s13287-019-1339-1

Liang, C. Y., Wang, L. J., Chen, C. P., Chen, L. F., Chen, Y. H., & Chen, H. (2010). GCM1 regulation of the expression of syncytin 2 and its cognate receptor MFSD2A in human placenta. *Biol Reprod*, *83*(3), 387-395. https://doi.org/10.1095/biolreprod.110.083915

Lin, F. Y., Chang, C. W., Cheong, M. L., Chen, H. C., Lee, D. Y., Chang, G. D., & Chen, H. (2011). Dual-specificity phosphatase 23 mediates GCM1 dephosphorylation and activation. *Nucleic Acids Res*, *39*(3), 848-861. https://doi.org/10.1093/nar/gkq838

Liu, D., Chen, Y., Ren, Y., Yuan, P., Wang, N., Liu, Q., Yang, C., Yan, Z., Yang, M., Wang, J., Lian, Y., Yan, J., Zhai, F., Nie, Y., Zhu, X., Chen, Y., Li, R., Chang, H. M., Leung, P. C. K., . . . Yan, L. (2022). Primary specification of blastocyst trophectoderm by scRNA-seq: New insights into embryo implantation. *Sci Adv*, *8*(32), eabj3725. https://doi.org/10.1126/sciadv.abj3725

Liu, H., Yu, L., Ding, Y., Peng, M., & Deng, Y. (2023). Progesterone Enhances the Invasion of Trophoblast Cells by Activating PI3K/AKT Signaling Pathway to Prevent Preeclampsia. *Cell Transplant*, *32*, 9636897221145682. https://doi.org/10.1177/09636897221145682

Liu, X., & Polo, J. M. (2024). Human blastoid as an in vitro model of human blastocysts. *Curr Opin Genet Dev*, *84*, 102135. https://doi.org/10.1016/j.gde.2023.102135

Liu, X., Tan, J. P., Schröder, J., Aberkane, A., Ouyang, J. F., Mohenska, M., Lim, S. M., Sun, Y. B. Y., Chen, J., Sun, G., Zhou, Y., Poppe, D., Lister, R., Clark, A. T., Rackham, O. J. L., Zenker, J., & Polo, J. M. (2021). Modelling human blastocysts by reprogramming fibroblasts into iBlastoids. *Nature*, *591*(7851), 627-632. https://doi.org/10.1038/s41586-021-03372-y

Liu, Y., Fan, X., Wang, R., Lu, X., Dang, Y. L., Wang, H., Lin, H. Y., Zhu, C., Ge, H., Cross, J. C., & Wang, H. (2018). Single-cell RNA-seq reveals the diversity of trophoblast subtypes and patterns of differentiation in the human placenta. *Cell Res*, *28*(8), 819-832. https://doi.org/10.1038/s41422-018-0066-y

Loregger, T., Pollheimer, J., & Knöfler, M. (2003). Regulatory transcription factors controlling function and differentiation of human trophoblast--a review. *Placenta*, *24 Suppl A*, S104-110. https://doi.org/10.1053/plac.2002.0929

Lu, J., Zhang, S., Nakano, H., Simmons, D. G., Wang, S., Kong, S., Wang, Q., Shen, L., Tu, Z., Wang, W., Wang, B., Wang, H., Wang, Y., van Es, J. H., Clevers, H., Leone, G., Cross, J. C., & Wang, H. (2013). A positive feedback loop involving Gcm1 and Fzd5 directs

chorionic branching morphogenesis in the placenta. *PLoS Biol*, *11*(4), e1001536. https://doi.org/10.1371/journal.pbio.1001536

Lu, X., Wang, R., Zhu, C., Wang, H., Lin, H. Y., Gu, Y., Cross, J. C., & Wang, H. (2017). Fine-Tuned and Cell-Cycle-Restricted Expression of Fusogenic Protein Syncytin-2 Maintains Functional Placental Syncytia. *Cell Rep*, *21*(5), 1150-1159. https://doi.org/10.1016/j.celrep.2017.10.019

Lv, B., An, Q., Zeng, Q., Zhang, X., Lu, P., Wang, Y., Zhu, X., Ji, Y., Fan, G., & Xue, Z. (2019). Single-cell RNA sequencing reveals regulatory mechanism for trophoblast cell-fate divergence in human peri-implantation conceptuses. *PLoS Biol*, *17*(10), e3000187. https://doi.org/10.1371/journal.pbio.3000187

Lyall, F., Bulmer, J. N., Kelly, H., Duffie, E., & Robson, S. C. (1999). Human trophoblast invasion and spiral artery transformation: the role of nitric oxide. *Am J Pathol*, *154*(4), 1105-1114. https://doi.org/10.1016/S0002-9440(10)65363-1

Macklon, N. S., Geraedts, J. P., & Fauser, B. C. (2002). Conception to ongoing pregnancy: the 'black box' of early pregnancy loss. *Hum Reprod Update*, *8*(4), 333-343. https://doi.org/10.1093/humupd/8.4.333

Maltepe, E., & Fisher, S. J. (2015). Placenta: the forgotten organ. *Annu Rev Cell Dev Biol*, *31*, 523-552. https://doi.org/10.1146/annurev-cellbio-100814-125620

Maltepe, E., Schmidt, J. V., Baunoch, D., Bradfield, C. A., & Simon, M. C. (1997). Abnormal angiogenesis and responses to glucose and oxygen deprivation in mice lacking the protein ARNT. *Nature*, *386*(6623), 403-407. https://doi.org/10.1038/386403a0

Mansilla, M., Wang, Y., Lim, R., Palmer, K., & Nie, G. (2021). HtrA4 is up-regulated during trophoblast syncytialization and BeWo cells fail to syncytialize without HtrA4. *Sci Rep*, *11*(1), 14363. https://doi.org/10.1038/s41598-021-93520-1

Martin, M. (2011). Cutadapt removes adapter sequences from high-throughput sequencing reads. *EMBnet.journal; Vol 17, No 1: Next Generation Sequencing Data Analysis*. https://doi.org/10.14806/ej.17.1.200

Matsuoka, S., Edwards, M. C., Bai, C., Parker, S., Zhang, P., Baldini, A., Harper, J. W., & Elledge, S. J. (1995). p57KIP2, a structurally distinct member of the p21CIP1 Cdk inhibitor family, is a candidate tumor suppressor gene. *Genes Dev*, *9*(6), 650-662. https://doi.org/10.1101/gad.9.6.650

Matsuura, K., Jigami, T., Taniue, K., Morishita, Y., Adachi, S., Senda, T., Nonaka, A., Aburatani, H., Nakamura, T., & Akiyama, T. (2011). Identification of a link between Wnt/β-catenin signalling and the cell fusion pathway. *Nat Commun*, *2*, 548. https://doi.org/10.1038/ncomms1551

Meinhardt, G., Haider, S., Kunihs, V., Saleh, L., Pollheimer, J., Fiala, C., Hetey, S., Feher, Z., Szilagyi, A., Than, N. G., & Knöfler, M. (2020). Pivotal role of the transcriptional co-activator YAP in trophoblast stemness of the developing human placenta. *Proc Natl Acad Sci U S A*, *117*(24), 13562-13570. https://doi.org/10.1073/pnas.2002630117

Messmer, T., von Meyenn, F., Savino, A., Santos, F., Mohammed, H., Lun, A. T. L., Marioni, J. C., & Reik, W. (2019). Transcriptional Heterogeneity in Naive and Primed Human Pluripotent Stem Cells at Single-Cell Resolution. *Cell Rep*, *26*(4), 815-824.e814. https://doi.org/10.1016/j.celrep.2018.12.099

Mischler, A., Karakis, V., Mahinthakumar, J., Carberry, C. K., San Miguel, A., Rager, J. E., Fry, R. C., & Rao, B. M. (2021). Two distinct trophectoderm lineage stem cells from human pluripotent stem cells. *J Biol Chem*, *296*, 100386. https://doi.org/10.1016/j.jbc.2021.100386

Moffett, A., Chazara, O., & Colucci, F. (2017). Maternal allo-recognition of the fetus. *Fertil Steril*, *107*(6), 1269-1272. https://doi.org/10.1016/j.fertnstert.2017.05.001

Moffett, A., & Loke, C. (2006). Immunology of placentation in eutherian mammals. *Nat Rev Immunol*, *6*(8), 584-594. https://doi.org/10.1038/nri1897

Nakamura, T., Okamoto, I., Sasaki, K., Yabuta, Y., Iwatani, C., Tsuchiya, H., Seita, Y., Nakamura, S., Yamamoto, T., & Saitou, M. (2016). A developmental coordinate of pluripotency among mice, monkeys and humans. *Nature*, *537*(7618), 57-62. https://doi.org/10.1038/nature19096

Napso, T., Yong, H. E. J., Lopez-Tello, J., & Sferruzzi-Perri, A. N. (2018). The Role of Placental Hormones in Mediating Maternal Adaptations to Support Pregnancy and Lactation. *Front Physiol*, *9*, 1091. https://doi.org/10.3389/fphys.2018.01091

Natsuizaka, M., Naganuma, S., Kagawa, S., Ohashi, S., Ahmadi, A., Subramanian, H., Chang, S., Nakagawa, K. J., Ji, X., Liebhaber, S. A., Klein-Szanto, A. J., & Nakagawa, H. (2012). Hypoxia induces IGFBP3 in esophageal squamous cancer cells through HIF-

1alpha-mediated mRNA transcription and continuous protein synthesis. *FASEB J*, *26*(6), 2620-2630. https://doi.org/10.1096/fj.11-198598

Ng, R. K., Dean, W., Dawson, C., Lucifero, D., Madeja, Z., Reik, W., & Hemberger, M. (2008). Epigenetic restriction of embryonic cell lineage fate by methylation of Elf5. *Nat Cell Biol*, *10*(11), 1280-1290. https://doi.org/10.1038/ncb1786

Nguyen, N. M., & Slim, R. (2014). Genetics and Epigenetics of Recurrent Hydatidiform Moles: Basic Science and Genetic Counselling. *Curr Obstet Gynecol Rep*, *3*(1), 55-64. https://doi.org/10.1007/s13669-013-0076-1

Niakan, K. K., & Eggan, K. (2013). Analysis of human embryos from zygote to blastocyst reveals distinct gene expression patterns relative to the mouse. *Dev Biol*, *375*(1), 54-64. https://doi.org/10.1016/j.ydbio.2012.12.008

Nichols, J., & Smith, A. (2009). Naive and primed pluripotent states. *Cell Stem Cell*, *4*(6), 487-492. https://doi.org/10.1016/j.stem.2009.05.015

Nikas, G., Ao, A., Winston, R. M., & Handyside, A. H. (1996). Compaction and surface polarity in the human embryo in vitro. *Biol Reprod*, *55*(1), 32-37. https://doi.org/10.1095/biolreprod55.1.32

Niwa, H., Toyooka, Y., Shimosato, D., Strumpf, D., Takahashi, K., Yagi, R., & Rossant, J. (2005). Interaction between Oct3/4 and Cdx2 determines trophectoderm differentiation. *Cell*, *123*(5), 917-929. https://doi.org/10.1016/j.cell.2005.08.040

Okae, H., Chiba, H., Hiura, H., Hamada, H., Sato, A., Utsunomiya, T., Kikuchi, H., Yoshida, H., Tanaka, A., Suyama, M., & Arima, T. (2014). Genome-wide analysis of DNA methylation dynamics during early human development. *PLoS Genet*, *10*(12), e1004868. https://doi.org/10.1371/journal.pgen.1004868

Okae, H., Toh, H., Sato, T., Hiura, H., Takahashi, S., Shirane, K., Kabayama, Y., Suyama, M., Sasaki, H., & Arima, T. (2018). Derivation of Human Trophoblast Stem Cells. *Cell Stem Cell*, *22*(1), 50-63.e56. https://doi.org/10.1016/j.stem.2017.11.004

Ottosen, L. D., Hindkaer, J., Husth, M., Petersen, D. E., Kirk, J., & Ingerslev, H. J. (2006). Observations on intrauterine oxygen tension measured by fibre-optic microsensors. *Reprod Biomed Online*, *13*(3), 380-385. https://doi.org/10.1016/s1472-6483(10)61443-5

Outhwaite, J. E., McGuire, V., & Simmons, D. G. (2015). Genetic ablation of placental sinusoidal trophoblast giant cells causes fetal growth restriction and embryonic lethality. *Placenta*, *36*(8), 951-955. https://doi.org/10.1016/j.placenta.2015.05.013

Papuchova, H., & Latos, P. A. (2022). Transcription factor networks in trophoblast development. *Cell Mol Life Sci*, *79*(6), 337. https://doi.org/10.1007/s00018-022-04363-6

Pastor, W. A., Chen, D., Liu, W., Kim, R., Sahakyan, A., Lukianchikov, A., Plath, K., Jacobsen, S. E., & Clark, A. T. (2016). Naive Human Pluripotent Cells Feature a Methylation Landscape Devoid of Blastocyst or Germline Memory. *Cell Stem Cell*, *18*(3), 323-329. https://doi.org/10.1016/j.stem.2016.01.019

Pastor, W. A., Liu, W., Chen, D., Ho, J., Kim, R., Hunt, T. J., Lukianchikov, A., Liu, X., Polo, J. M., Jacobsen, S. E., & Clark, A. T. (2018). TFAP2C regulates transcription in human naive pluripotency by opening enhancers. *Nat Cell Biol*, *20*(5), 553-564. https://doi.org/10.1038/s41556-018-0089-0

Petropoulos, S., Edsgärd, D., Reinius, B., Deng, Q., Panula, S. P., Codeluppi, S., Plaza Reyes, A., Linnarsson, S., Sandberg, R., & Lanner, F. (2016). Single-Cell RNA-Seq Reveals Lineage and X Chromosome Dynamics in Human Preimplantation Embryos. *Cell*, *165*(4), 1012-1026. https://doi.org/10.1016/j.cell.2016.03.023

Pfeffer, P. L. (2018). Building Principles for Constructing a Mammalian Blastocyst Embryo. *Biology (Basel)*, *7*(3). https://doi.org/10.3390/biology7030041

Pijnenborg, R., Bland, J. M., Robertson, W. B., & Brosens, I. (1983). Uteroplacental arterial changes related to interstitial trophoblast migration in early human pregnancy. *Placenta*, *4*(4), 397-413. https://doi.org/10.1016/s0143-4004(83)80043-5

Pijnenborg, R., Dixon, G., Robertson, W. B., & Brosens, I. (1980). Trophoblastic invasion of human decidua from 8 to 18 weeks of pregnancy. *Placenta*, *1*(1), 3-19. https://doi.org/10.1016/s0143-4004(80)80012-9

Płusa, B., & Piliszek, A. (2020). Common principles of early mammalian embryo self-organisation. *Development*, *147*(14). https://doi.org/10.1242/dev.183079

Pollheimer, J., Loregger, T., Sonderegger, S., Saleh, L., Bauer, S., Bilban, M., Czerwenka, K., Husslein, P., & Knöfler, M. (2006). Activation of the canonical wingless/T-cell factor signaling pathway promotes invasive differentiation of human trophoblast. *Am J Pathol*, *168*(4), 1134-1147. https://doi.org/10.2353/ajpath.2006.050686

Pollheimer, J., Vondra, S., Baltayeva, J., Beristain, A. G., & Knofler, M. (2018). Regulation of Placental Extravillous Trophoblasts by the Maternal Uterine Environment. *Front Immunol*, *9*, 2597. https://doi.org/10.3389/fimmu.2018.02597

Qin, H., Hejna, M., Liu, Y., Percharde, M., Wossidlo, M., Blouin, L., Durruthy-Durruthy, J., Wong, P., Qi, Z., Yu, J., Qi, L. S., Sebastiano, V., Song, J. S., & Ramalho-Santos, M. (2016). YAP Induces Human Naive Pluripotency. *Cell Rep*, *14*(10), 2301-2312. https://doi.org/10.1016/j.celrep.2016.02.036

Ray, S., Saha, A., Ghosh, A., Roy, N., Kumar, R. P., Meinhardt, G., Mukerjee, A., Gunewardena, S., Kumar, R., Knöfler, M., & Paul, S. (2022). Hippo signaling cofactor, WWTR1, at the crossroads of human trophoblast progenitor self-renewal and differentiation. *Proc Natl Acad Sci U S A*, *119*(36), e2204069119. https://doi.org/10.1073/pnas.2204069119

Renaud, S. J., Chakraborty, D., Mason, C. W., Rumi, M. A., Vivian, J. L., & Soares, M. J. (2015). OVO-like 1 regulates progenitor cell fate in human trophoblast development. *Proc Natl Acad Sci U S A*, *112*(45), E6175-6184. https://doi.org/10.1073/pnas.1507397112

Rijlaarsdam, M. A., Tax, D. M., Gillis, A. J., Dorssers, L. C., Koestler, D. C., de Ridder, J., & Looijenga, L. H. (2015). Genome wide DNA methylation profiles provide clues to the origin and pathogenesis of germ cell tumors. *PLoS One*, *10*(4), e0122146. https://doi.org/10.1371/journal.pone.0122146

Roberts, R. M., Loh, K. M., Amita, M., Bernardo, A. S., Adachi, K., Alexenko, A. P., Schust, D. J., Schulz, L. C., Telugu, B. P., Ezashi, T., & Pedersen, R. A. (2014). Differentiation of trophoblast cells from human embryonic stem cells: to be or not to be? *Reproduction*, *147*(5), D1-12. https://doi.org/10.1530/rep-14-0080

Roberts, V. H. J., Morgan, T. K., Bednarek, P., Morita, M., Burton, G. J., Lo, J. O., & Frias, A. E. (2017). Early first trimester uteroplacental flow and the progressive disintegration of spiral artery plugs: new insights from contrast-enhanced ultrasound and tissue histopathology. *Hum Reprod*, *32*(12), 2382-2393. https://doi.org/10.1093/humrep/dex301

Rodesch, F., Simon, P., Donner, C., & Jauniaux, E. (1992). Oxygen measurements in endometrial and trophoblastic tissues during early pregnancy. *Obstet Gynecol*, *80*(2), 283-285. https://www.ncbi.nlm.nih.gov/pubmed/1635745

Romero, R., Dey, S. K., & Fisher, S. J. (2014). Preterm labor: one syndrome, many causes. *Science*, *345*(6198), 760-765. https://doi.org/10.1126/science.1251816

Romero, R., Kusanovic, J. P., Chaiworapongsa, T., & Hassan, S. S. (2011). Placental bed disorders in preterm labor, preterm PROM, spontaneous abortion and abruptio placentae. *Best Pract Res Clin Obstet Gynaecol*, *25*(3), 313-327. https://doi.org/10.1016/j.bpobgyn.2011.02.006

Rossant, J., & Tam, P. P. L. (2022). Early human embryonic development: Blastocyst formation to gastrulation. *Dev Cell*, *57*(2), 152-165. https://doi.org/10.1016/j.devcel.2021.12.022

Ruebner, M., Langbein, M., Strissel, P. L., Henke, C., Schmidt, D., Goecke, T. W., Faschingbauer, F., Schild, R. L., Beckmann, M. W., & Strick, R. (2012). Regulation of the human endogenous retroviral Syncytin-1 and cell-cell fusion by the nuclear hormone receptors PPARγ/RXRα in placentogenesis. *J Cell Biochem*, *113*(7), 2383-2396. https://doi.org/10.1002/jcb.24110

Rugg-Gunn, P. J., Ferguson-Smith, A. C., & Pedersen, R. A. (2007). Status of genomic imprinting in human embryonic stem cells as revealed by a large cohort of independently derived and maintained lines. *Hum Mol Genet*, *16 Spec No. 2*, R243-251. https://doi.org/10.1093/hmg/ddm245

Saha, B., Ganguly, A., Home, P., Bhattacharya, B., Ray, S., Ghosh, A., Rumi, M. A. K., Marsh, C., French, V. A., Gunewardena, S., & Paul, S. (2020). TEAD4 ensures postimplantation development by promoting trophoblast self-renewal: An implication in early human pregnancy loss. *Proc Natl Acad Sci U S A*, *117*(30), 17864-17875. https://doi.org/10.1073/pnas.2002449117

Sathyanarayanan, A., Ing-Simmons, E., Chen, R., Jeong, H. W., Ozguldez, H. O., Fan, R., Duethorn, B., Kim, K. P., Kim, Y. S., Stehling, M., Brinkmann, H., Scholer, H. R., Adams, R. H., Vaquerizas, J. M., & Bedzhov, I. (2022). Early developmental plasticity enables the induction of an intermediate extraembryonic cell state. *Sci Adv*, *8*(44), eabl9583. https://doi.org/10.1126/sciadv.abl9583

Sato, T., Vries, R. G., Snippert, H. J., van de Wetering, M., Barker, N., Stange, D. E., van Es, J. H., Abo, A., Kujala, P., Peters, P. J., & Clevers, H. (2009). Single Lgr5 stem cells build crypt-villus structures in vitro without a mesenchymal niche. *Nature*, *459*(7244), 262-265. https://doi.org/10.1038/nature07935

Sato, Y. (2020). Endovascular trophoblast and spiral artery remodeling. *Mol Cell Endocrinol*, *503*, 110699. https://doi.org/10.1016/j.mce.2019.110699

Sheridan, M. A., Zhao, X., Fernando, R. C., Gardner, L., Perez-Garcia, V., Li, Q., Marsh, S. G. E., Hamilton, R., Moffett, A., & Turco, M. Y. (2021). Characterization of primary models of human trophoblast. *Development*, *148*(21). https://doi.org/10.1242/dev.199749

Shimizu, T., Oike, A., Kobayashi, E. H., Sekiya, A., Kobayashi, N., Shibata, S., Hamada, H., Saito, M., Yaegashi, N., Suyama, M., Arima, T., & Okae, H. (2023). CRISPR screening in human trophoblast stem cells reveals both shared and distinct aspects of human and mouse placental development. *Proc Natl Acad Sci U S A*, *120*(51), e2311372120. https://doi.org/10.1073/pnas.2311372120

Simon, M. C., & Keith, B. (2008). The role of oxygen availability in embryonic development and stem cell function. *Nat Rev Mol Cell Biol*, *9*(4), 285-296. https://doi.org/10.1038/nrm2354

Smilinich, N. J., Day, C. D., Fitzpatrick, G. V., Caldwell, G. M., Lossie, A. C., Cooper, P. R., Smallwood, A. C., Joyce, J. A., Schofield, P. N., Reik, W., Nicholls, R. D., Weksberg, R., Driscoll, D. J., Maher, E. R., Shows, T. B., & Higgins, M. J. (1999). A maternally methylated CpG island in KvLQT1 is associated with an antisense paternal transcript and loss of imprinting in Beckwith-Wiedemann syndrome. *Proc Natl Acad Sci U S A*, *96*(14), 8064-8069. https://doi.org/10.1073/pnas.96.14.8064

Smith, S. D., Dunk, C. E., Aplin, J. D., Harris, L. K., & Jones, R. L. (2009). Evidence for immune cell involvement in decidual spiral arteriole remodeling in early human pregnancy. *Am J Pathol*, *174*(5), 1959-1971. https://doi.org/10.2353/ajpath.2009.080995

Smith, Z. D., Shi, J., Gu, H., Donaghey, J., Clement, K., Cacchiarelli, D., Gnirke, A., Michor, F., & Meissner, A. (2017). Epigenetic restriction of extraembryonic lineages mirrors the somatic transition to cancer. *Nature*, *549*(7673), 543-547. https://doi.org/10.1038/nature23891

Soejima, H., & Higashimoto, K. (2013). Epigenetic and genetic alterations of the imprinting disorder Beckwith-Wiedemann syndrome and related disorders. *J Hum Genet*, *58*(7), 402-409. https://doi.org/10.1038/jhg.2013.51

Soncin, F., Khater, M., To, C., Pizzo, D., Farah, O., Wakeland, A., Arul Nambi Rajan, K., Nelson, K. K., Chang, C. W., Moretto-Zita, M., Natale, D. R., Laurent, L. C., & Parast,

M. M. (2018). Comparative analysis of mouse and human placentae across gestation reveals species-specific regulators of placental development. *Development*, *145*(2). https://doi.org/10.1242/dev.156273

Soncin, F., Morey, R., Bui, T., Requena, D. F., Cheung, V. C., Kallol, S., Kittle, R., Jackson, M. G., Farah, O., Chousal, J., Meads, M., Pizzo, D., Horii, M., Fisch, K. M., & Parast, M. M. (2022). Derivation of functional trophoblast stem cells from primed human pluripotent stem cells. *Stem Cell Reports*, *17*(6), 1303-1317. https://doi.org/10.1016/j.stemcr.2022.04.013

Sonderegger, S., Pollheimer, J., & Knofler, M. (2010). Wnt signalling in implantation, decidualisation and placental differentiation--review. *Placenta*, *31*(10), 839-847. https://doi.org/10.1016/j.placenta.2010.07.011

Stirparo, G. G., Boroviak, T., Guo, G., Nichols, J., Smith, A., & Bertone, P. (2018). Integrated analysis of single-cell embryo data yields a unified transcriptome signature for the human pre-implantation epiblast. *Development*, *145*(3). https://doi.org/10.1242/dev.158501

Takahashi, S., Okae, H., Kobayashi, N., Kitamura, A., Kumada, K., Yaegashi, N., & Arima, T. (2019). Loss of p57(KIP2) expression confers resistance to contact inhibition in human androgenetic trophoblast stem cells. *Proc Natl Acad Sci U S A*, *116*(52), 26606-26613. https://doi.org/10.1073/pnas.1916019116

Takashima, Y., Guo, G., Loos, R., Nichols, J., Ficz, G., Krueger, F., Oxley, D., Santos, F., Clarke, J., Mansfield, W., Reik, W., Bertone, P., & Smith, A. (2014). Resetting transcription factor control circuitry toward ground-state pluripotency in human. *Cell*, *158*(6), 1254-1269. https://doi.org/10.1016/j.cell.2014.08.029

Takeda, K., Ho, V. C., Takeda, H., Duan, L. J., Nagy, A., & Fong, G. H. (2006). Placental but not heart defects are associated with elevated hypoxia-inducible factor alpha levels in mice lacking prolyl hydroxylase domain protein 2. *Mol Cell Biol*, *26*(22), 8336-8346. https://doi.org/10.1128/MCB.00425-06

Tan, J. P., Liu, X., & Polo, J. M. (2022). Establishment of human induced trophoblast stem cells via reprogramming of fibroblasts. *Nat Protoc*, *17*(12), 2739-2759. https://doi.org/10.1038/s41596-022-00742-2

Tanaka, S., Kunath, T., Hadjantonakis, A. K., Nagy, A., & Rossant, J. (1998). Promotion of trophoblast stem cell proliferation by FGF4. *Science*, *282*(5396), 2072-2075. https://doi.org/10.1126/science.282.5396.2072

Tarazi, S., Aguilera-Castrejon, A., Joubran, C., Ghanem, N., Ashouokhi, S., Roncato, F., Wildschutz, E., Haddad, M., Oldak, B., Gomez-Cesar, E., Livnat, N., Viukov, S., Lokshtanov, D., Naveh-Tassa, S., Rose, M., Hanna, S., Raanan, C., Brenner, O., Kedmi, M., . . . Hanna, J. H. (2022). Post-gastrulation synthetic embryos generated ex utero from mouse naive ESCs. *Cell*, *185*(18), 3290-3306 e3225. https://doi.org/10.1016/j.cell.2022.07.028

Theunissen, T. W., Friedli, M., He, Y., Planet, E., O'Neil, R. C., Markoulaki, S., Pontis, J., Wang, H., Iouranova, A., Imbeault, M., Duc, J., Cohen, M. A., Wert, K. J., Castanon, R., Zhang, Z., Huang, Y., Nery, J. R., Drotar, J., Lungjangwa, T., . . . Jaenisch, R. (2016). Molecular Criteria for Defining the Naive Human Pluripotent State. *Cell Stem Cell*, *19*(4), 502-515. https://doi.org/10.1016/j.stem.2016.06.011

Theunissen, T. W., Powell, B. E., Wang, H., Mitalipova, M., Faddah, D. A., Reddy, J., Fan, Z. P., Maetzel, D., Ganz, K., Shi, L., Lungjangwa, T., Imsoonthornruksa, S., Stelzer, Y., Rangarajan, S., D'Alessio, A., Zhang, J., Gao, Q., Dawlaty, M. M., Young, R. A., . . . Jaenisch, R. (2014). Systematic identification of culture conditions for induction and maintenance of naive human pluripotency. *Cell Stem Cell*, *15*(4), 471-487. https://doi.org/10.1016/j.stem.2014.07.002

Thomson, J. A., Itskovitz-Eldor, J., Shapiro, S. S., Waknitz, M. A., Swiergiel, J. J., Marshall, V. S., & Jones, J. M. (1998). Embryonic stem cell lines derived from human blastocysts. *Science*, *282*(5391), 1145-1147. https://doi.org/10.1126/science.282.5391.1145

Treissman, J., Yuan, V., Baltayeva, J., Le, H. T., Castellana, B., Robinson, W. P., & Beristain, A. G. (2020). Low oxygen enhances trophoblast column growth by potentiating differentiation of the extravillous lineage and promoting LOX activity. *Development*, *147*(2). https://doi.org/10.1242/dev.181263

Turco, M. Y., Gardner, L., Kay, R. G., Hamilton, R. S., Prater, M., Hollinshead, M. S., McWhinnie, A., Esposito, L., Fernando, R., Skelton, H., Reimann, F., Gribble, F. M., Sharkey, A., Marsh, S. G. E., O'Rahilly, S., Hemberger, M., Burton, G. J., & Moffett, A.

(2018). Trophoblast organoids as a model for maternal-fetal interactions during human placentation. *Nature*, *564*(7735), 263-267. https://doi.org/10.1038/s41586-018-0753-3

Turco, M. Y., & Moffett, A. (2019). Development of the human placenta. *Development*, *146*(22). https://doi.org/10.1242/dev.163428

Tuuli, M. G., Longtine, M. S., & Nelson, D. M. (2011). Review: Oxygen and trophoblast biology--a source of controversy. *Placenta*, *32 Suppl 2*(0 2), S109-118. https://doi.org/10.1016/j.placenta.2010.12.013

Uhlén, M., Fagerberg, L., Hallström, B. M., Lindskog, C., Oksvold, P., Mardinoglu, A., Sivertsson, Å., Kampf, C., Sjöstedt, E., Asplund, A., Olsson, I., Edlund, K., Lundberg, E., Navani, S., Szigyarto, C. A., Odeberg, J., Djureinovic, D., Takanen, J. O., Hober, S., . . . Pontén, F. (2015). Proteomics. Tissue-based map of the human proteome. *Science*, *347*(6220), 1260419. https://doi.org/10.1126/science.1260419

Uy, G. D., Downs, K. M., & Gardner, R. L. (2002). Inhibition of trophoblast stem cell potential in chorionic ectoderm coincides with occlusion of the ectoplacental cavity in the mouse. *Development*, *129*(16), 3913-3924. https://doi.org/10.1242/dev.129.16.3913

Varberg, K. M., Dominguez, E. M., Koseva, B., Varberg, J. M., McNally, R. P., Moreno-Irusta, A., Wesley, E. R., Iqbal, K., Cheung, W. A., Schwendinger-Schreck, C., Smail, C., Okae, H., Arima, T., Lydic, M., Holoch, K., Marsh, C., Soares, M. J., & Grundberg, E. (2023). Extravillous trophoblast cell lineage development is associated with active remodeling of the chromatin landscape. *Nat Commun*, *14*(1), 4826. https://doi.org/10.1038/s41467-023-40424-5

Varberg, K. M., Iqbal, K., Muto, M., Simon, M. E., Scott, R. L., Kozai, K., Choudhury, R. H., Aplin, J. D., Biswell, R., Gibson, M., Okae, H., Arima, T., Vivian, J. L., Grundberg, E., & Soares, M. J. (2021). ASCL2 reciprocally controls key trophoblast lineage decisions during hemochorial placenta development. *Proc Natl Acad Sci U S A*, *118*(10). https://doi.org/10.1073/pnas.2016517118

Velicky, P., Meinhardt, G., Plessl, K., Vondra, S., Weiss, T., Haslinger, P., Lendl, T., Aumayr, K., Mairhofer, M., Zhu, X., Schutz, B., Hannibal, R. L., Lindau, R., Weil, B., Ernerudh, J., Neesen, J., Egger, G., Mikula, M., Rohrl, C., . . . Pollheimer, J. (2018). Genome amplification and cellular senescence are hallmarks of human placenta development. *PLoS Genet*, *14*(10), e1007698. https://doi.org/10.1371/journal.pgen.1007698

Vento-Tormo, R., Efremova, M., Botting, R. A., Turco, M. Y., Vento-Tormo, M., Meyer, K. B., Park, J. E., Stephenson, E., Polanski, K., Goncalves, A., Gardner, L., Holmqvist, S., Henriksson, J., Zou, A., Sharkey, A. M., Millar, B., Innes, B., Wood, L., Wilbrey-Clark, A., . . . Teichmann, S. A. (2018). Single-cell reconstruction of the early maternal-fetal interface in humans. *Nature*, *563*(7731), 347-353. https://doi.org/10.1038/s41586-018-0698-6

Wakeland, A. K., Soncin, F., Moretto-Zita, M., Chang, C. W., Horii, M., Pizzo, D., Nelson, K. K., Laurent, L. C., & Parast, M. M. (2017). Hypoxia Directs Human Extravillous Trophoblast Differentiation in a Hypoxia-Inducible Factor-Dependent Manner. *Am J Pathol*, *187*(4), 767-780. https://doi.org/10.1016/j.ajpath.2016.11.018

Wallace, A. E., Fraser, R., & Cartwright, J. E. (2012). Extravillous trophoblast and decidual natural killer cells: a remodelling partnership. *Hum Reprod Update*, *18*(4), 458-471. https://doi.org/10.1093/humupd/dms015

Wang, L. J., Chen, C. P., Lee, Y. S., Ng, P. S., Chang, G. D., Pao, Y. H., Lo, H. F., Peng, C. H., Cheong, M. L., & Chen, H. (2022a). Functional antagonism between DeltaNp63alpha and GCM1 regulates human trophoblast stemness and differentiation. *Nat Commun*, *13*(1), 1626. https://doi.org/10.1038/s41467-022-29312-6

Wang, L. J., Chen, C. P., Lee, Y. S., Ng, P. S., Chang, G. D., Pao, Y. H., Lo, H. F., Peng, C. H., Cheong, M. L., & Chen, H. (2022b). Functional antagonism between ΔNp63α and GCM1 regulates human trophoblast stemness and differentiation. *Nat Commun*, *13*(1), 1626. https://doi.org/10.1038/s41467-022-29312-6

Wang, L. J., Cheong, M. L., Lee, Y. S., Lee, M. T., & Chen, H. (2012). High-temperature requirement protein A4 (HtrA4) suppresses the fusogenic activity of syncytin-1 and promotes trophoblast invasion. *Mol Cell Biol*, *32*(18), 3707-3717. https://doi.org/10.1128/mcb.00223-12

Wang, Y., & Zhao, S. (2010). Integrated Systems Physiology: from Molecules to Function to Disease. In *Vascular Biology of the Placenta*. Morgan & Claypool Life Sciences

https://doi.org/10.4199/c00016ed1v01y201008isp009

Weatherbee, B. A. T., Gantner, C. W., Iwamoto-Stohl, L. K., Daza, R. M., Hamazaki, N., Shendure, J., & Zernicka-Goetz, M. (2023). Pluripotent stem cell-derived model of the

post-implantation human embryo. *Nature*, *622*(7983), 584-593. https://doi.org/10.1038/s41586-023-06368-y

Wei, X. W., Zhang, Y. C., Wu, F., Tian, F. J., & Lin, Y. (2022). The role of extravillous trophoblasts and uterine NK cells in vascular remodeling during pregnancy. *Front Immunol*, *13*, 951482. https://doi.org/10.3389/fimmu.2022.951482

Wei, Y., Wang, T., Ma, L., Zhang, Y., Zhao, Y., Lye, K., Xiao, L., Chen, C., Wang, Z., Ma, Y., Zhou, X., Sun, F., Li, W., Dunk, C., Li, S., Nagy, A., Yu, Y., Pan, G., Lye, S. J., & Shan, Y. (2021). Efficient derivation of human trophoblast stem cells from primed pluripotent stem cells. *Sci Adv*, *7*(33). https://doi.org/10.1126/sciadv.abf4416

Whitley, G. S., & Cartwright, J. E. (2010). Cellular and molecular regulation of spiral artery remodelling: lessons from the cardiovascular field. *Placenta*, *31*(6), 465-474. https://doi.org/10.1016/j.placenta.2010.03.002

Windsperger, K., Dekan, S., Pils, S., Golletz, C., Kunihs, V., Fiala, C., Kristiansen, G., Knöfler, M., & Pollheimer, J. (2017). Extravillous trophoblast invasion of venous as well as lymphatic vessels is altered in idiopathic, recurrent, spontaneous abortions. *Hum Reprod*, *32*(6), 1208-1217. https://doi.org/10.1093/humrep/dex058

Woods, L., Perez-Garcia, V., & Hemberger, M. (2018). Regulation of Placental Development and Its Impact on Fetal Growth-New Insights From Mouse Models. *Front Endocrinol (Lausanne)*, *9*, 570. https://doi.org/10.3389/fendo.2018.00570

Xi, Y., & Li, W. (2009). BSMAP: whole genome bisulfite sequence MAPping program. *BMC Bioinformatics*, *10*, 232. https://doi.org/10.1186/1471-2105-10-232

Xiang, L., Yin, Y., Zheng, Y., Ma, Y., Li, Y., Zhao, Z., Guo, J., Ai, Z., Niu, Y., Duan, K., He, J., Ren, S., Wu, D., Bai, Y., Shang, Z., Dai, X., Ji, W., & Li, T. (2020). A developmental landscape of 3D-cultured human pre-gastrulation embryos. *Nature*, *577*(7791), 537-542. https://doi.org/10.1038/s41586-019-1875-y

Xu, R. H., Chen, X., Li, D. S., Li, R., Addicks, G. C., Glennon, C., Zwaka, T. P., & Thomson, J. A. (2002). BMP4 initiates human embryonic stem cell differentiation to trophoblast. *Nat Biotechnol*, *20*(12), 1261-1264. https://doi.org/10.1038/nbt761

Yang, L., Liang, P., Yang, H., & Coyne, C. B. (2024). Trophoblast organoids with physiological polarity model placental structure and function. *J Cell Sci*, *137*(5). https://doi.org/10.1242/jcs.261528

Yang, L., Semmes, E. C., Ovies, C., Megli, C., Permar, S., Gilner, J. B., & Coyne, C. B. (2022). Innate immune signaling in trophoblast and decidua organoids defines differential antiviral defenses at the maternal-fetal interface. *Elife*, *11*. https://doi.org/10.7554/eLife.79794

Yang, M., Lei, Z. M., & Rao Ch, V. (2003). The central role of human chorionic gonadotropin in the formation of human placental syncytium. *Endocrinology*, *144*(3), 1108-1120. https://doi.org/10.1210/en.2002-220922

Yu, C., Shen, K., Lin, M., Chen, P., Lin, C., Chang, G. D., & Chen, H. (2002). GCMa regulates the syncytin-mediated trophoblastic fusion. *J Biol Chem*, *277*(51), 50062-50068. https://doi.org/10.1074/jbc.M209316200

Yu, L., Wei, Y., Duan, J., Schmitz, D. A., Sakurai, M., Wang, L., Wang, K., Zhao, S., Hon, G. C., & Wu, J. (2021). Blastocyst-like structures generated from human pluripotent stem cells. *Nature*, *591*(7851), 620-626. https://doi.org/10.1038/s41586-021-03356-y

Zhao, A., Yang, Y., Pan, X., Pan, Y., & Cai, S. (2020). Generation of keratinocyte stem-like cells from human fibroblasts via a direct reprogramming approach. *Biotechnol Prog*, *36*(3), e2961. https://doi.org/10.1002/btpr.2961

Zhao, H., Wong, R. J., & Stevenson, D. K. (2021). The Impact of Hypoxia in Early Pregnancy on Placental Cells. *Int J Mol Sci*, *22*(18). https://doi.org/10.3390/ijms22189675

Zhao, W. X., Wu, Z. M., Liu, W., & Lin, J. H. (2017). Notch2 and Notch3 suppress the proliferation and mediate invasion of trophoblast cell lines. *Biol Open*, *6*(8), 1123-1129. https://doi.org/10.1242/bio.025767

Zhou, W., Wang, H., Yang, Y., Guo, F., Yu, B., & Su, Z. (2022). Trophoblast Cell Subtypes and Dysfunction in the Placenta of Individuals with Preeclampsia Revealed by Single-Cell RNA Sequencing. *Mol Cells*, *45*(5), 317-328. https://doi.org/10.14348/molcells.2021.0211

Zhou, Y., Fisher, S. J., Janatpour, M., Genbacev, O., Dejana, E., Wheelock, M., & Damsky, C. H. (1997). Human cytotrophoblasts adopt a vascular phenotype as they differentiate. A strategy for successful endovascular invasion? *J Clin Invest*, *99*(9), 2139-2151. https://doi.org/10.1172/jci119387